

D I P L O M A R B E I T

M A S T E R ' S   T H E S I S

# A numerical model for slip curves of dowel connections and its application to timber structures

ausgeführt zum Zwecke der Erlangung des akademischen  
Grades eines Diplom-Ingenieurs

unter der Anleitung von

Univ.-Ass. Dipl.-Ing. Dr. techn. **Thomas K. Bader**

Proj.-Ass. Dipl.-Ing. **Georg Hochreiner**

Institut für Mechanik der Werkstoffe und Strukturen  
Fakultät für Bauingenieurwesen  
Technische Universität Wien

und

Univ.-Prof. Dipl.-Ing. Dr. techn. DDr. h.c. **Josef Eberhardsteiner**

Institut für Mechanik der Werkstoffe und Strukturen  
Fakultät für Bauingenieurwesen  
Technische Universität Wien

eingereicht an der Technischen Universität Wien  
Fakultät für Bauingenieurwesen

von

**Michael Schweigler**

Matr.Nr.: 07 28 165

Horngasse 5

A - 3140 Pottenbrunn

Wien, im Juni 2013

## Danksagung

Diese Diplomarbeit stellt den Abschluss meines Bachelor- und Masterstudiums an der Technischen Universität Wien dar. Fünfeinhalb lehrreiche und manchmal auch anstrengende Jahre an dieser Universität gehen zu Ende. Aus diesem Grund möchte ich die Gelegenheit nutzen Danke zu sagen. Danke, an all jene Personen, die mir dieses Studium überhaupt erst ermöglicht haben. Besonderer Dank gebührt hierbei meinen Eltern Maria und Kurt Schweigler, die mich auf meinem eingeschlagenen Weg stets unterstützt haben. Obwohl aus einfachen Verhältnissen stammend, haben sie mir und meinen Brüdern während des Studiums soweit als möglich finanziell unter die Arme gegriffen. Diesbezüglich gilt mein Dank auch allen öffentlichen Stellen, der Universität und anderen privaten Personen, welche versuchen durch finanzielle Unterstützung ein Studium für alle, unabhängig von der gesellschaftlichen Herkunft möglich zu machen. Gerade der Kontakt mit Studenten aus anderen Ländern während meines Auslandsstudiums, hat mir vor Augen geführt, dass dies keine Selbstverständlichkeit ist.

Des Weiteren gilt es meinen Studienkollegen für die gute Zusammenarbeit zu danken. Eine Zusammenarbeit die zu einem raschen und erfolgreichen Abschluss des Studiums geführt hat. Natürlich möchte ich mich auch bei meiner gesamten Familie und meinen Freunden für den sozialen Rückhalt während der Studienzeit bedanken.

Bezüglich der Erstellung der Diplomarbeit möchte ich mich bei allen Mitarbeitern des Institutes für Mechanik der Werkstoffe und Strukturen (IMWS) bedanken. Im Besonderen danke ich meinen zukünftigen Kollegen der Holzgruppe am IMWS für die freundliche Aufnahme. Ein herzliches Dankeschön richtet sich an meine Betreuer, die mir während der Erstellung der Diplomarbeit stets mit Rat und Tat zur Seite gestanden sind. Herrn Univ.-Ass. Dipl.-Ing. Dr. techn. Thomas Bader danke ich im Besonderen für die ausgezeichnete Betreuung und gewissenhafte Korrektur meiner Diplomarbeit. Herrn Proj.-Ass. Dipl.-Ing. Georg Hochreiner ist für sein kritisches Denken bezüglich aktueller Bemessungsstandards und für seine neuen Denkansätze, welche meine Diplomarbeit maßgebend beeinflusst haben, zu danken. Ein Danke sei auch an den ehemaligen Mitarbeiter Herrn Dipl.-Ing. Dr. techn. Michael Dorn gerichtet, dessen Begeisterung für den Werkstoff Holz, auch bei mir zu einem vertieften Interesse an diesem Material geführt hat. Abschließend richtet sich mein Dank an Univ.-Prof. Dipl.-Ing. Dr. techn. DDr. h.c. Josef Eberhardsteiner für seine Unterstützung während der Ausarbeitung der Diplomarbeit, und für die von ihm gebotene Möglichkeit auch in Zukunft in diesem Forschungsbereich tätig sein zu können.

## Abstract

Wood as a natural and renewable material currently experiences a revival as structural building material. New technologies and a new design standard request appropriate, modern design methods for timber structures. Particularly, the design of modern timber connections is of importance since more challenging timber constructions demand ambitious connections. Most connections in timber structures are compliant in the sense that relative deformations between the connected structural elements occur during load transfer. In particular dowel connections exhibit this behavior since load transfer in dowel connections is based on the compliant embedment behavior of stiff steel dowels in wood.

The aim of this thesis is to develop a model for a consistent calculation of the load-deformation relationship of connections. Additionally, this model is applied to timber structures to study the influence of compliant connections on the structural behavior. As a basis for the modeling of dowel connections, properties of single-dowel connections are presented. Different responses of wood in case of different loading directions, as well as several models for the calculation of single-dowel slip curves are discussed. Significant differences in the predicted load-deformation behavior of single-dowels can be observed among these approaches. A sub-model is used to determine realistic single-dowel slip curves for arbitrary connection configurations. Furthermore, the state-of-the-art approach for the determination of connection slip curves of multi-dowel connections is discussed. The restriction of this approach to some specific design situations is highlighted. These limitations of the current design approach are the motivation to develop a model for the calculation of slip curves of multi-dowel connections. This model enables a straight forward determination of member forces and connection slip curves for an arbitrary set of deformations. The single calculation steps and the feasibility of application on arbitrary connection configurations are discussed. Furthermore, a modification of the model to determine the deformation and force distribution within the connection for specific member forces is presented.

Finally, the model is applied to different connections to illustrate their behavior for simple design examples. Moreover, connection slip curves have been implemented in the structural analysis of a static indetermined system in order to illustrate the necessity of considering the compliance of connections in the design of timber structures. It is shown that negligence of the connection slip may lead to uneconomic or even unsafe timber structures. Furthermore, the importance of an exact definition of the connection slip curves is discussed. Even insignificant differences from standard configurations may lead to remarkable changes in the connection behavior and, consequently, in the behavior of the structure. Moreover, a considerable influence of the used method to describe the single-dowel behavior on the behavior of the connection and, consequently, on the structural behavior has been found.

## Kurzfassung

Der nachwachsende Werkstoff Holz erfährt zurzeit einen beachtlichen Aufschwung als Konstruktionsmaterial im Bauwesen. Neuentwicklungen auf diesem Sektor sowie eine neue normative Regelungen erfordern neue Bemessungsmethoden für die computerbasierte Bemessung von Holzkonstruktionen. Der Berechnung moderner Holzverbindungen kommt eine besondere Bedeutung zu, da immer aufwändigere Tragkonstruktionen zu komplexeren Verbindungen führen. Außerdem verhalten sich die meisten Verbindungen nachgiebig in Bezug auf das Verformungsverhalten zwischen den einzelnen Tragelementen. Besonders stark ausgeprägt ist das nachgiebige Verhalten bei Dübelverbindungen, da die Lastabtragung über nachgiebige Lochleibungsbettung des starren Dübels in der Holzmatrix erfolgt.

Das Ziel dieser Arbeit ist es, ein Berechnungsmodell zur konsistenten Ermittlung des Last-Verschiebungsverhaltens von Holzverbindungen zu entwickeln. Anschließend werden die mit diesem Modell ermittelten Nachgiebigkeiten in der Strukturanalyse verwendet, um den Einfluss auf das Tragverhalten der Struktur zu analysieren. Als Grundlage des Berechnungsmodells werden die Eigenschaften des Einzeldübels anhand von verschiedenen Modellen für unterschiedliche Belastungsrichtungen vorgestellt. Hierbei sind beachtliche Unterschiede im Last-Verschiebungsverhalten zwischen den einzelnen Berechnungsmodellen für den Einzeldübel erkennbar. Um eine realitätsnahe Abbildung des realen Tragverhaltens des Einzeldübels für eine beliebige Verbindung zu ermöglichen, wird auf eine baustatische Modellbildung zurückgegriffen. Des Weiteren wird ein aktuelles Bemessungsverfahren zur Ermittlung der Verbindungsnachgiebigkeit vorgestellt. Nachteile dieses Modells und die dadurch vorgenommenen Vereinfachungen und Einschränkungen werden aufgezeigt. Genau diese Einschränkungen dienen als Motivation zur Entwicklung eines allgemeingültigen Berechnungsverfahrens für die Nachgiebigkeit von Holzverbindungen. Das vorgestellte Berechnungsmodell ermöglicht, basierend auf einem beliebigen Verschiebungszustand, eine konsistente Ermittlung der Schnittgrößen und Nachgiebigkeit der Verbindung. Die einzelnen Berechnungsschritte sowie die allgemeingültige Anwendbarkeit auf beliebige Holzverbindungen werden diskutiert. Eine abgeänderte Version dieses Modells erlaubt es, ausgehend von Schnittgrößen, die Einzeldübelkräfte und Einzeldübelverschiebungen zu berechnen.

Abschließend werden die Fähigkeiten und Auswirkungen des vorgestellten Modells anhand von einfachen Konstruktionsbeispielen dargestellt. Das Modell wird sowohl auf einzelne Holzverbindungen als auch auf ein Tragsystem angewendet, um die Notwendigkeit der Berücksichtigung von Nachgiebigkeiten der Verbindungen aufzuzeigen. Es konnte gezeigt werden, dass ein Nichtbeachten der Nachgiebigkeit sowohl zu unwirtschaftlichen als auch unsicheren Tragkonstruktionen führen kann. Zusätzlich wird auf die Notwendigkeit der exakten Formulierung des Einzeldübelverhaltens und des Last-Verschiebungsverhaltens der Verbindung verwiesen, denn bereits geringfügige Abweichungen von den Standardkonfigurationen können zu signifikanten Änderungen im Deformationsverhalten der Verbindung und daraus resultierend im Tragverhalten der gesamten Struktur führen.

# Contents

<b>1</b>	<b>Introduction</b>	<b>3</b>
<b>2</b>	<b>Single-dowel connections</b>	<b>5</b>
2.1	Mechanical behavior of clear wood . . . . .	6
2.2	Mechanical behavior of single-dowel connections . . . . .	8
2.3	Design according to EC 5 . . . . .	13
2.4	Single-dowel slip curves as input for the calculation of connections . . . .	16
2.4.1	Description of calculation methods . . . . .	17
2.4.2	Determination of single-fastener slip curves for dowel connections by means of commercial structural analysis software . . . . .	18
2.5	Parameter study - single-fastener slip curves . . . . .	21
2.5.1	Structural analysis model for single-dowel connection . . . . .	21
2.5.2	Variation of dowel stiffness . . . . .	22
2.5.3	Variation of side member thickness $t_1$ . . . . .	26
<b>3</b>	<b>Multi-dowel connections</b>	<b>31</b>
3.1	Mechanical behavior of multi-dowel connections . . . . .	32
3.2	Current models considering the compliance of connections . . . . .	36
3.3	State-of-the-art calculation of connection slip curves and dowel verification	37
3.3.1	Design of connections . . . . .	37
3.3.2	Calculation of slip curves of connections . . . . .	37
3.3.3	Structural analysis considering the compliance of connections . . .	43
3.3.4	Verification of connection . . . . .	43
3.3.5	Limits and restrictions of the model . . . . .	46
3.3.6	Flow chart - State-of-the-art design of dowel connections . . . . .	47
<b>4</b>	<b>Modeling approach for the calculation of connection slip curves and dowel forces</b>	<b>48</b>
4.1	Model for the calculation of connection slip curves . . . . .	49
4.1.1	Description of the model . . . . .	49
4.1.2	Flow chart - calculation of connection slip curves . . . . .	54
4.2	Back-calculation of dowel forces . . . . .	55
4.2.1	Description of the model . . . . .	55
4.2.2	Flow chart - back-calculation of dowel forces . . . . .	58

---

<b>5</b>	<b>Design examples</b>	<b>59</b>
5.1	Slip curves and limit surfaces of multi-dowel connections . . . . .	60
5.1.1	Dowel connection design examples . . . . .	60
5.1.2	Typical connections of a timber frame structure . . . . .	75
5.2	Influence of connection slip on structural behavior . . . . .	79
<b>6</b>	<b>Summary and conclusions</b>	<b>85</b>
<b>A</b>	<b>Description of MATLAB Code for the calculation of connection slip curves</b>	<b>89</b>
<b>B</b>	<b>Description of MATLAB Code for back-calculation of dowel forces</b>	<b>101</b>

# Chapter 1

---

## Introduction

Most connections in timber structures are compliant in the sense that relative deformations between the connected structural elements occur during load transfer. Particularly dowel connections exhibit this behavior since load transfer in dowel connection is based on the compliant embedment behavior of stiff steel dowels in wood.

The aim of this thesis is the development of a model for the calculation of multi-dowel connection slip curves and its application to typical design examples in timber structures.

Wood as a natural and renewable material is undoubtedly one of the oldest building materials. Impressive constructions have been made of wood even several hundred years ago. Later, the building material wood has mostly been replaced by other building materials like steel and concrete. New technologies and increasing environmental awareness may be two of several reasons for the revival of wood as building material. New design standard as well as more challenging timber constructions with wide spans request appropriate design methods. Therefore, the behavior of connections might significantly influence the distribution of internal forces and the deformation of timber structures. Moreover, compared to structural elements made of timber, connections can be designed as elasto-plastic elements in timber structures. This is particularly desired for energy dissipation in case of seismic loading. Consequently, a consistent formulation of the load-deformation relationship of connections is required as input for the structural analysis of timber structures. This is essential for a realistic model of force-redistributions in and corresponding deformations of a structure.

Since wood is a natural and anisotropic material, the connection behavior depends on the corresponding force-to-grain angle at the single dowels. Larger deformations are encountered perpendicular to grain than along the grain due to the weaker stiffness of wood perpendicular to grain. The mechanical behavior of wood and the characteristics of single-dowel connections are discussed in Chapter 2. The current standard for the design of timber structures ÖNORM EN 1995-1-1 (EC 5) [2] requests a realistic consideration of the connection compliance in the structural analysis. However, only limited and

simplified information on the load-deformation behavior of single connectors is given. In Chapter 2, different approaches for the determination of single-dowel slip curves are presented and compared to each other.

The mechanical behavior of multi-dowel connections and the current state-of-the-art of the calculation of slip curves of connections is discussed in Chapter 3. The corresponding modeling approach is based on dowel characteristics provided by EC 5. A drawback of this model is particularly the independent formulation of the strength of a connection and its deformations. Moreover, the dependence of the stiffness of connections on the loading direction is not considered.

Therefore, a novel model for the calculation of dowel connection slip curves, as developed in this thesis, is presented in Chapter 4. It is based on the behavior of single dowels as discussed in Chapter 3 and gives access to consistent deformation-reaction force relationships. Moreover, limit states of connections related to the maximum deformation of single-dowels can be illustrated. This gives access to the strength of connections in case of the interaction of internal forces. The model is also applied to back-calculate single-dowel forces and connection deformations for a specific set of internal forces. The application of different single-dowel slip curves as presented in Chapter 3 and its influence on the predicted behavior of dowel connections is discussed.

Thereon, model predictions for the behavior of typical dowel connections are given in Chapter 5. Design examples of centric and excentric connections as well as of dowel connections with contact behavior of the connected structural element are studied. Additionally, slip curves of typical connections for timber frame structures are analyzed. Finally, the influence of connection slip curves on the distribution of internal forces in and on deformations of a structure is assessed.

Even if the presented model for calculation of connections is discussed for dowels only, this model is generally applicable to all kinds of fasteners. Moreover, the model appropriately accounts for a combination of different types of fasteners within a connection, as shown by the design example including contact behavior.

# Chapter 2

## Single-dowel connections

In general, dowel connections consist of the timber members, the fasteners and for indirect connections of one or multiple connecting element(s), by means of steel plates, timber elements or any engineered wood products (Figure 2.1). Connections are called direct connections, in the case of a direct load-transfer between the timber elements, while for indirect connections a gusset plate is used to transfer the forces between the timber elements. This limited number of components makes the design and assembly process quite simple and enables a large number of variations. Position and size of the dowels can be chosen arbitrarily, in order to adjust the connection to the specific situation. Single fasteners transfer loads through embedment behavior in wood and bending of the dowel. Connections, composed of a group of fasteners, can be designed to transfer normal forces, shear forces and bending moments. This load-bearing characteristic makes the connection suitable for a wide range of purposes, like joints for beams, frame corners or connections between secondary and primary structure. The compliant behav-

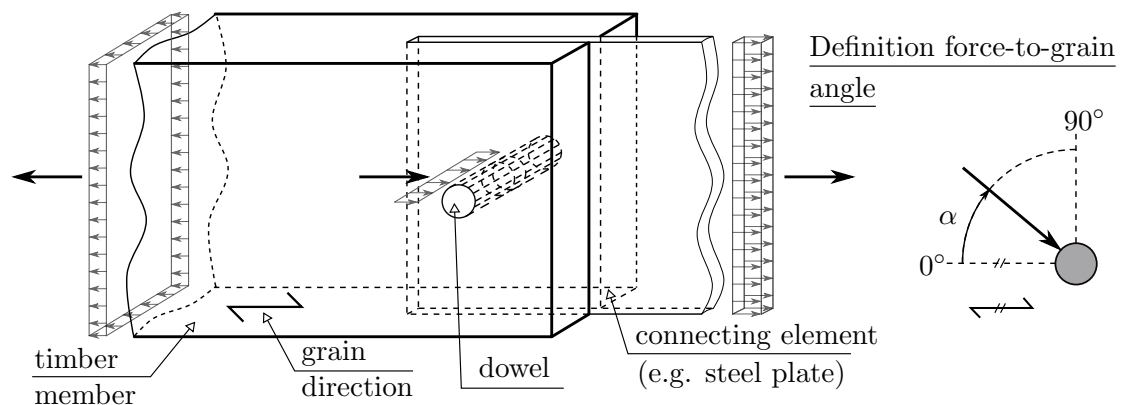


Figure 2.1: Typical single-dowel connection loaded in tension parallel to the wood fiber direction, and definition of the force-to-grain angle.

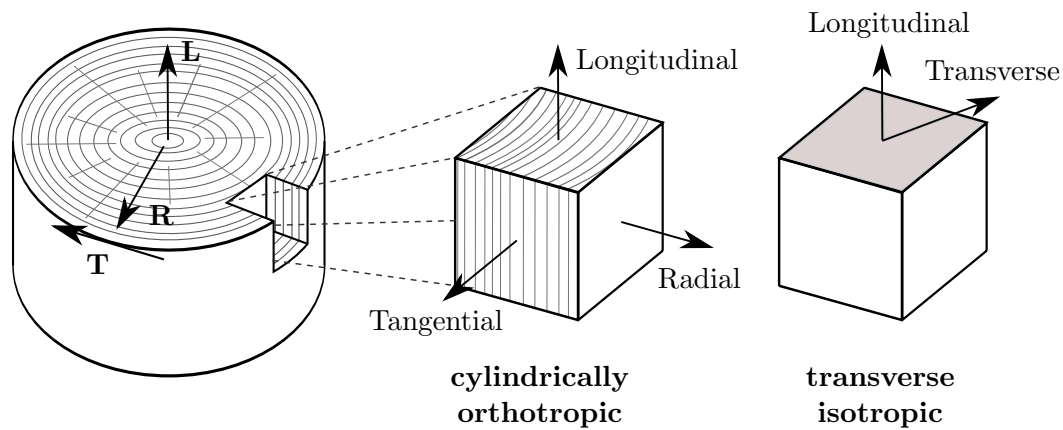


Figure 2.2: Principal material directions of wood in cylindrically orthotropic and transverse isotropic reference systems.

ior of dowel-type timber connections, i.e. the deformation characteristics during loading, requires special consideration in their design and the structural analysis of timber structures.

In the following, mechanical characteristics of the clear wood as well as of single-dowel connections are discussed in detail.

## 2.1 Mechanical behavior of clear wood

### Anatomy of wood

Wood is mainly composed of longitudinal (L), stem parallel hollow cells. These cells have the function to mechanically stabilize the tree structure and to provide pathways for water and mineral-transport. Simplified, the cell structure can be seen as a bonded, stem parallel bunch of fibers. This model makes it obvious that the mechanical properties of wood depend on the loading direction with respect to the grain direction. For example it is easier to deform this bunch of fibers in cross direction then in longitudinal direction. Additionally, wood properties are different within the cross sectional at plane. While in radial (R) direction (from pith to bark) cell walls of the fibers are straight, in tangential (T) direction cell walls are out of phase. Consequently, there is a difference in mechanical properties in radial and tangential direction. Furthermore, direction-dependency does not only take effect on mechanical properties, such as stiffness and strength, but also on moisture and temperature transport behavior.

### Anisotropy and inhomogeneity

As a result of the anatomical structure as discussed before, wood exhibits a strong direction-dependency of the mechanical properties as well as of the moisture and temperature transport behavior, i.e. it is anisotropic. Usually a cylindrical reference system with L-R-T axis is used, which indicates the longitudinal, radial and tangential direction

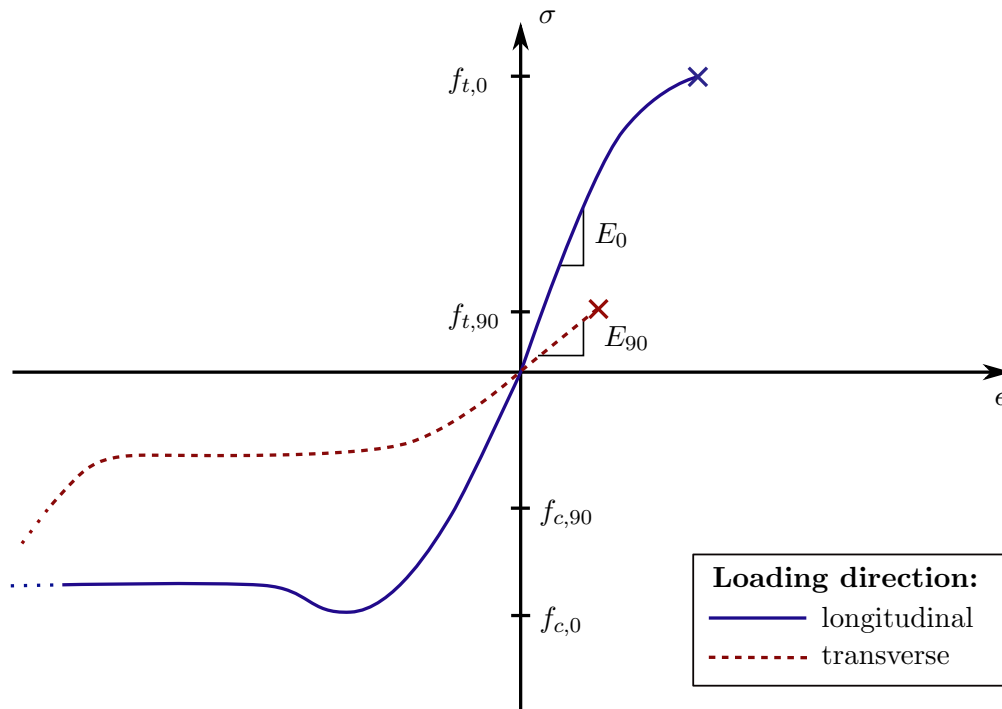


Figure 2.3: Stress-strain curves for clear wood under compression and tension for loading in longitudinal and transverse direction.

in the stem (see Figure 2.2). This special case of anisotropy is called orthotropy.

In order to simplify the mechanical properties of wood for the calculation of timber structures, most standards use the model of transverse isotropy. In this case, differences of the properties in radial and tangential direction are neglected. A transversely isotropic material exhibits one principal material directions, which is the longitudinal direction, and an isotropic plane perpendicular to it. The models presented in this thesis assume wood to be a transversely isotropic and homogenous material.

## Failure mechanisms

The anisotropy of wood leads to different failure mechanisms depending on the type of loading and the force-to-grain angle, while the inhomogeneity additionally causes the variation of these properties. Wood shows brittle failure under tension, both in longitudinal and transverse direction. While high stresses can be carried in longitudinal direction, in transverse direction, wood fails at a low stress level. Generally, brittle behavior is undesirable in structures, since failure occurs without warning and may lead to a collapse of the structure.

Compared to brittle behavior of wood under tension, the behavior in compression is different. In general, the response can be described as elasto-plastic. The material exhibits a ductile failure mechanism in longitudinal and transverse direction. As regards structures, this failure mode has the advantage of warning signs before collapse, such as

large visible deformations. Longitudinally stressed wood, indicated by 0, which denotes the force-to-grain angle, reacts approximately linear elastic until the peak load is reached. However, compared to wood under tension, further deformations are observed by approximately constant load. Increasing the force-to-grain angle changes the shape of the load-displacement curve. At the beginning, transverse loaded wood under compression also shows linear elastic but considerably softer behavior, followed by plastic plateau. At large deformation, a remarkable stress increase is observed. Figure 2.3 presents the different behavior of longitudinal and transverse properties of wood under compression as well as under tension. The bearing capacity is indicated by  $f$ . The first subscript is related to the type of loading, where  $t$  stands for tension and  $c$  for compression. The second subscript gives the loading direction (0 - for longitudinal and 90 - for transverse).

## 2.2 Mechanical behavior of single-dowel connections

Since loads between timber and steel dowel act on a small area compared to the total cross-section of the timber element, the load-carrying behavior of the connection strongly depends on the strength of the contact area. This local fictitious stress in wood is called embedment strength.

### Embedment behavior and embedment strength of dowels

According to DIN EN 383 [3] the embedment strength is defined as the fictitious stress at a dowel displacement of 5 mm or the maximum stress in case of failure before a displacement of 5 mm is reached. It is the stress that can be carried by the timber element when forces are transferred between the dowel and the timber element. The term fictitious stress is used since the embedment strength is specified as the interaction force between fastener and wood divided by the fictitious contact area, which is estimated by the fastener diameter times the fastener length.

According to the embedment strength definition of the current design standard for timber structures (EC 5), the embedment strength depends on the dowel diameter, the density of the wood and the force-to-grain angle. This simplified approach is of experimental origin, and neglects parameters like the dowel roughness and the roughness of the bore-hole, which do not influence the embedment strength itself, but the shape of the load-deformation curve of the embedment behavior. In general, increasing roughness of the dowel increases the ductility of the interaction single dowel - wood, since the failure mode may change from lateral splitting to shear failure of wood. Additionally, the roughness of the bore-hole strongly influences the initial stiffness of the embedment configuration. These effects are discussed in detail in [8].

Basically, the load-deformation behavior of the single dowel slightly differs from the behavior of clear wood. The embedment strength and corresponding deformations depend on the force-to-grain direction. In the following, the embedment behavior is discussed in detail for loads parallel to the grain as well as perpendicular to the grain, and illustrated in Figure 2.4.

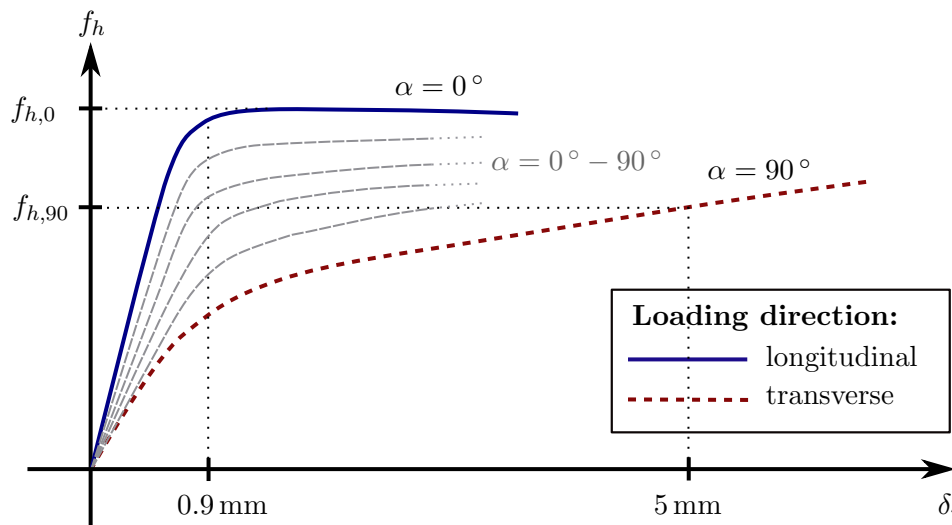


Figure 2.4: Embedment behavior (slip curve) of single dowels for loading in longitudinal and transverse direction.

**Loading in grain direction:** The load-carrying characteristic is similar to the one of clear wood, but the embedment strength is only about 60 % of the strength of wood, since the real contact area is approximately 60 % of the fictitious contact area, which is used to calculate the embedment strength. Simplified, the load-deformation curve can be described as bi-linear curve. The first part describes the linear-elastic part of the embedment behavior. As illustrated in Figure 2.4, the transition for an elastic to an approximately ideally plastic behavior takes place at a displacement of about 0.9 mm (cf. [6] and [9]).

**Loading perpendicular to the grain direction:** In addition to the effect of hardening of the sound wood at large deformations (see Section 2.1), the so called rope effect leads to a remarkable increase of the embedment stress at the stage of plastic deformations, until the strength of the grain parallel loaded wood is reached. The increasing embedment stress caused by the rope effect is based on the activation of the wood perpendicular to the loading direction. While large deformations in loading direction occur beneath the fastener, the surrounding wood can be considered to behave elastic. This causes tension stresses in fiber direction, since the deformations perpendicular to the fiber direction elongates the wood fibers. As illustrated in Figure 2.4, the embedment behavior perpendicular to the grain is significantly softer than in grain direction. The elastic limit is approximately reached at the same deformation level like for grain parallel loading. Compared to longitudinally loaded wood, plastic deformations lead to a remarkable increase of the embedment forces, due to the effect of hardening and the rope effect (cf. [6] and [9]).

**Loading at an arbitrary force-to-grain angle:** The stress-deformation behavior in case of loading at an angle to the grain lies in-between the longitudinal and perpendicular to grain behavior. According to EC 5, the embedment strength for loads under an angle between  $0^\circ$  and  $90^\circ$ , follows a S-shaped curve. Depending on the material, the

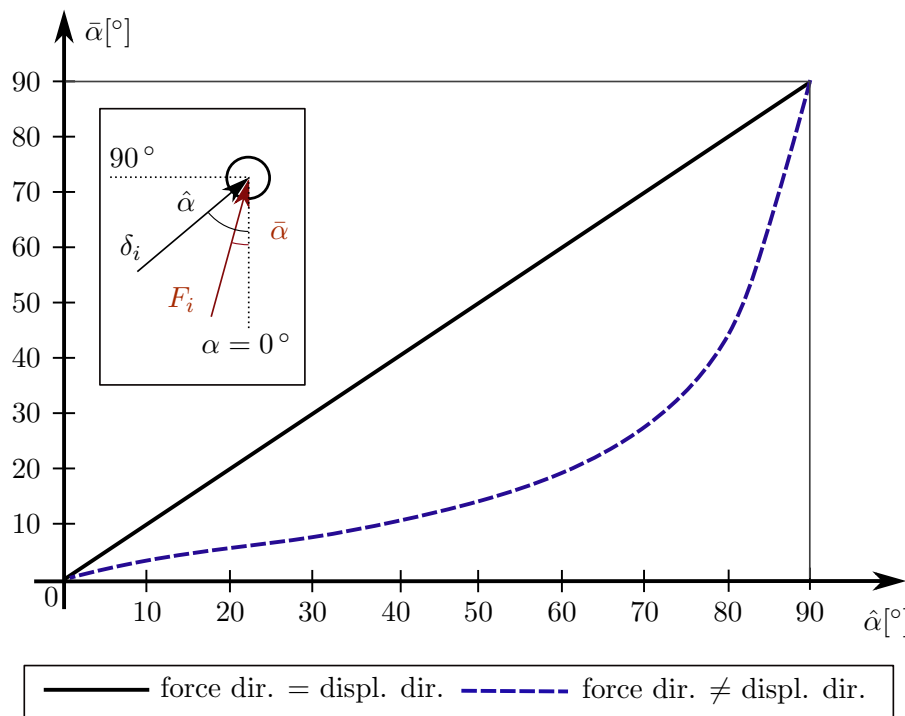


Figure 2.5: Relationship between the displacement direction  $\hat{\alpha}$  and the force direction  $\bar{\alpha}$  of a loaded single-dowel related to the grain direction  $\alpha$ , according to [17].

embedment strength perpendicular to the grain direction is reduced to approximately 2/3 of the embedment strength parallel to the grain.

This design approach has been verified by several test, e.g. Bleron et al. [6] conducted experimental tests with single-dowel joints loaded at different angles (for North fir specimens). The results were further used as data basis for a FEM model. Compared to these experimental tests the model used in EC 5 gives realistic but weakly overestimated values. They also highlighted in their experiments that the direction of the displacement of the dowel is not collinear with the resultant force on the dowel, with the exception of loading under  $0^\circ$  or  $90^\circ$ . Furthermore, experiments and simulations related to the behavior of dowel-type connections for loads under an arbitrary angle have been conducted by Pederson et al. [18] and by Yasumura et al. [21]. The same characteristic has been observed in FEM-analysis of dowel-type connections in [16] and in [17] (see Figure 2.5).

While the embedment strength is defined as the maximum stress during the test or as stress at a deformation of 5 mm, and is therefore only one point of the load-deformation curve, also the deformation behavior from the initial load up to failure is of interest. This has been studied for LVL products of New Zealand timber by Franke et al. [9], for European hardwoods by Hübner et al. [11] and for Shorea obtusa (a tropical hardwood) by Awaludin et al. [4]. Since the design formulas of EC 5, relating to the determination of the embedment strength, are based on substantial and fundamental experiences with softwood species, the aim of these papers is to provide design approaches for the investigated materials. Therefore, experimental results have been compared to the design

formulas of EC 5, and if necessary modified design approaches were proposed.

The different shapes of the load-displacement curves (see Figure 2.4) are caused by different failure modes for different force-to-grain angles as described previously. Experimental and theoretical analysis of the different failure modes have been done by Minoru Masuda and Kei Tabata [15]. For this purpose, the Digital Image Correlation method (DIC) and the Finite Small Area Fracture Criterion (FSAFC) have been used. In case of loading parallel to the grain large shear strains were observed as the dominant reason for failure. Fracture in mixed mode of tension and shear was observed in case of a force-to-grain angle of  $10^\circ$ . In case of larger angles, tension perpendicular to the grain was found to govern failure.

### Steel properties of dowels

In general, conventional steel of average quality (e.g. S235) is used for dowel fasteners. Usually electrogalvanized, cylindrical steel bolts are applied. Their strength is described by the characteristic yield stress  $f_{y,k}$  and the ultimate stress  $f_{u,k}$ . Up to the stress level of  $f_{y,k}$ , steel exhibits a linear-elastic behavior. This is followed by yielding and consecutively hardening of the steel until the stress level of  $f_{u,k}$  is reached. Further increase of deformations leads to decreasing stresses, until brittle failure. It should be mentioned that the description of the stress-deformation behavior considers the stress to be calculated by division of the loading by the initial cross section of the steel bolt. Concluding, steel bolts show a highly ductile behavior with increasing strength in the plastic state.

### Bearing capacity of single-dowel connections - Johansen formulas

Design formulas for the load-bearing capacity of dowel-type timber connections were first developed by Johansen [12]. This approach forms the basis for most design codes such as EC 5. Based on the assumptions of ideal-plastic behavior of wood under compression and of the dowels in bending, he studied the load-bearing mechanisms of timber-to-timber connections for dowels in single shear as well as in double shear connections. Johansen derived design rules by formulating equilibrium of forces and moments. For bolt connections the tensioning of the bolt (rope effect of the bolt) according to EC 5 was not considered. Kinematic constraints were also neglected. The assumptions of plasticity of the wood and the dowels as well as the derived formulas were verified by tests. Assuming ideal-plastic behavior of the wood and of the dowel makes it impossible to calculate the deformation of the connection at the level of the bearing capacity. However in current standards, Johansen's equations are used for all kinds of metal fasteners loaded in shear, such as dowels, bolts, nails and screws.

## Influence parameters on the bearing capacity of single-dowel connections

In this subsection, main influences on the bearing capacity of single-dowel timber-to-timber or timber-to-steel connections, are discussed. Based on the observations of Johansen, different failure modes have to be considered. The specific failure mode governing the strength of a specific connection is mainly influenced by the ratio of dowel diameter to side member thickness, as well as by wood quality, dowel diameter and steel quality. Depending on these parameters, translation of the dowel in case of embedment failure of wood, and bending of the dowel, which leads to plastic hinges in the metal fastener, may occur. For single shear connections, rotations of the dowel are possible. All failure modes are based on ductile behavior of the dowel as well as of the wood under compression.

- **Dowel diameter:** Increasing the dowel diameter leads to an increased resistance of the dowel. This means that the dowel gets stiffer compared to the side members, which ends up at an increased contact area between the dowel and wood, since the contact length and width increase. In consequence, higher loads can be transferred.
- **Steel quality:** Changes in steel quality of the dowel have similar effects like changes of the dowel diameter. Higher steel quality means higher yield and ultimate strength, which leads in the case of failure modes with plastic hinges, to an increased bearing capacity of the connection, since plastic hinges develop at higher stress levels.
- **Wood quality:** Since the embedment strength, expressed as force by area, depends on the density of the wood, increased density leads to an increased embedment strength and stiffness of the connection. In consequence, in case of constant side member thickness and increasing embedment strength, the first plastic hinges develop at a lower deformation level.
- **Side member thickness:** A small side member thickness gives a high ratio between dowel and side member stiffness. With increasing side member thickness the bearing capacity of the connection increases linearly, as long as no plastic hinges at the dowel are obtained. Further increase of the side member thickness leads to bending of the dowel and the formation of plastic hinges. The bearing capacity stays constant even for higher side member thicknesses as soon as the maximum number of plastic hinges in the dowel are formed.

Illustrations of the described failure modes, by means of a double-shear steel-to-timber connection, are given in Section 2.5, where a parameter study of the single-dowel behavior is conducted.

## 2.3 Design according to EC 5

Several models presented in the thesis at hand are based at least partially on the current design code EC 5. In this section a design guideline for double-shear steel-to-timber connections, including stiffness and strength determination, is discussed.

### Stiffness of single-dowels

According to EC 5, the stiffness up to the Serviceability Limit State (SLS) of dowel-type fasteners, like dowels, bolts, screws and pre-drilled nails, is estimated as

$$K_{ser} = \rho_m^{1.5} d / 23, \quad (2.1)$$

where  $K_{ser}$  is the slip modulus per shear plane in N/mm,  $\rho_m$  the mean density of the wood in kg/m<sup>3</sup> and  $d$  the dowel diameter in mm. Since this slip modulus  $K_{ser}$  is given for timber-to-timber connections, for steel-to-timber connections,  $K_{ser}$  should be based on  $\rho_m$  for the timber member and be multiplied by a factor of 2.0.

The slip modulus  $K_u$  as the secant modulus up to the Ultimate Limit State (ULS) can be derived from

$$K_u = 2/3 K_{ser}, \quad (2.2)$$

with  $K_u$  and  $K_{ser}$  in N/mm. The inconsistency in units in Equation (2.2) underlines the empirical origin.

### Strength of single-dowels

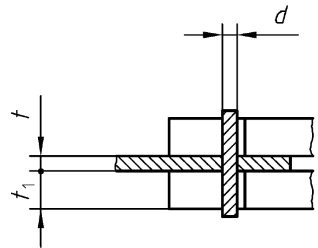
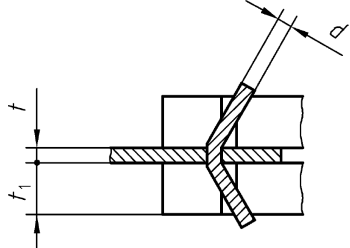
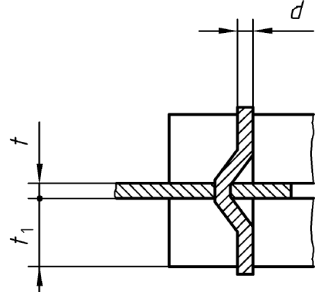
The determination of the load-carrying capacity of single dowels follows the rules of Johansen. Depending on the connection configuration, different failure modes in a single fastener from a rigid dowel and embedment failure up to the development of several plastic hinges are possible. As an example, Table 2.1 shows the determination of the load-carrying capacity  $F_{v,Rk}$  for a double-shear dowel-type steel-to-timber connection according to EC 5.

The characteristic load-carrying capacity is the minimum of all potential failure modes:

$$F_{v,Rk} = \min \{F_{v,Rk}(f), F_{v,Rk}(g), F_{v,Rk}(h)\}, \quad (2.3)$$

where  $F_{v,Rk}$  is the characteristic load-carrying capacity of one fastener for one shear plane in Newton. Lines in Table 2.1 [(f), (g) and (h)] are related to the possible failure modes according to EC 5, where failure mode (f) describes fasteners without formation of a plastic hinge, (g) describes a fastener with one plastic hinge and (h) a fastener with one plastic hinge in the middle and two additional ones located in the side members.

Table 2.1: Load-carrying capacity  $F_{v,Rk}$  for a double-shear dowel-type steel-to-timber connection, based on EC 5.

load-carrying capacity	failure mode	
$F_{v,Rk} = f_{h,\alpha,k} t_1 d$	(f)	
$F_{v,Rk} = f_{h,1,k} t_1 d \left[ \sqrt{2 + \frac{4M_{y,k}}{f_{h,\alpha,k} d t_1^2}} - 1 \right]$	(g)	
$F_{v,Rk} = \sqrt{2} \sqrt{2M_{y,k} f_{h,\alpha,k} d}$	(h)	

In the formulas of Table 2.1,  $f_{h,\alpha,k}$  stands for the characteristic embedment strength under a specific force-to-grain angle of one fastener in  $\text{N/mm}^2$ . This can be calculated by

$$f_{h,\alpha,k} = \frac{f_{h,0,k}}{k_{90} \sin^2 \alpha + \cos^2 \alpha}, \quad (2.4)$$

where  $f_{h,0,k}$  is the characteristic embedment strength parallel to grain, in  $\text{N/mm}^2$ , and  $k_{90}$  is a factor that takes into account the type of material. These two values can be calculated as

$$f_{h,0,k} = 0.082(1 - 0.01d)\rho_k \quad (2.5)$$

and

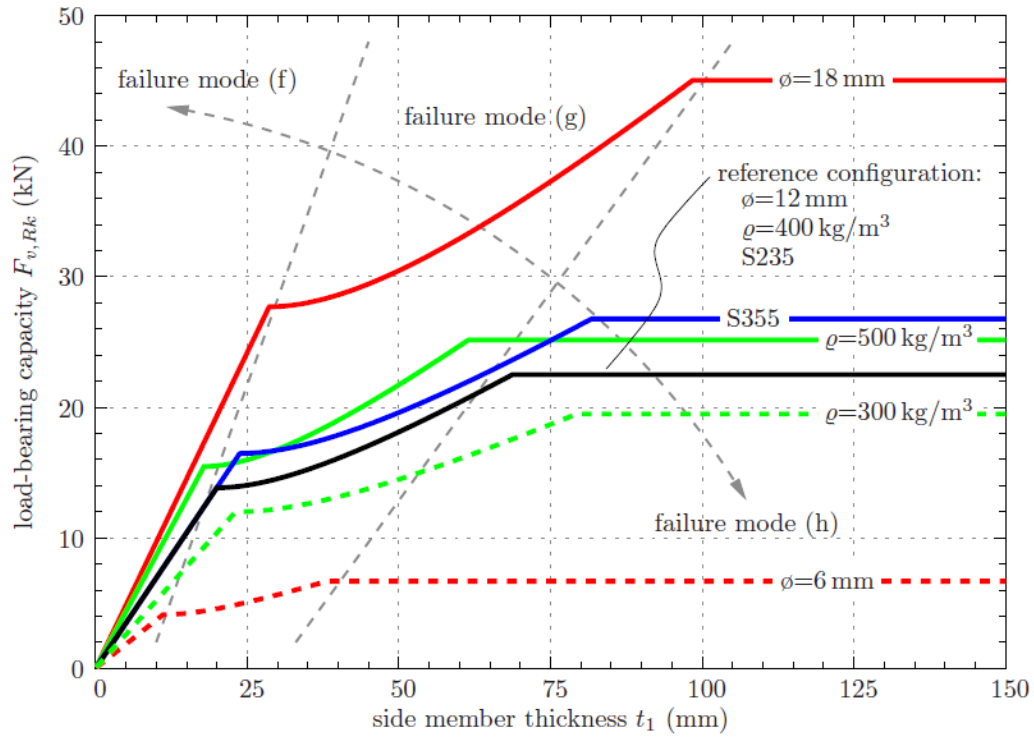


Figure 2.6: Load-carrying capacity  $F_{v,Rk}$  for double-shear single-dowel steel-to-timber connections according to EC 5 for a variation of wood density, dowel diameter, and steel quality, depending on the connection width [8].

$$k_{90} = \begin{cases} 1.35 + 0.015d & \text{for softwoods} \\ 1.30 + 0.015d & \text{for LVL} \\ 0.90 + 0.015d & \text{for hardwoods} \end{cases} \quad (2.6)$$

where  $d$  is the dowel diameter in mm and  $\rho_k$  the characteristic density of the wood in  $\text{kg/m}^3$ . Further in Table 2.1,  $t_1$  indicates the side member thickness in mm and  $M_{y,Rk}$  the characteristic plastic moment of the dowel in Nmm, which is calculated as

$$M_{y,Rk} = 0.3f_{u,k}d^{2.6}, \quad (2.7)$$

with  $f_{u,k}$  as the characteristic tensile strength of the dowel in  $\text{N/mm}^2$ . Again, the inconsistency of the units in the formulas underlines their empirical origin.

Figure 2.6 visualizes the main influence parameters for the load-carrying capacity  $F_{v,Rk}$  of double-shear single-dowel steel-to-timber connections. It is based on EC 5 formulas and shows the dependence on wood density, dowel diameter, steel quality and connection width.

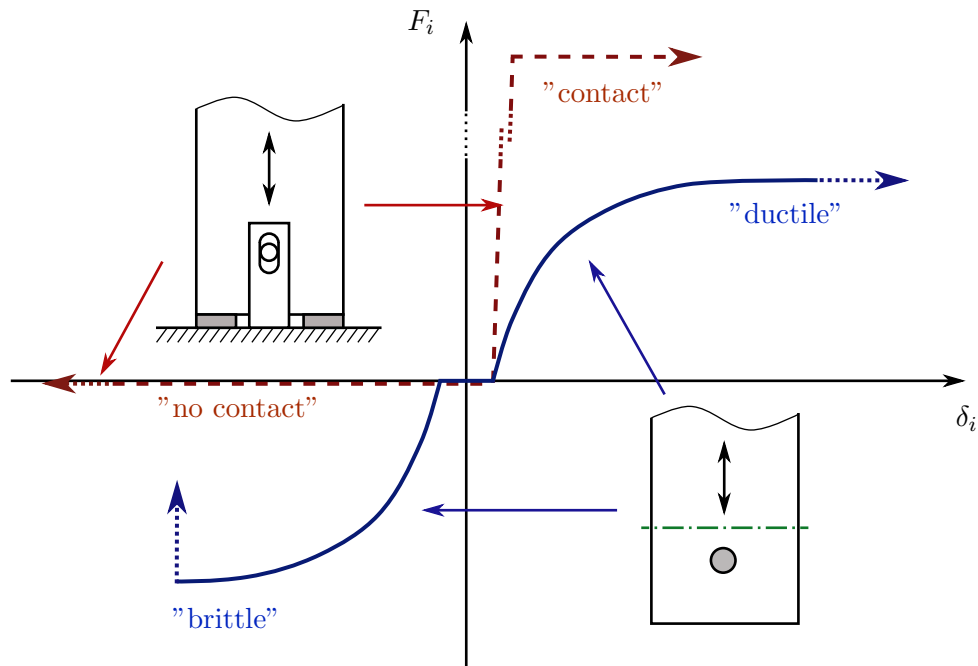


Figure 2.7: Single-dowel slip curves for a contact condition (red, dashed line) and a single-dowel connection (blue, continuous line).

## 2.4 Single-dowel slip curves as input for the calculation of connections

Besides geometric properties and global settings, single-dowel slip curves are the main input parameters for the calculation of the global slip curves of multi-dowel connections. The characteristic shape of single-dowel slip curves is illustrated in Figure 2.7. This section focuses on the different calculation approaches of single-dowel slip curves, which are used in this thesis. First, different approaches for the calculation of single-dowel slip curves are discussed in detail, followed by, a comparison between simplified single-dowel slip curves based on EC 5 and more realistic single-dowel slip curves calculated by means of a commercial structural analysis software. Two parameter studies are conducted for this purpose.

Figure 2.7 illustrates asymmetric single-dowel slip curves for two typical situations. The red, dashed line describes the behavior of a hinged column base. In the case of uplifting forces no forces can be transmitted (left part of the slip curve  $\rightarrow$  negative displacement). In the opposite direction, the connection acts as a stiff element, which transmits high forces (right part of the slip curve  $\rightarrow$  positive displacement).

The blue, continuous line illustrates the behavior of a single-dowel connection. Forces in the one direction may cause brittle failure by means of splitting (left part of the slip curve  $\rightarrow$  negative displacement). Forces in the opposite direction may lead to a ductile embedment failure in case of reinforced dowels (right part of the slip curve  $\rightarrow$  positive displacement).

### 2.4.1 Description of calculation methods

First, two methods based on information given in EC 5 are discussed. Since the standard only gives specifications related to the bearing capacity and the elastic (partly plastic) stiffness of the single dowel, but no load-consistent deformation behavior, assumptions for the development of plastic deformations are required. As a third method, the calculation by means of a sub-model using a structural analysis software is presented. In this case, only the embedment strength according to EC 5 is used as input, while the corresponding deformations of the wood are assumed based on experiments well documented in literature (see Section 2.2). Furthermore, contact behavior of single elements in a connection and the corresponding slip curve is discussed.

In this thesis, the following methods are used to determine single-dowel slip curves (see Table 2.2):

- Simplified method based on EC 5:** The determination of single-dowel slip curves follows the principles of EC 5 discussed in Section 2.3. A tri-linear curve is assembled by the elastic part (first section), a zone related to the change from elastic to plastic behavior (second section) and the horizontal plastic plateau (third section). The gradient of the elastic section is equal to the stiffness  $K_{ser}$  according to EC 5. The sketch of the slip curves in Table 2.2 highlights the independence of the connection-stiffness from the force-to-grain angle according to EC 5. The elastic limit is assumed to be the bearing capacity of the single-dowel divided by a factor of 1.4. Since EC 5 gives no information about the maximum elastic loading, the elastic limit is assumed to be the bearing capacity of the single-dowel divided by the arithmetic mean of the partial factors  $\gamma_G$  and  $\gamma_Q$ , which is 1.4. Compared to the stiffness, the bearing capacity of the single-dowel depends on the force to grain angle. The change to plastic behavior is estimated by calculating the stiffness at the ultimate limit state  $K_u$  and the bearing capacity. This point is connected to the end of the elastic section. For the calculation of the bearing capacity itself, formulas according to EC 5 are used. The different formulas are related to different failure modes. The maximum displacement of the single dowel is assumed to be twice the dowel diameter. This restriction of maximum deformation of single dowels is done for all single-dowel slip curves presented in this thesis.
- Advanced method based on EC 5:** The slip curves are again based on the information available in EC 5. However, additional assumptions on the load-deformation behavior are considered for a more realistic model that accounts for the anisotropic material properties of wood. These assumptions are valid for a single-dowel connection that fails due to embedment failure. An extension to failure modes related to plastic deformations in the steel dowel would be possible. Again a tri-linear curve is used. Compared to the first method, not only the elastic limit but also the stiffness is considered to depend on the force-to-grain angle. In this method, the elastic section is assumed to end at a displacement of 0.9 mm. The maximum elastic force is the bearing capacity reduced by the factor considering the direction dependency of the bearing capacity according to EC 5. For force-to-grain angles unequal to  $\alpha = 0^\circ$  the rope effect and hardening is assumed,

which leads to an increase of the connection strength until the bearing capacity of a longitudinal loaded wood is reached. This is assumed to be the case at a deformation of 1.5 times the dowel diameter. The maximum displacement considered herein, is again twice the dowel diameter. The assumptions related to the displacement limits of 0.9 mm, 1.5  $\phi$  and 2.0  $\phi$  are based on experiments documented in literature (see Section 2.2).

- **Single-dowel slip curves determined by means of a sub-model:** The slip curves are derived from a sub-model with the principle load-deformation behavior of wood and steel dowel as input for a model of the specific dowel configuration. The corresponding slip curves are characterized by a nonlinear shape. The calculation is done by means of a commercial structural analysis software. The shape of the curve depends on the configuration of the connection, and therefore, differs for each connection. A detailed description of the sub-model is given in Section 2.4.2.
- **Contact condition:** The contact condition describes a situation where the connection acts in one deformation direction as stiff element transmitting high forces, while no forces can be carried in opposite direction. This is considered by a single-dowel slip curve with an asymmetric (load-direction dependent) curve. In one direction, a stiffness equal to zero, and in the other displacement direction, an extremely high stiffness is used. An example of a contact condition is illustrated in Figure 2.7.

#### 2.4.2 Determination of single-fastener slip curves for dowel connections by means of commercial structural analysis software

EC 5 as the current design code for timber structures demands a realistic consideration of the connection stiffness in the structural analysis. However, only limited and simplified information on the behavior of single dowels is given. The numerical model for single dowel joints, as presented in [10], allows to calculate realistic slip curves for dowel-type single-fasteners by means of commercial structural analysis software. The advantages of the model over formulas provided by EC 5 lies in its high flexibility according to the configuration of the connection and its connection members. It is based on the characteristic behavior of wood under embedment loading and on the elasto-plastic behavior of steel dowels. Furthermore, the elastic limit can be deduced as well as the load-deformation curve for different force-to-grain angles. Both, the elastic limit and the characteristic of the load-deformation curve cannot be determined by the European yield model of EC 5, since the design formulas do not provide consistent deformations. Additionally, the model visualizes failure mechanisms which supports the engineer in the optimization of the connection.

#### Description of the sub-model for single-dowel slip curves [10]

**Model of the embedding behavior of wood:** The basic elements of the model are presented in Figure 2.8. The first group of elements includes the vertical couple-beams,

Table 2.2: Single-dowel slip curves used as input for models of connections.

Method	Description	Single-dowel slip curve ( <i>Only one side of the slip curve is shown</i> )
1	<b>Simplified method based on EC 5</b> stiffness independent ( $K_{ser}$ , $K_u$ ); bearing capacity dependent on the force-to-grain angle according to EC 5	
2	<b>Advanced method based on EC 5</b> stiffness assumed to depend on the force-to-grain angle; bearing capacity (based on EC 5) assumed to be independent on the force-to-grain angle	
3	<b>Slip curve determined by a sub-model</b> The determination of the slip curves by means of a commercial structural analysis software is shown in Subsection 2.4.2. The slip curves are adjusted for a specific single-dowel connection	
4	<b>Contact condition</b> The contact condition describes a situation where the connection acts in one deformation direction as stiff element transmitting high forces, while no forces can be transmitted in opposite direction. (Only the stiff side is shown.)	

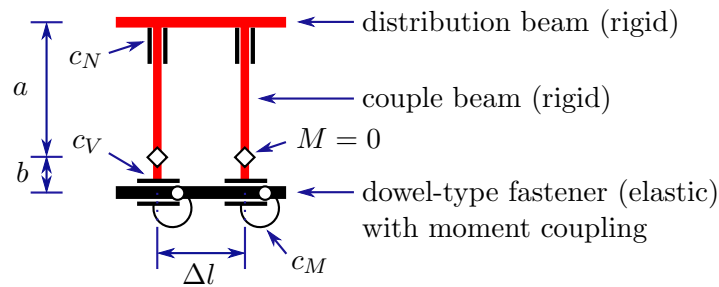


Figure 2.8: Basic elements of the model according to [10].

the spring stiffnesses  $c_N$  and  $c_V$  as well as the hinge. These elements are used to model the embedment behavior of wood.

- **Couple beams:** Represent the support of the fastener in the wood matrix. Its main purpose is to host the different springs representing the embedment situation.
- **$c_N$  :** On the top of the couple beams, springs with nonlinear load-deformation behavior are situated. These springs stand for the embedment properties perpendicular to the fastener axis. The ultimate load of this spring is calculated according to the formulas for embedment strength as given at EC 5. The proportionality limit is assumed to be at a deformation of 0.9 mm. Wood loaded in grain direction is assumed to reach the ultimate load at this deformation. For other force-to-grain angles the force is reduced by the EC 5 specifications according to Equation (2.4). In these situations, further loading leads to hardening of the wood, until the ultimate limit is reached at an deformation of  $1.5 \phi$ . The maximum deformation is reached at a displacement of two times the fastener diameter. In summary, the load-deformation behavior of wood is considered as discussed in the second method presented in Table 2.2.
- **Moment hinge:** The moment hinge allows an adaptation of the embedment zone in case of bending deformations of the fastener, whereby embedment forces remain parallel or transverse to the fastener axis, respectively.
- **$c_V$  :** The shear-force-hinges are considered at the intersections of the couple beam with the fastener. The spring stiffness  $c_V$  is used to model the embedment properties in axial direction. Depending on the surface roughness of the fastener, a corresponding spring stiffness may be chosen. For conventional dowels with a smooth surface the friction between dowel and wood can be neglected. In this case,  $c_V$  is equal to zero.

**Model of the plastic rotation of the dowel-type fastener:** The plastic moment-rotation behavior of the fastener itself is modeled by means of nonlinear torsional springs  $c_M$ . In order to model a continuous bending line, the fastener is divided into several beam sections, which are connected by nonlinear springs. The elastic deformation of the dowel is represented by the bending-stiffness  $EI$  of the fastener itself.

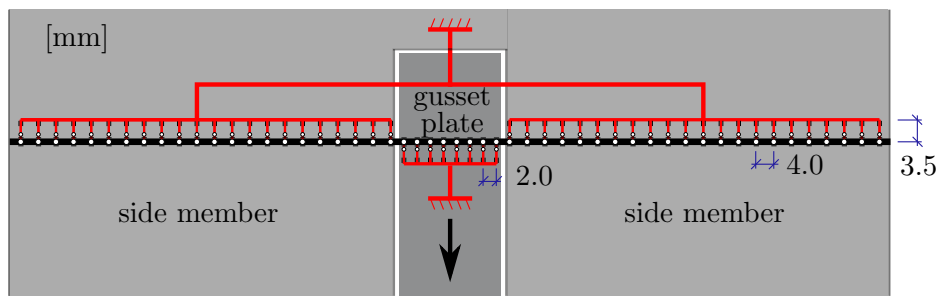


Figure 2.9: System of structural analysis model (sub-model).

**Modeling of the connection members:** Since elastic and plastic deformations are concentrated mainly in the very narrow contact-area between fastener and wood, the wood matrix outside of this load transmission zone can be assumed to be rigid. Therefore, the embedment forces, transferred by the vertical couple beams presented before, are connected to a fastener-parallel rigid beam. This beam itself is fixed at the axis of the connection member, where the member forces of the connection can be recorded.

## 2.5 Parameter study - single-fastener slip curves

Two different parameter studies on single-dowel slip curves determined by means of the structural analysis model presented in 2.4.2, are discussed for a typical single-dowel connection. The properties of the connection are illustrated in Figure 2.8 and the corresponding model is shown in Figure 2.9.

Since the reaction forces as a result of deformations can be recorded, slip curves are generated for force-to-grain angles of  $0^\circ$  and  $90^\circ$  for a reference condition. Furthermore, the failure mode as well as the bearing capacity are studied for different dowel-stiffnesses and side member thicknesses. The collected data are compared to the values calculated by EC 5 formulas. Finally, the elastic limit is determined and compared to the approximate approach suggested in Section 2.4.1, where the elastic limit is assumed to be the ultimate load divided by 1.4. Moreover, it should be mentioned that several wood properties are based on mean values.

### 2.5.1 Structural analysis model for single-dowel connection

For the structural analysis model of single dowel connections, the commercial structural analysis software RSTAB (Ing. Dlubal GmbH, Germany) has been used (see Figure 2.9). The two outer groups of elements, consisting of couple beams and springs ( $c_N$ ,  $c_V$ ) represent the embedment behavior of the dowel perpendicular and parallel to the dowel axis, respectively. The group in the middle illustrates the gusset plate, where again springs ( $c_N$ ,  $c_V$ ) are situated, which represent the embedment behavior of the dowel in the steel plate. The horizontal chain of beams, connected by torsion springs, models the dowel itself. With respect to the notation in Figure 2.8, the length of the couple beam between the spring  $c_N$  and the moment hinge  $a=2.7$  mm, and the distance between

Table 2.3: Configurations used for the parameter study, related to the variation of dowel stiffness.

Notation	dowel diameter $d$ [mm]	failure mode
$M_{pl,1}$	40	rigid dowel (mode $f$ in EC 5)
$M_{pl,2}$	20	one plastic hinge in the dowel (mode $g$ in EC 5)
$M_{pl,3}$	16	reference configuration (between $g$ and $h$ in EC 5)
$M_{pl,4}$	12	two plastic hinges in the dowel (mode $h$ in EC 5)

moment hinge and the spring  $c_V$   $b=0.8$  mm have been chosen. One element of the dowel beam chain exhibits a length of 4.0 mm at the wooden side member parts, and a length of 2.0 mm at the gusset plate.

Since the dowel shows a smooth surface, no forces are considered parallel to the dowel axis. The slip curve representing the embedment situation has been determined according to EC 5, as described in Section 2.4.2. The torsion spring is based on the moment-rotation curve for dowels according to [5].

The single dowel is loaded by means of a displacement perpendicular to the dowel axis at the bearing of the gusset plate. The reaction force can then be recorded as vertical supporting force of the two wooden side members, bounded together in the middle of the connection. The other supporting forces are equal to zero, since the loading and geometry is symmetric to the connection.

### 2.5.2 Variation of dowel stiffness

For loadings in and perpendicular to the grain, the stiffness of the dowel is continuously changed. Consequently, a transition from a rigid dowel to failure modes with plastic hinges is modeled. In order to vary the stiffness of the dowel, the dowel diameter is changed. Therefore, the elastic stiffness of the dowel changes. The plastic moment-rotation behavior is varied by adapting the slip curve of the torsional spring. In order to highlight only the influence of the dowel stiffness on the behavior of the single dowel, the embedment behavior perpendicular to the dowel axis is constant.

In total, 13 variations with dowel diameters between 8.0 mm and 60 mm are investigated. Three representative configurations, related to the three possible failure modes, and the reference configuration have been chosen for detailed discussion and for comparison of the results with a simplified model according to EC 5. The notation of these four configurations and the related dowel diameter as well as the failure mode are given in Table 2.3, where the stiffness of the dowel decreases from  $M_{pl,1}$  to  $M_{pl,4}$ . The failure modes differ in the number of plastic hinges in the dowel. Dowels of high stiffness are rigid (failure mode  $f$  in EC 5), which means forces can be transferred into the wood along the entire dowel. Decreasing stiffness of the dowel leads to one (failure mode  $g$  in EC 5) or two plastic hinges in the steel dowel (failure mode  $h$  in EC 5) and, as a result, to a decreasing contact area between dowel and wood. Consequently, increasing stiffness of the dowel increases the bearing capacity of the single-dowel connection.

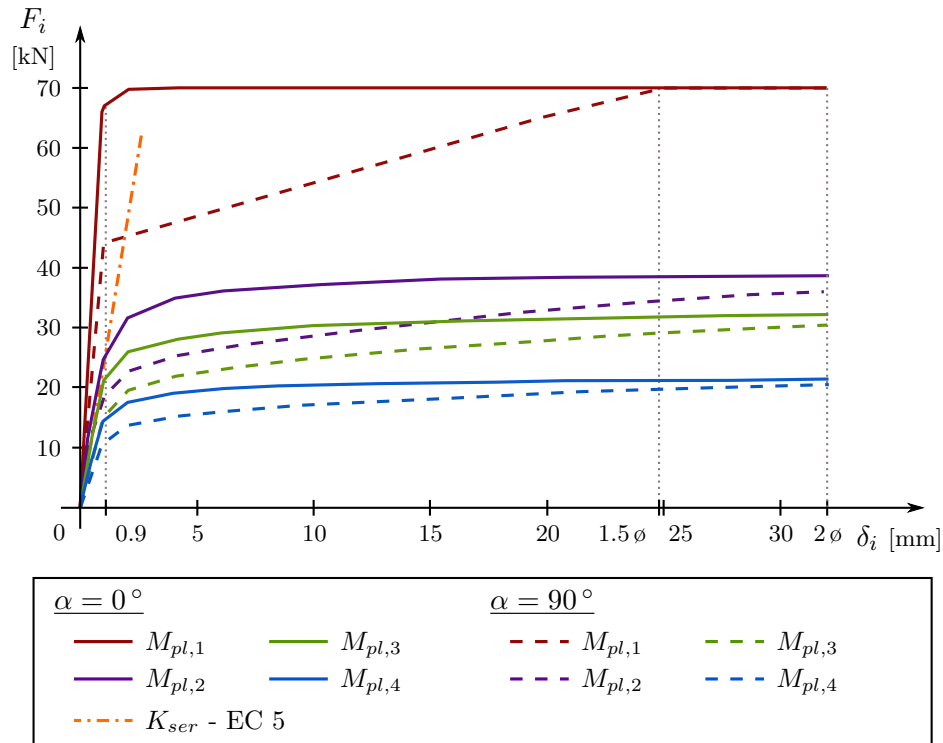


Figure 2.10: Slip curves for different dowel stiffnesses ( $M_{pl}$ ) for force-to-grain angles of  $\alpha = 0^\circ$  and  $\alpha = 90^\circ$ .

The corresponding slip curves are shown in Figure 2.10 for four configurations. The continuous lines are related to loading in grain direction, the dashed ones to loading perpendicular to the grain direction. Further, the dash-dot line stands for the stiffness  $K_{ser}$  according to EC 5. It should be highlight that the estimation of  $K_{ser}$  is based on the dowel diameter of the reference configuration ( $d=16$  mm).

The shape of the slip curve for the stiffest dowel ( $M_{pl,1}$ ) is equal to the shape of the embedment curve, since no plastic deformations develop in the dowel. For  $\alpha = 0^\circ$ , an almost linear elastic - ideal plastic behavior is found. The insignificant deviation from the embement curve at a deformation of 0.9 mm results from elastic bending of the dowel. This means that the embedment loading of wood behaves partly elastic and partly plastic. This deviation cannot be seen in the slip curve for  $\alpha = 90^\circ$ , because the ratio of stiffness of the dowel to stiffness of the wood is considerably higher, which leads to almost no bending of the dowel and, consequently, to a failure mode  $f$  according to EC 5.

The other curves in Figure 2.10 are related to the failure modes with one or two plastic hinges. Since the shape of these curves is similar for both modes, only a general description is given. The load-deformation behavior is characterized by non-linearity. The shape is mainly a result of the shape of the plastic moment-rotation relationship of the steel dowel, since the first plastic zone develops at approximately  $u = 0.2$  mm. The following reduction of the stiffness of the interaction dowel-wood is caused, on the one hand, by the change from elastic to plastic behavior of wood (approximately at

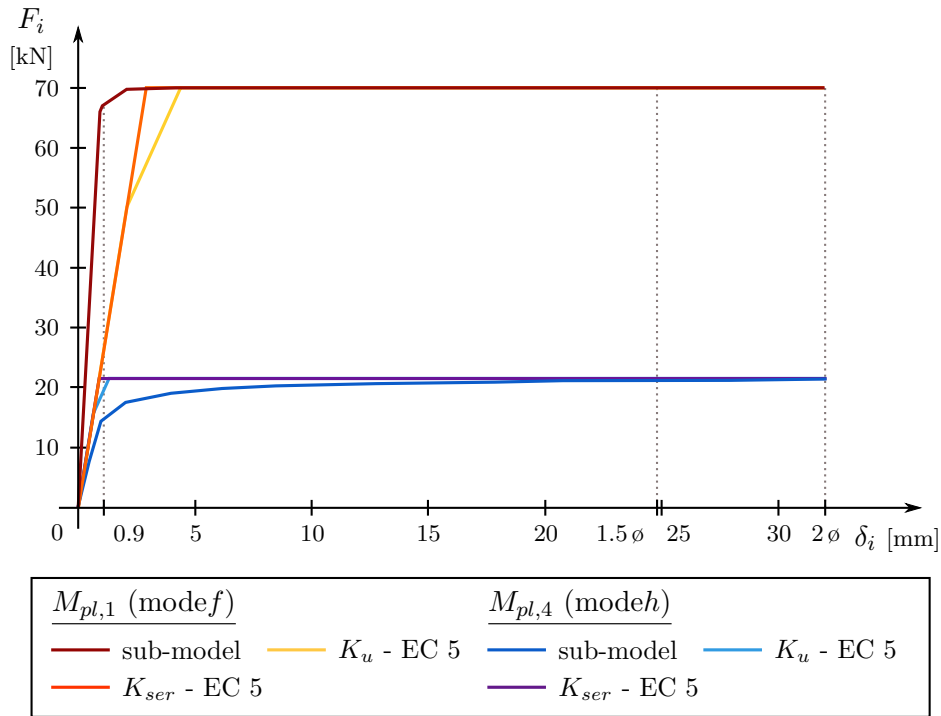


Figure 2.11: Comparison of the sub-model (method 3) with EC 5, by means of slip curves for failure mode  $f$  and  $h$  for a force-to-grain angle of  $\alpha = 0^\circ$ .

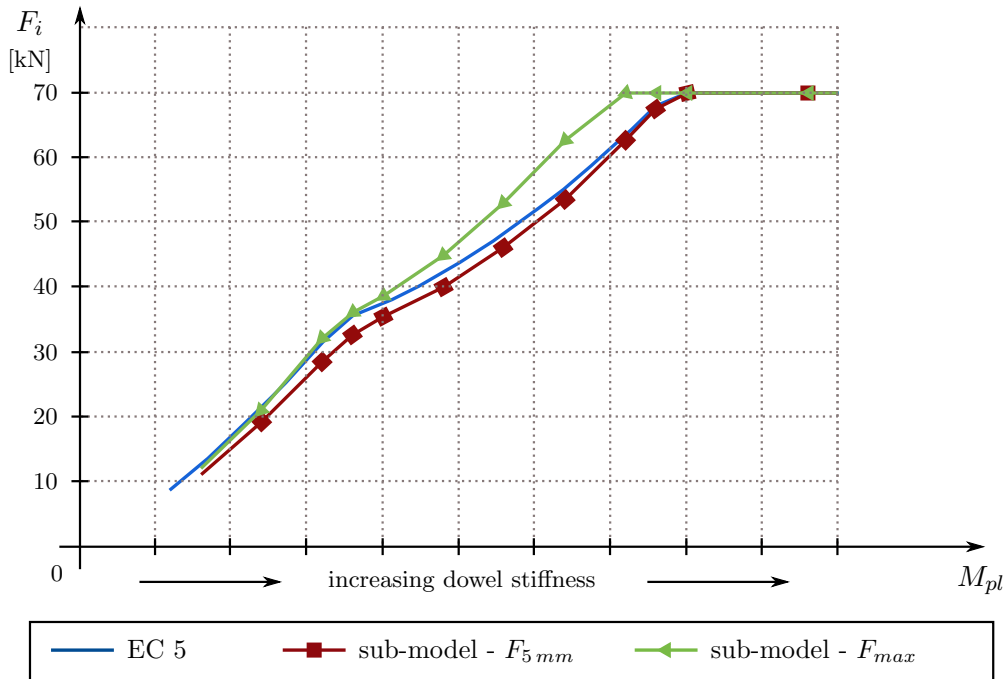
$u = 0.9$  mm), as well as by the loss of stiffness of the dowel. The difference of the slip curves for  $\alpha = 0^\circ$  and  $\alpha = 90^\circ$  can be explained by the soft behavior of wood loaded perpendicular to the grain. Further loading leads to hardening and, consequently, to an increasing bearing capacity, until the load level of grain-parallel loaded wood is reached.

Figure 2.11 shows a comparison between the slip curves determined by the structural analysis model and the simplified method based on EC 5 for both limit cases: the stiff dowel (no plastic hinges) and the soft dowel (two plastic hinges), under grain-parallel load. Once again it should be mentioned that the stiffness estimation according to EC 5 ( $K_{ser}$  and  $K_u$ ) is based on a dowel diameter of 16 mm. It becomes obvious, that EC 5 underestimates the stiffness of the stiff dowel (failure mode  $f$ ), while the ultimate load fits well to the load determined using the structural analysis model. The stiffness of the soft dowel (failure mode  $h$ ) estimated by EC 5 is significantly higher than calculated by the structural analysis model. Only at low deformations a good correlation has been found. After first plastic deformations in steel and in wood, the stiffness decreases rapidly. Again, the ultimate load correlates quite well.

EC 5 gives no information on the elastic limit of single-dowel connections. The standard only postulates that no elastic limit has to be checked for the case of verification of the ultimate load. Since the elastic limit is used for the serviceability limit state, which works with characteristic loads, one approach is to estimate the elastic limit by division of the ultimate load through the averaged partial factor, which is approximately 1.4. The elastic limit is marked by the break of the slip curve in Figure 2.11. For the stiff

Table 2.4: Failure modes and corresponding dowel stiffness according to EC 5.

Dowel diameter $d$ [mm]		$\alpha = 0^\circ$	$\alpha = 90^\circ$
2 plastic hinges (failure mode $h$ )	from/to	0 - 16	0 - 14
1 plastic hinge (failure mode $g$ )	from/to	18 - 38	16 - 32
rigid dowel (failure mode $f$ )	from/to	40 - $\infty$	34 - $\infty$

Figure 2.12: Comparison of the ultimate load calculated by the sub-model (method 3) and according to EC 5 for different dowel stiffnesses for  $\alpha = 0^\circ$ .

dowel the elastic limit is underestimated by this simple approximation, but for the soft dowel, plastic deformations occur much earlier than assumed. In this case, it has to be distinguished between plasticity of the dowel and plasticity of the wood. While the bearing forces at the state of the first plastic deformations of the dowel is more than 70% less than the assumed elastic limit, the elastic limit of the wood is approximately 15% overestimated by this simple approach.

In general the statements in question of loads in grain direction are also valid for connections loaded perpendicular to the grain. However, the ultimate load determined by the structural analysis model is much higher than the one of EC 5, since EC 5 does not consider the effect of hardening of the wood. The deviation is about 60% for the stiff dowel and about 20% for the soft dowel. A comparison between single-dowel slip curves determined by the sub-model and the simplified method based on EC 5 for loads perpendicular to the grain is not shown.

Failure modes corresponding to the stiffness of the dowel are shown in Table 2.4. These

values, calculated according to EC 5, correlate quite well with the values determined by the structural analysis model. In the transition from one failure mode to an other, only limited plastic hinges may occur.

Since EC 5 gives no specification of the deformation at level of the ultimate load, the definition of the standard DIN EN 383 [3] to determine the embedment strength of dowel-type fasteners is used. The ultimate load is defined as the maximum load or the load at a deformation of 5 mm plus the initial deformation. Based on this definition, the ultimate load for wood loaded in grain direction, as calculated by EC 5, is compared to the bearing force at a deformation of 5 mm ( $F_{5mm}$ ) as well as to the maximum force ( $F_{ultimate}$ ) as determined by the sub-model (see Figure 2.12). In general, the results of EC 5 correlate well with the results of the structural analysis model. For soft dowels, ultimate loads  $F_{ultimate}$  are almost equal to the one according to EC 5. For increasing stiffness of the dowel the results of EC 5 fit better to the bearing forces from the sub-model at a deformation of 5 mm ( $F_{5mm}$ ). As soon as the stiffness of the dowel reaches a level where the dowel behaves rigid, EC 5 forces are equal to  $F_{ultimate}$  and  $F_{5mm}$  from the sub-model.

For loading perpendicular to the grain, the ultimate load determined by EC 5 fits better to the bearing force of the sub-model at a deformation of 5 mm ( $F_{5mm}$ ), while the ultimate load  $F_{ultimate}$  determined by the structural analysis model is higher. The deviation increases with increasing stiffness of the dowel, since for stiff dowels the ultimate load mainly depends on the embedment strength of wood. The difference is due to the hardening effect of wood that is considered in the sub-model but not in the simplified calculation according to EC 5. This comparison is not shown.

### 2.5.3 Variation of side member thickness $t_1$

The same configuration as described in 2.5.1 has been used. Again, variations are done for loadings in and perpendicular to the grain direction. In this case, all properties are kept constant, except the side member thickness  $t_1$ . Since exactly the same input data are used for EC 5 and the sub-model, a direct comparison of both models is possible.

Starting from the reference configuration with  $t_1 = 84$  mm, the side member thickness has been increased as well as decreased. The reference configuration leads to a failure mode between one and two plastic hinges ( $g+h$ ). Increasing side member thickness increases the stiffness of the wooden parts, while the stiffness of the dowel is unchanged. A large side member thickness is related to a low ratio of dowel to side member stiffness. Consequently, starting from the reference configuration, an increase of  $t_1$  leads to the failure mode with two plastic hinges ( $h$ ). Decreasing  $t_1$  gives the failure mode with one plastic hinge (mode  $g$ ) and, for a further decrease of  $t_1$ , failure mode  $f$  (no plastic hinge).

In total, 16 different assessments, with side member thicknesses between 20 mm and 200 mm have been investigated. In addition to the reference configuration, three representative configurations, related to the three possible failure modes, have been chosen to be discussed in detail.

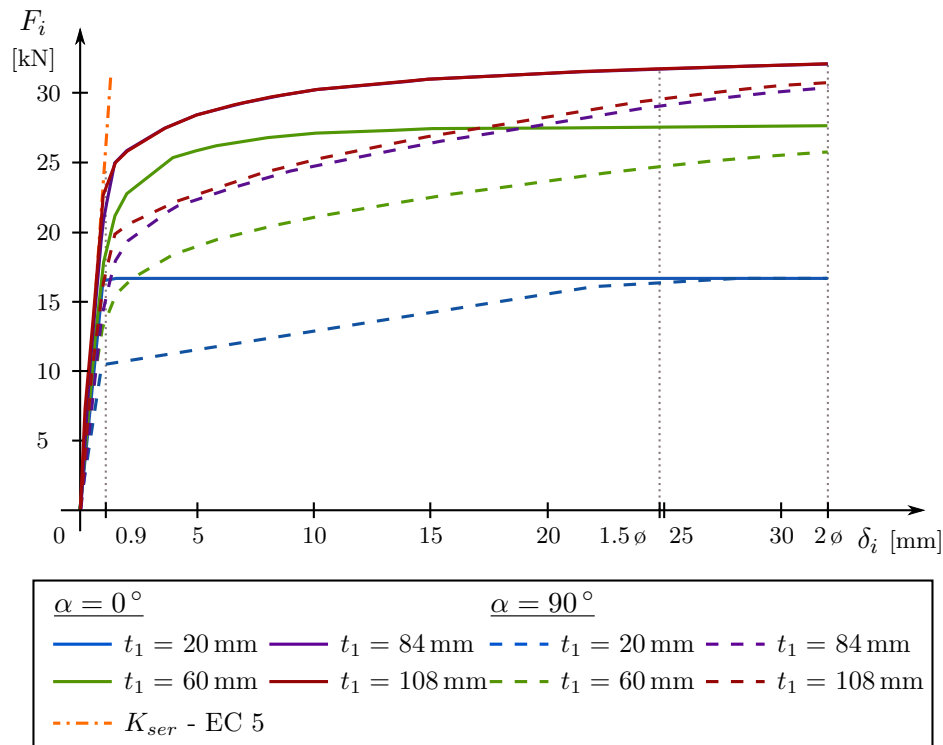


Figure 2.13: Slip curves for different side member thicknesses for force-to-grain angles of  $\alpha = 0^\circ$  and  $\alpha = 90^\circ$ .

The corresponding slip curves are shown in Figure 2.13 for four different configurations. The continuous lines are related to loading in grain direction and the dashed ones to loading perpendicular to the grain. Further, the dash-dot line stands for the stiffness  $K_{ser}$  according to EC 5.

In general, the statements given in Section 2.5.2 are also valid here. Only the bearing capacity of the different side member thicknesses and, consequently, of the different failure modes cannot be directly compared, since the bearing capacity depends on  $t_1$ . This is the reason for a higher bearing capacity of the dowels with plastic hinges than the ones without a plastic hinge. Furthermore, the slip curves of the configurations  $t_1 = 84$  mm and  $t_1 = 108$  mm are very similar. This indicates that the bearing capacity is independent from the side member thickness for the failure mode with two plastic hinges. Consequently, this is the maximum load of the single-dowel connection.

Figure 2.14 shows the comparison of the slip curves determined by the sub-model (method 3) and according to EC 5 for the both limit cases: the stiff dowel (no plastic hinges) and the soft dowel (two plastic hinges), under grain-parallel load. The stiffness  $K_{ser}$  according to EC 5 only depends on the dowel diameter and the density of the wood, but is independent of the side member thickness. Consequently, the stiffness of the configuration with a large  $t_1$  (failure mode with two hinges) is underestimated and the configuration with a low  $t_1$  (failure mode without plastic hinge) is overestimated, respectively. As regards the ultimate load, conclusions given in Section 2.5.2 are also

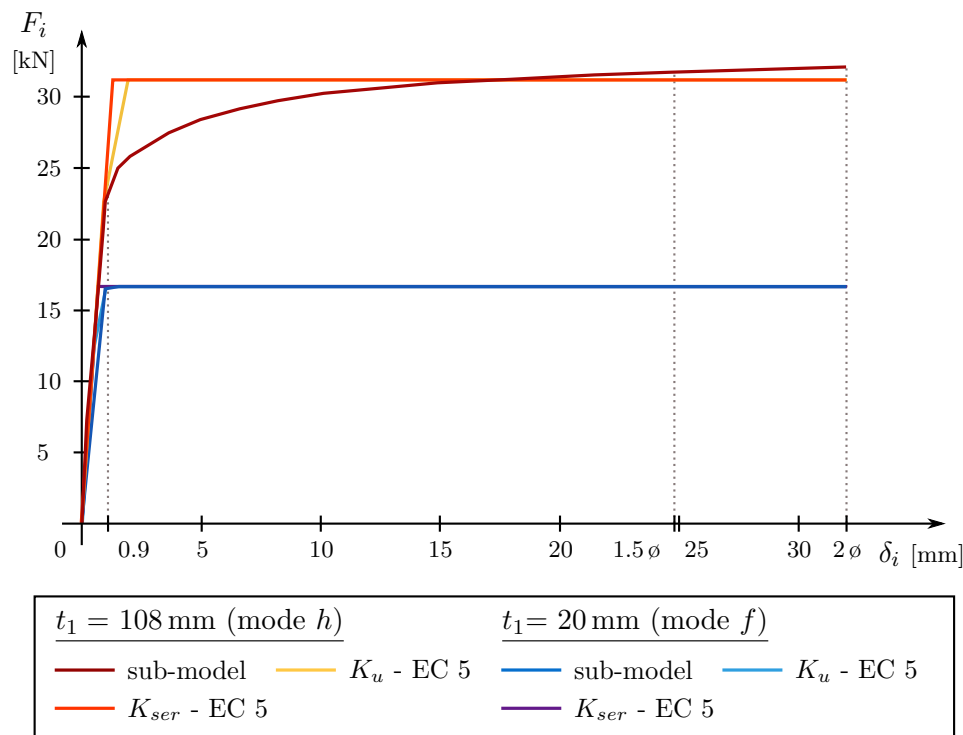


Figure 2.14: Comparison of the sub-model (method 3) with EC 5 by means of slip curves for failure mode  $f$  and  $h$  for a force-to-grain angle of  $\alpha = 0^\circ$ .

true in this case. This means that the ultimate load correlates quite well for the two different methods.

As described in Section 2.5.2, the elastic limit is an additional information from the sub-model not available in EC 5.

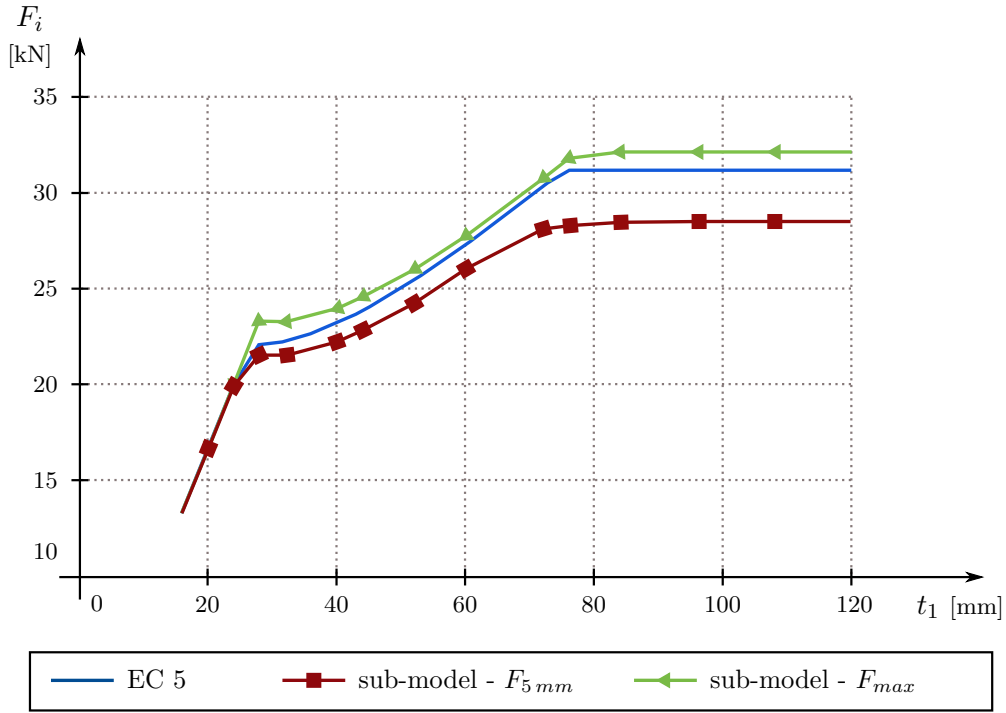
In general, the statements given for loading in grain direction are also valid for connections loaded perpendicular to the grain (not shown). Since the wood behaves softer in this loading direction, also the connection itself shows a softer behavior at the beginning, followed by the effect of hardening at plastic deformations. This means that the stiffness in case of failure mode  $f$  is considerably overestimated by EC 5. Again, the ultimate load of both configurations is considerably underestimated by EC 5, since the standard does not consider the effect of hardening.

Failure modes according to EC 5 corresponding to the side member thickness  $t_1$ , are shown in Table 2.5. These values correlate quite well to the values determined by the structural analysis model. In the transition from one failure mode to an other, only limited plastic hinges may occur.

Again, the definition of the ultimate load according to DIN EN 383 is used (see Section 2.5.2). Based on this definition the ultimate load for wood loaded in grain direction as determined by EC 5 is compared to the bearing force at a deformation of 5 mm ( $F_{5mm}$ ) as well as to the maximum force ( $F_{ultimate}$ ) of the sub-model (see Figure 2.15). For failure

Table 2.5: Failure modes and corresponding side member thickness  $t_1$  according to EC 5.

Side member thickness $t_1$	[mm]	$\alpha = 0^\circ$	$\alpha = 90^\circ$
rigid dowel (failure mode $f$ )	from/to	0 - 24	0 - 32
1 plastic hinge (failure mode $g$ )	from/to	28 - 72	36 - 92
2 plastic hinges (failure mode $h$ )	from/to	76 - $\infty$	96 - $\infty$

Figure 2.15: Comparison of the ultimate load calculated by the structural analysis model (method 3) and EC 5 for different side member thickness  $t_1$ , for  $\alpha = 0^\circ$ .

mechanisms without plastic deformations of the dowel, EC 5 calculations match more or less exactly the values of the structural analysis model for  $F_{ultimate}$  as well as for  $F_{5mm}$ . Increasing side member thickness leads to the failure mode with one plastic hinge. As observed in the parameter studies for different dowel stiffness, EC 5 calculations are close to  $F_{5mm}$  at the change from failure mode  $f$  to  $g$ , and close to  $F_{ultimate}$  at the change from failure mode  $g$  to  $h$ . As soon as the failure mode with two plastic hinges is reached ( $h$ ), an increasing side member thickness does no longer increase the bearing force. As a result, forces are only transferred at the area between the second plastic hinge and the gusset plate. EC 5 model assumes a constant embedment force distribution along this contact area at the size of the embedment strength. In comparison, the structural analysis model accounts for the non-uniform distribution of embedment stresses. Also, elastic deformations occur next to the second plastic hinge. This means that the transferred loads are lower than the one assumed in EC 5 and, as a consequence, the bearing capacity is lower.

For loading perpendicular to the grain, the ultimate load calculated by EC 5 fits better to the bearing force at a deformation of 5 mm  $F_{5mm}$ , while the ultimate load  $F_{ultimate}$  determined by the structural analysis model is higher. The difference is due to the hardening effect of wood that is considered in the sub-model but not in the simplified calculation according to EC 5. Additionally, the different embedment force distribution, for the failure mode with two plastic hinges, between the structural analysis model and EC 5, takes effect here.

## Multi-dowel connections

### Load-carrying principle of dowel connections

Regardless of the connection configuration or if the connection is loaded by normal forces in tension or compression, or even by bending moments, there are principal load-carrying characteristics of dowel connections, which are discussed in the following.

Starting for the timber part, the load is transferred by means of contact forces between the timber and the dowel. For indirect connections, the connecting element is loaded via bending of the fastener and/or contact forces between the fastener and connecting element. Thereon, the second timber element is again loaded via bending of the dowel and/or contact forces between the dowel and the timber element. For direct connections the load is transferred directly from the one timber element to the other via bending of the fastener and/or contact forces between the timber elements and the fastener. Typical direct and indirect dowel connections can be seen at Figure 3.1.

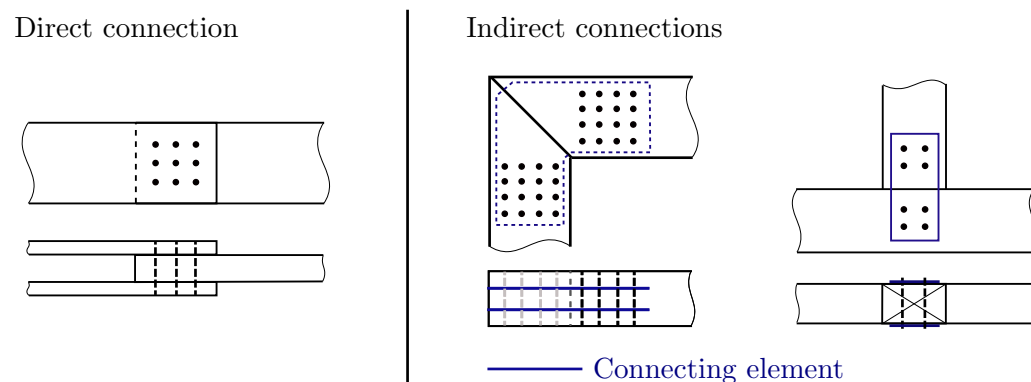


Figure 3.1: Typical direct and indirect dowel connections.

### 3.1 Mechanical behavior of multi-dowel connections

The following discussions are related to two-dimensional problems. In this case, loading of the connection consists of three internal forces, namely normal force  $N$ , shear force  $V$  and moment  $M$ . Consequently, the deformation of the connection is described by the longitudinal deformation  $u$ , the transverse deformation  $w$  and the rotation  $\phi$ , respectively. The loading and deformation components are assembled in the load vector ( $\mathbf{F}$ ) and deformation vector ( $\mathbf{u}$ ) respectively. These two vectors are connected by the so called stiffness matrix ( $\mathbb{K}$ ), with 9 non-zero elements in the general case (see Equation (3.1)).

$$\mathbf{F} = \mathbb{K} \cdot \mathbf{u} \quad (3.1)$$

Simplified, the bearing capacity of the multi-dowel connection can be considered to be the sum of the bearing capacity of the single dowels. Figure 3.2 shows the general way of the determination of the bearing capacity of the connection in case of uniform loading conditions. In the following, a description of Figure 3.2 is given.

- The three columns are related to the three member forces.
- Line 1: The deformation distribution ( $\mu_i$ ,  $\omega_i$  or  $\delta_{\phi,i}$ ) within the connection caused by external longitudinal deformation  $u$ , transverse deformation  $w$  and rotation  $\phi$  is shown.
- Line 2: Via the slip curve of the single-dowel, the deformation of the single-dowel is related to the reaction force ( $R_i$ ) of the specific dowel.
- Line 3: Summation of the calculated reaction forces of each dowel, gives the bearing capacity of the entire connection for a specific uniform external deformation condition (=one point in the slip curve of the connection). Repeating this process for a number of deformation steps gives the slip curve of the connection.

This simplified approach is only valid for the specific case of a dowel group with their center of gravity (COG) at the reference point of the connection. The reference point itself, is a point within the connection, at which the external deformations ( $u$ ,  $w$  and  $\phi$ ) are acting on the connection. As a result, a longitudinal deformation ( $u$ ) causes only a normal force ( $N$ ), a transverse deformation ( $w$ ) leads only to a shear force ( $V$ ) and the rotation ( $\phi$ ) causes only a moment ( $M$ ). This means only the three diagonal elements of the stiffness matrix are non-zero elements and no additional forces are caused by a uniform external deformation. In the case of excentricity between the reference point and the COG, also some other elements of the stiffness matrix are unequal zero. E.g. an axial excentricity leads to an additional bending moment caused by the transverse displacement  $w$ , and to an additional shear force caused by the rotation  $\phi$ . Furthermore, the separated consideration of the three deformations  $u$ ,  $w$  and  $\phi$  is also only an approximation. For example, while the fasteners are at an elastic stage for each of the three deformations, the interaction may already be of plastic manner (see Figure 3.3), which leads to force redistribution within the connection. In addition, the resulting displacement of the single dowel leads to a resulting reaction force of the single dowel,

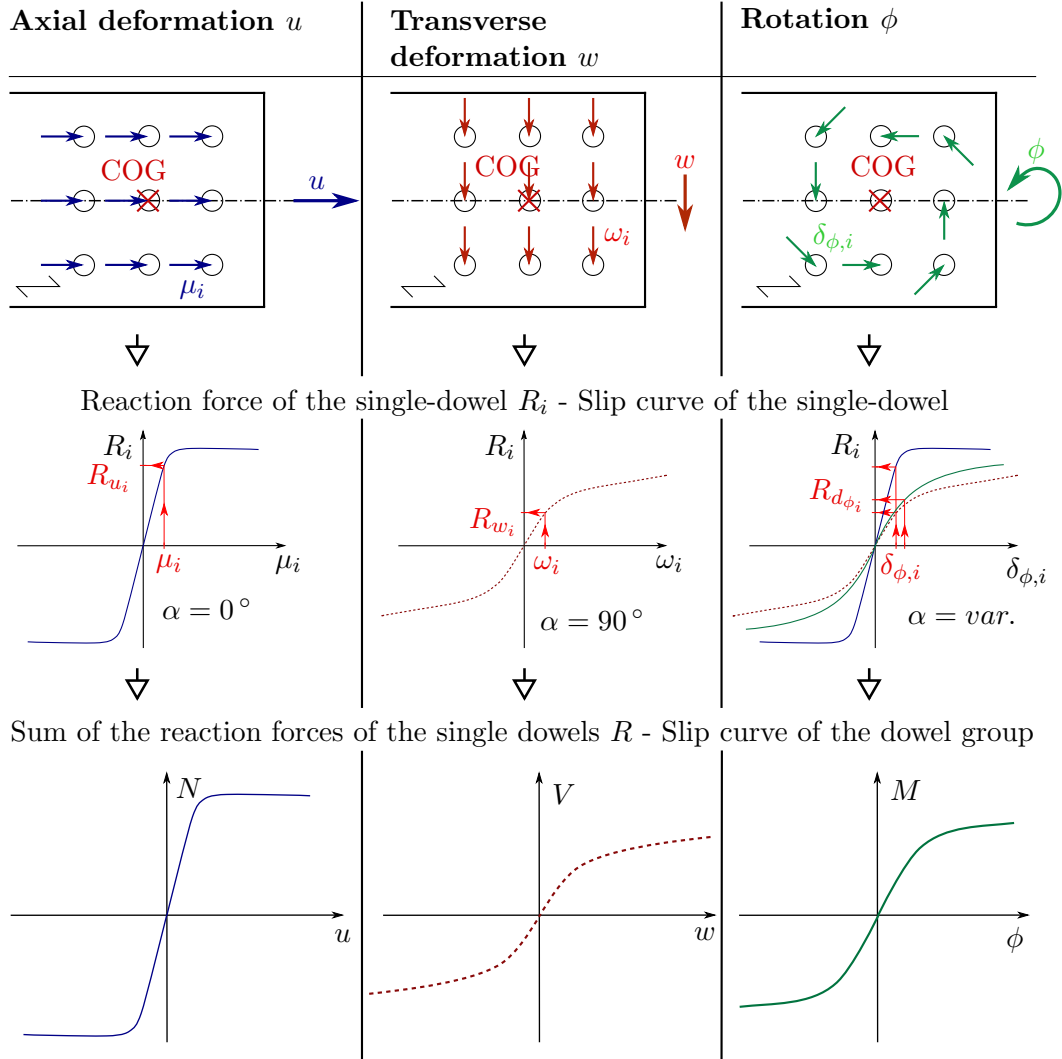


Figure 3.2: Simplified force distribution in a multi-dowel connection for the specific case of a double-symmetric connection under uniform loading conditions.

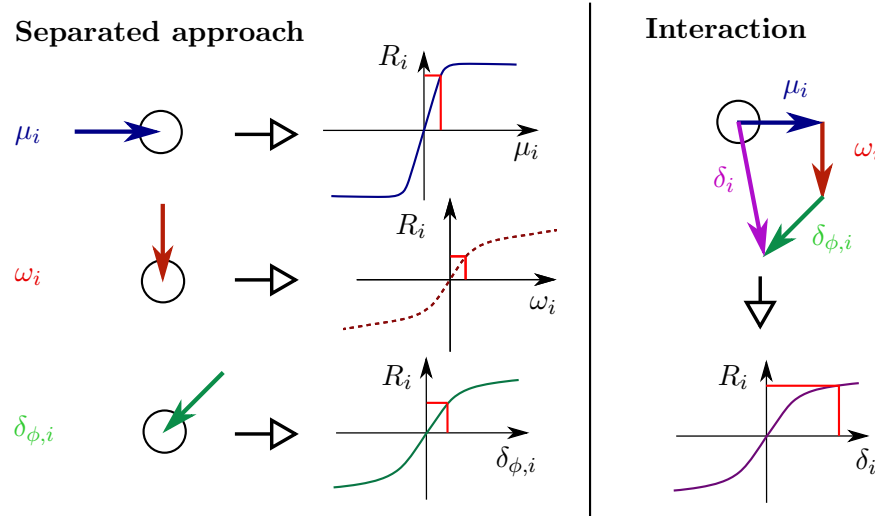


Figure 3.3: Comparison of the separated approach and the approach with interaction of the deformations at the estimation of the bearing capacity of the connection.

determined with the corresponding force-to-grain direction. In general, this resulting force is not equal to the sum of the resulting forces of the separated approach, since the relation between reaction force and force-to-grain angle is nonlinear. Concluding, the separated approach would only be valid for a direction independent behavior of the wood and a pure linear elastic behavior of all dowels.

Apart from force redistributions caused by plasticity of single fasteners, an uneven force distribution can be generated by different load-carrying characteristics of the individual fasteners. Depending on the stiffness of the single fastener it will bear more or less of the loading. Furthermore, antisymmetric slip curves of the single connectors are possible. This is e.g. the case for contact conditions, which act in one deformation direction as stiff element transmitting high forces, while no forces can be carried in opposite direction.

The previous descriptions assume the direction of the reaction force to be equal to the deformation direction. As mentioned in Section 2.2, this is only valid for deformations in and perpendicular to the grain direction ( $\alpha = 0^\circ$  and  $90^\circ$ ). For intermediate force-to-grain angles the force direction differs from the deformation direction. This takes effect on the force distribution within the connection, since the reaction forces tend to lean to the stiffer axial direction (see Figure 2.5).

### Brittle failure modes

In addition to ductile failure in case of embedment failure and fastener bending, brittle failure in terms of lateral splitting, row shear failure and block shear failure may occur (see Figure 3.4). This brittle behavior can be prevented by using slender dowels and by increasing the distance between the fasteners. Additionally, lateral reinforcement by means of internal reinforcing elements, such as screws, or by glued-on elements can be used. Herein, these brittle failure modes are not considered and goes beyond the scope of the thesis.

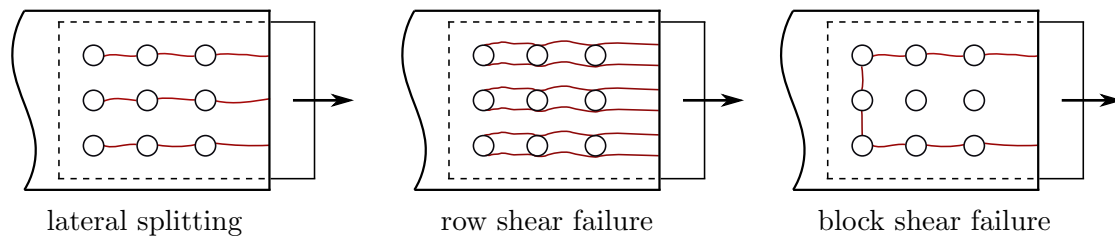


Figure 3.4: Typical brittle failure modes in multi-dowel connections [8].

## Ductility of dowel connections

Ductility goes always hand in hand with large deformations, which generally means plastic deformations in the connection members. Plastic design approaches significantly change the force distribution within the connection and within structure, respectively. Jorissen and Fragiacomio discusses in [13] ductility in timber structures in general. Different approaches of the definition of ductility and highlights why ductility in structures is desirable are discussed. Four reasons have been listed, including:

1. announced failure of the structure, by means of large deformations (static ductility),
2. stress redistribution within a cross-section and force redistribution among different cross-sections in statically indeterminate structures (static ductility),
3. energy dissipation under seismic loading (dynamic ductility), and
4. structural robustness, which means the structure can accommodate large displacements and rotation demands caused by sudden failure of a single member within the structural system.

Also different theoretical and experimental approaches to obtain ductility at the structural design are given. Since timber members in bending, tension and/or shear behave brittle, the ductility of the structure is provided mainly by the joints of timber structures. In order to allow plastic deformations in dowel connections, a reinforcement, for example by means of screws perpendicular to the dowel, has to be installed. The scope of the paper does not include a detailed description of the determination of slip curves (moment-rotation relationship). Only general ideas of different approaches, like experimental determination, the EEEP (Equivalent Energy Elastic-Plastic) method and EC 5 formulas, are presented.

In [20] and [7], the design of timber structures considering the plastic behavior of the connections is discussed. It generally deals about the load redistribution caused by the ductility of the joints. To illustrate the effect of plasticity in connections, in both papers a two span-beam example is analyzed. In [20], the load-slip-relation of the joint is simplified considered by Innsbrucks component method for steel structures, and in [7] the moment-rotation capacity of the connection is studied experimentally.

The papers presented above highlight the advantages of considering plasticity in timber-joints, but a satisfactorily approach to determine the load-slip-relation of a specific joint

has not been given. Since the load redistribution in timber structures in case of plastic behavior of joints is sensitive to the slip curve of the joint, a realistic design approach for joints requires taking into account the anisotropic stiffness and strength properties of wood.

### 3.2 Current models considering the compliance of connections

This section gives an overview of current methods for the consideration of the compliance of connections in the structural analysis. In [19] an overview of different methods for semi-rigid connections in the structural analysis of timber structures is given. It focuses on the transfer of the basic idea of the method and gives no guideline for execution in detail. The following models are presented: Simplified analytical model based on the virtual work principle, mechanical model (spring model), finite element model and experimental methods.

Further, the force distribution in moment-stiff timber connections has been reviewed in [16] and [17]. In [16] comparison of the force distribution in a frame corner determined by hand calculation and by FEM-analysis is shown. The hand calculation is based on a method presented in Larsen and Enjily 2009 [14], where the distribution of internal forces between the dowels is found by considering the frame corner connection as an eccentrically loaded connection with unknown line of force action. In this approach, the force distribution only depends on the geometry of the connection, which means the magnitude of the resulting force of the dowel increases with increasing distance from the center of gravity, independent of the force-to-grain angle of the corresponding force. As a conclusion, it has been found, that the resulting forces calculated by the FEM-analysis are stronger oriented in grain direction and reaction forces at force-to-grain angles close to  $90^\circ$  are significantly lower than determined by hand calculation.

The second paper presents an improved method for calculating force distributions in moment-stiff timber connections [17]. Based on a numerical simulation the deviation of the dowel force direction from the theoretical direction (= direction of displacement) is shown by means of a specific problem. Also the direction dependency of the arm to the force and slip modulus is shown. Finally, a refined hand calculation approach is presented and has been compared to conventional hand calculation. The influence on the stiffness of the entire connection and, as a result, the influence on the force distribution in the system has not been shown.

A lot of research has already been done in the field of ductility of timber-joints and their influence on the structure, as well as in the load distribution within the connection. But most of the papers concentrate only on a specific problem of this topic, in example on the load distribution within the connection or on the load redistribution of the structure caused by ductile joints. So far, no consistent way for the estimation of the load-deformation behavior of the single joint and the load distribution within a connection up to the structural analysis has been shown. Such a guideline is presented by means of a simplified model in Section 3.3 and by means of an improved model in Chapter 4.

### 3.3 State-of-the-art calculation of connection slip curves and dowel verification

In the following, a model for simplified calculation of connection slip curves based on the current design standard EC 5 is discussed. It displays the current state-of-the-art in the engineering design of dowel connections. It is based on estimation of single-dowel slip curves. Additionally, the verification of the connection based on EC 5 is shown. Since an elastic approach is used, the bearing capacity of the connection is limited by the maximum stressed dowel. In general, EC 5 approves also formation of plastic deformations, but without providing specifications for its uses in practice.

The model is based on following assumptions and restricted by:

- elastic approach according to EC 5, which means elastic and minor plastic deformations, and plastic strengths of the single-dowel connection, are used,
- two-dimensional load-bearing characteristics (x-z plane),
- homogenous connections: Only one fastener type or fastener of equal stiffness are allowed within the connection,
- decoupled approach: Member forces and their corresponding deformation are considered to be independent, and
- force direction is equal to the direction of displacement: This means that at each dowel the direction of the displacement vector, caused by member forces, is equal to the direction of the reaction-force vector.

As a result of this assumptions, satisfactorily results are only given for connections with their center of gravity at the beam axis and unlimited linear elastic behavior of the single fastener. In the following, the calculation procedure is presented in detail:

#### 3.3.1 Design of connections

Since the internal forces (member forces) and, therefore, the number of necessary fasteners are dependent on the stiffness distribution in the structural system, and at the same time the stiffness distribution of the system is dependent on the number of fasteners, the verification of a statically indeterminate system is an iterative process. Therefore, the first step is to design the connection configuration. The following parameters are necessary as input parameters: Number, size, position and material of the fasteners as well as dimensions, grain direction and properties of the timber members. For the design of a connection, member forces estimated by a static system without considering compliances may be used as a starting point.

#### 3.3.2 Calculation of slip curves of connections

Based on the connection configuration, corresponding slip curves as input for the structural analysis of timber structures are calculated.

### Connection stiffness

In addition to the assumptions mentioned at the beginning of this section, the following assumptions are done and restrictions are given:

- only layer configurations according to EC 5 and layer combinations which lead to compatible failure modes are permitted,
- the principle of superposition is only valid until the service load is reached, and
- direction independence of the stiffness modulus. This means that the connection reacts in transverse direction as stiff as in longitudinal direction.

The determination of the stiffness of single-dowel connections in the Serviceability Limit State (SLS) and in the Ultimate Limit State (ULS) is given in Section 2.3 in Equation (2.1) and (2.2) respectively. In case of loading by means of normal forces and shear forces, the slip modulus ( $K_{v,N}$ ,  $K_{v,V}$ ) of the dowel group is calculated as the sum of the single-dowel slip moduli.

$$K_{v,ser,N} = \sum_{i=1}^n K_{ser,i} \quad K_{v,u,N} = \frac{2}{3} K_{v,ser,N} \quad \dots \text{in case of normal force} \quad (3.2)$$

$$K_{v,ser,V} = \sum_{i=1}^n K_{ser,i} \quad K_{v,u,V} = \frac{2}{3} K_{v,ser,V} \quad \dots \text{in case of shear force} \quad (3.3)$$

For the calculation of the rotation modulus ( $C_\phi$ ) of the dowel group following assumptions are made:

- direction independence of the slip modulus  $K_{ser}$ ,
- linear elastic material behavior of wood, and
- validation of the superposition principle.

The rotation modulus is calculated from:

1. Determination of the center of gravity of the dowel group.
2. Determination of the local moment of inertia for each fastener

$$I_{p,i} = r_i^2 = x_i^2 + z_i^2 \quad (3.4)$$

where  $r_i$  is the distance between the fastener  $i$  and the center of gravity, and  $x_i$  and  $z_i$  the distance between fastener and center of gravity in  $x$  and  $z$  direction respectively. The used notations are illustrated in Figure 3.5.

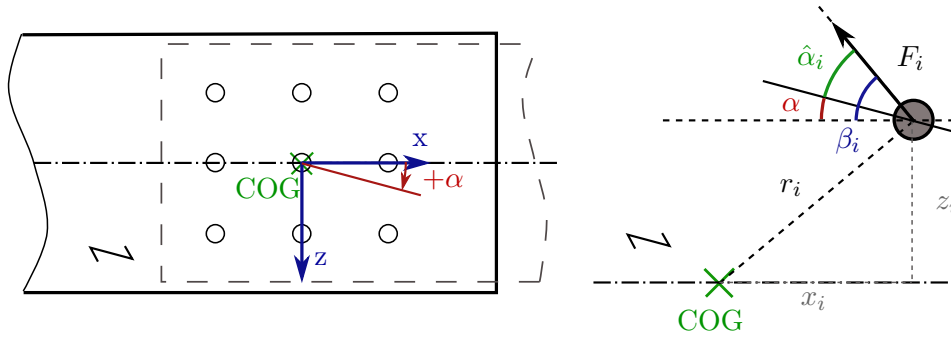


Figure 3.5: Notations and coordinate system used for the state-of-the-art calculation of slip curves.

3. The polar moment of inertia of the entire connection is the sum of the local moment of inertias:

$$I_p = \sum_{i=1}^n I_{p,i} \quad (3.5)$$

4. Finally, the rotation modulus is calculated as:

$$C_{\phi,ser} = \sum_{i=1}^n I_{p,i} K_{ser,i} \quad C_{\phi,u} = \frac{2}{3} C_{\phi,ser} \quad \dots \text{in case of bending moment} \quad (3.6)$$

### Connection strength

The second step for the calculation of slip curves is the bearing capacity of timber-to-timber or steel-to-timber connections according to EC 5. Section 2.3 shows the procedure to calculate the bearing capacity of a single-dowel, by means of a dowel double-shear steel-to-timber connection. The most important steps are repeated here. Since the embedment strength depends on the loading direction with respect to the grain direction, also the bearing capacity is direction-dependent. As a result of different force directions for different member forces, different bearing capacities are necessary for each kind of member forces.

In the following, the procedure to determine the bearing capacity in case of normal force, shear force and bending moment, is presented. In general, the following steps are executed:

- calculation of the embedment strength of wood for each material layer with respect to the force-to-grain angle,
- determination of the plastic moment of the dowel,
- axial withdrawal capacity of the fastener,
- calculation of the bearing capacity of a single-dowel, and
- determination of the bearing capacity of the dowel group.

**Normal force:** Normal forces are forces acting in longitudinal direction of the beam. Therefore, if the grain direction is equal to the direction of the axis, the embedment strength is calculated for a force-to-grain angle  $\alpha = 0^\circ$ . Strength of the connection is determined by:

1. Determination of the embedment strength for each layer with respect to the force-to-grain angle. First, the embedment strength parallel to grain  $f_{h,0,k}$ , according to Equ. (2.5), valid for dowel-type connections, is calculated. In the case of a force-to-grain angle  $\alpha \neq 0^\circ$ , the embedment strength under this specific force-to-grain angle  $f_{h,\alpha,k}$  can be determined according to Equation (2.4).
2. Determination of the plastic moment of the steel dowel. In order to calculate the bearing capacity of the dowel, it is necessary to identify the plastic moment of the dowel according to Equation (2.7).
3. In case of bolted connections, additionally, the axial withdrawal capacity of the fastener can be taken into account according to EC 5 section 8.5.2.
4. Determination of the bearing capacity of a single dowel. Depending on the connection configuration different failure modes may occur. EC 5 gives equation for different connection configurations in timber-to-timber and steel-to-timber connections. The load-carrying capacity of the single-dowel is then the minimum of all potential failure modes. The basic procedure is shown in Section 2.3 by means of a dowel double-shear steel-to-timber connection.
5. Determination of the bearing capacity of the dowel group. Finally, the total bearing capacity of the connection  $F_{v,R,N}$  in Newton can be calculated as the sum of the bearing capacities of the single dowels:

$$F_{v,R,N} = n n_{shear} F_{v,R,Ni}, \quad (3.7)$$

where  $n$  means the number of dowels within the connection,  $n_{shear}$  the number of shear planes and  $F_{v,R,Ni}$  the bearing capacity of the single dowel for one shear plane.

**Shear force:** Shear forces are forces acting in transverse direction of the beam. In general, the embedment strength is determined for a force-to-grain angle  $\alpha = 90^\circ$ . For the case of deviating grain direction from the axial direction of the beam, the force-to-grain direction changes to an angle less than  $90^\circ$ . Since the procedure to calculate the bearing capacity of the connection is identical to the procedure shown for the normal force, no further explanations are given. The only difference lies in the determination of the embedment strength, where the force-to-grain direction differ  $90^\circ$  from the force direction loaded by normal force.

**Bending moment:** Based on the assumptions mentioned at the beginning of this section, the moment bearing capacity of the connection is limited by the highest loaded dowel of the connection. On the one hand, increasing distance from the center of gravity, increases the load per dowel. On the other hand, the bearing capacity of the single-dowel

depends on the local force-to-grain direction. This means that the most exterior dowel is not necessarily the dowel with the highest relative load with respect to its strength. The general procedure is equal to the procedure presented for normal force and shear force. However, since each dowel has a different force-to-grain angle, also the embedment strength and the bearing capacity changes from dowel to dowel.

In the following, a computer supported procedure and an alternatively procedure is presented. The first method requires following calculation steps:

1. The local force-to-grain direction can be determined, when the reaction force is assumed to act on the dowel tangential to a circle with the center of gravity as basis.
2. Determination of the embedment strength of each dowel, considering the local force-to-grain angle at each dowel.
3. Calculation of the plastic moment and axial withdrawal capacity of the dowel.
4. Calculation of the bearing capacity of each dowel.
5. The moment bearing capacity of the connection can be estimated by

$$M_{Ri} = \frac{F_{v,Ri} I_p}{r_i}, \quad (3.8)$$

where  $M_{Ri}$  is the moment bearing capacity in Nmm caused by the bearing capacity of the dowel  $i$ .  $I_p$  stands for the polar moment of inertia in  $\text{mm}^2$  and  $r_i$  is the distance between center of gravity and the dowel  $i$  in mm.

6. Finally, the moment bearing capacity of the connection  $M_R$  is determined as minimum of the moment bearing capacity caused by the bearing capacity of the dowel  $i$ .

$$M_R = \min(M_{Ri}) \quad (3.9)$$

Alternatively, the following procedure can be followed (point 1 to 4 is equal to the procedure shown previously):

1. Determination of the local force-to-grain angle.
2. Determination of the embedment strength of each dowel, consisting local force-to-grain angle.
3. Calculation of the plastic moment and axial withdrawal capacity of the dowel.
4. Calculation of the bearing capacity of each dowel.
5. Determination of an approximate loading factor, given by

$$f_{M_{Ri}} = \frac{I_p}{r_i}, \quad (3.10)$$

where  $I_p$  is the polar moment of inertia in  $\text{mm}^2$  and  $r_i$  the distance between the center of gravity and the dowel  $i$  in mm. The minimum value of  $f_{M_{Ri}}$  marks the probably decisive dowel.

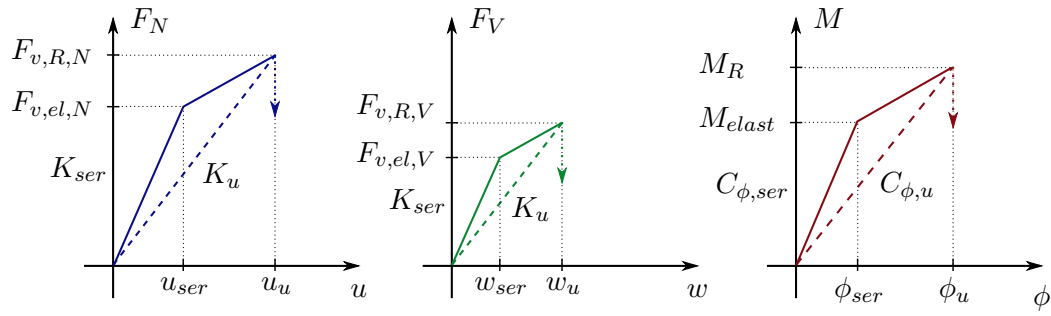


Figure 3.6: Slip curves of the connection corresponding to normal force (left), shear force (middle) and moment (right).

6. The bearing capacity of this dowel is taken as starting point for the calculation of the moment bearing capacity of the connection according to Equation (3.8).
7. Since this bearing capacity is based on an approximation, every dowel has to be checked, if the stress does not exceeds the strength of the dowel. The loading of each dowel is:

$$F_i = \frac{M_R}{I_p} r_i \quad (3.11)$$

where  $M_R$  is the approximated bearing capacity of the connection. Followed by the check:

$$F_i \leq F_{v,Ri}, \quad (3.12)$$

If the condition at Equation (3.12) is fulfilled for each dowel, than the exact moment bearing capacity is found. Otherwise, the moment bearing capacity is calculated using the dowel with the next higher  $f_{M_{Ri}}$ , and so on (iterative process).

### Assembling of slip curves

Having at hand the stiffness as well as the bearing capacity of the connection, the slip curves can be assembled (see Figure 3.6). The only unknown parameter is the elastic limit. No specifications for the calculation of the elastic limit of connection are given in EC 5. Therefore, it is assumed that the elastic limit can be determined by division of the bearing capacity of the connection by the arithmetic mean of the partial factors  $\gamma_G$  and  $\gamma_Q$ . Consequently, the elastic limit is given for normal forces by:

$$F_{v,el,N} = F_{v,R,N}/1.4, \quad (3.13)$$

for shear forces by:

$$F_{v,el,V} = F_{v,R,V}/1.4, \quad (3.14)$$

and for moment loading:

$$M_{elast} = M_R/1.4. \quad (3.15)$$

Since the stiffness, which is equivalent to the slope of the sectional linear curve, and the elastic limit as well as the bearing capacity is known, the corresponding displacements and rotations can be calculated.

Additionally, manufacturing inaccuracies can be considered by adding initial slips. This procedure describes the behavior of connection up to the ultimate limit of connections. No specifications of further deformation are given in the design standards. In general, a brittle behavior of the connection at the ultimate load should be considered. In case of reinforced connections, a ductile behavior of the connection is possible. Moreover, additional failure modes that would lead to premature failure of the connection should be considered in the determination of slip curves of dowel connections.

### 3.3.3 Structural analysis considering the compliance of connections

**Review:** The slip curves estimated in Section 3.3.2 are based on the design of connection configuration. The compliance of the connection together with the compliance of the timber elements gives the total stiffness of the system. Based on this stiffness the member forces acting on the connections can be calculated. If the loads of single dowels exceed the bearing capacity of the dowel, a new configuration has to be adopted. This changes again the stiffness of the system, and as a result the contribution of the member forces. For a two-dimensional problem, three slip curves by means of normal force  $N$  - with corresponding longitudinal displacement  $u$ , as well as shear force  $V$  - with corresponding transverse displacement  $w$ , and bending moment  $M$  - with corresponding rotation  $\phi$  at the center of gravity of the related connection are used for the structural analysis (see Figure 3.6).

### 3.3.4 Verification of connection

Compared to the determination of slip curves, the opposite way is followed. Starting at the member forces, calculated by means of a structural analysis software considering compliance of the connection, the load of each dowel is determined. In order to verify the connection, the bearing capacity for the actual load-to-grain direction is calculated, considering the effective number of dowels  $n_{ef}$ . Moreover, further verifications related to the group behavior is required.

#### Loading of each dowel

First, the calculated member forces from the structural analysis at the center of gravity of the connection are divided to elements in axial and transverse direction. The elements in axial direction, caused by normal force and bending moment as well as the transverse forces, caused by shear force and bending moment are summed up. Finally, resulting forces and the corresponding force-to-grain angles are determined for each dowel.

In order to sum up the forces in a correct way, the coordinate definition shown at Figure 3.5 has to be used. Load of each dowel in axial and transverse direction are then given as:

$$F_{i,x} = \frac{N_x}{n} + \frac{M_y}{I_p} z_i \quad \dots \text{load in axial direction on dowel } i \quad (3.16)$$

$$F_{i,z} = \frac{V_z}{n} - \frac{M_y}{I_p} x_i \quad \dots \text{load in transverse direction on dowel } i \quad (3.17)$$

where  $N_x$  indicates the normal force in Newton,  $n$  the number of dowels,  $M_y$  the bending moment around the y-axis in Nmm and  $z_i$  the distance between dowel  $i$  and the center of gravity parallel to the longitudinal direction in mm.  $V_z$  stands for the shear force in Newton and  $x_i$  is the distance between dowel  $i$  and the center of gravity normal to the axial direction in mm.

Combination of the loads yields the resulting force on the dowel as

$$F_i = \sqrt{F_{i,x}^2 + F_{i,z}^2} \quad (3.18)$$

The corresponding loading direction is given by

$$\beta_i = \arctan \left( \frac{F_{i,z}}{F_{i,x}} \right) \quad (3.19)$$

Finally, in the case of deviating grain direction from the beam axis, the force-to-grain angle can be calculated by

$$\hat{\alpha} = |\beta_i - \alpha| \quad (3.20)$$

where  $\beta_i$  is the loading direction per dowel in  $^\circ$  and  $\alpha$  the grain direction in  $^\circ$  (see Figure 3.5).

### Bearing capacity of each dowel

The general procedure to determine the bearing capacity of each dowel is equivalent to the procedure shown in Section 3.3.2 for the estimation of the slip curves.

However the procedure is briefly repeated:

1. Calculation of the embedment strength for each layer at each dowel with respect to the actual force-to-grain angle. For dowel-type connections Equation (2.4) and (2.5) may be used.
2. Determination of the plastic moment of the dowel (according to 2.7).
3. Determination of the axial withdrawal of the fastener (if necessary).
4. Based on point 1 to 3 the bearing capacity of the single-dowel can be determined as shown at Section 2.3.

### Verification

Before the load is compared to the strength of each dowel, the bearing capacity has to be reduced by the factor considering the group effect in multiple connections. This means

$$F_{R,i} = \frac{F_{v,R}}{f_i}, \quad (3.21)$$

where  $F_{R,i}$  is the reduced strength of each dowel in Newton,  $F_{v,R}$  the bearing capacity of the single dowel in Newton, and  $f_i$  the reduction factor to consider the group effect.

The reduction factor  $f_i$  reduces the bearing capacity to a limit, where brittle behavior caused by splitting can be excluded. For this purpose, EC 5 decreases the total number of fasteners  $n$  to an effective number of fasteners  $n_{ef}$ . For dowel connections  $n_{ef}$  is calculated by

$$n_{ef} = \min \left\{ \begin{array}{l} n_{row} \\ n_{row}^{0.9} \sqrt[4]{\frac{a_1}{13d}} \end{array} \right. ,$$

where  $n_{ef}$  is the effective number of dowels in grain direction,  $n_{row}$  the total number of dowels in series in grain direction,  $a_1$  the spacing between dowels in the grain direction in mm and  $d$  the dowel diameter in mm.

Based on the effective number of dowels  $n_{ef}$ , according to DIN 1052 [1], and linear interpolation between  $n_{ef}$  and  $n$  for force-to-grain angles between  $0^\circ$  and  $90^\circ$ , the reduction factor  $f_i$  can be determined by

$$f_i = \frac{n_{row}}{n_{ef} \frac{90 - \hat{\alpha}}{90} + n_{row} \frac{\hat{\alpha}}{90}} \quad (3.22)$$

Finally, the load can be compared to the reduced strength of each dowel.

$$F_{E,i} \leq F_{R,i}. \quad (3.23)$$

Additionally, a capacity factor

$$f_{R,i} = \frac{F_{E,i}}{F_{R,i}}, \quad (3.24)$$

illustrates the utilization of each dowel with respect to its strength.

### Further verifications

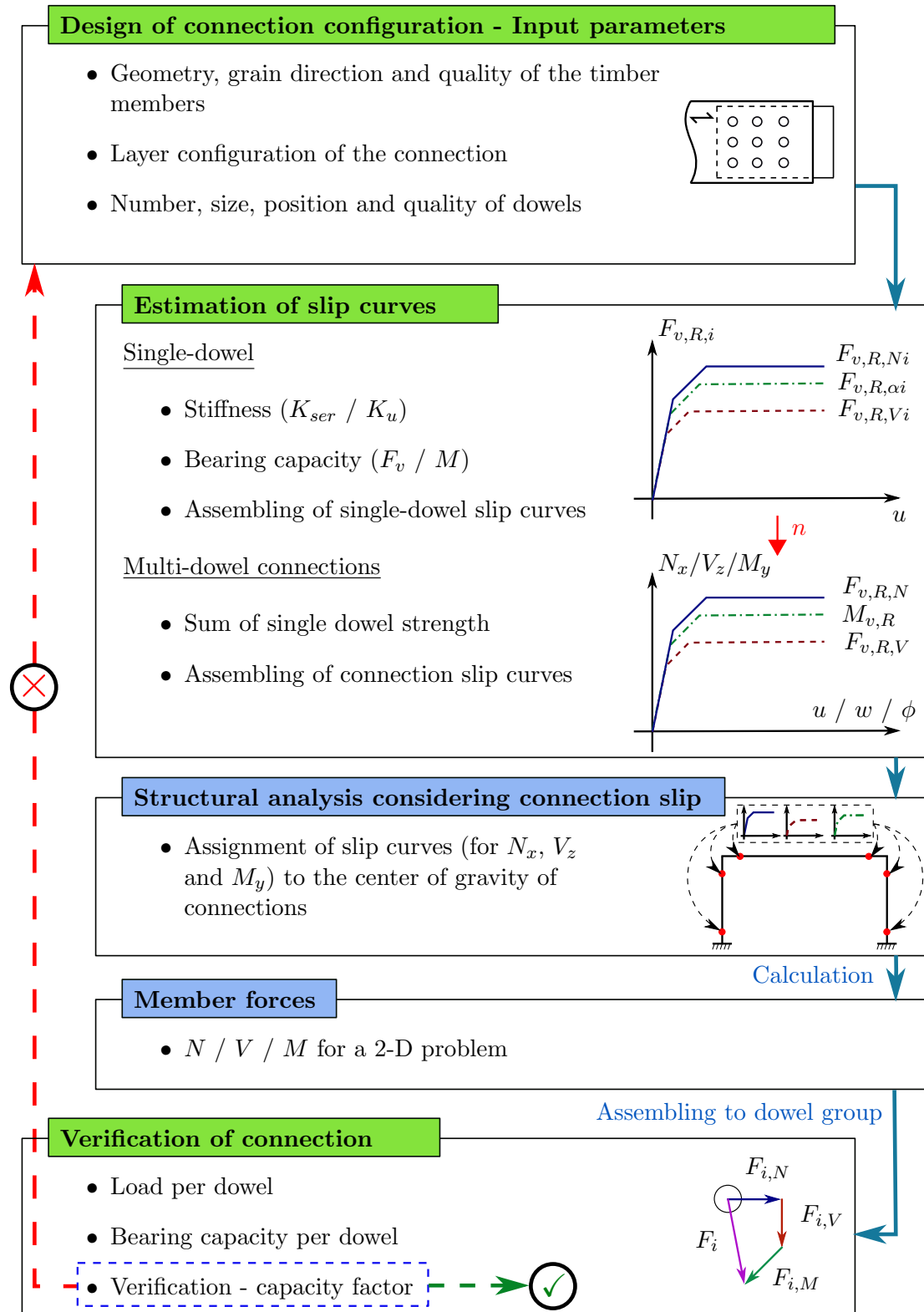
Further verifications, like block shear failure or verification of the net cross-section are required for verification of connections. However, these failure modes are not discussed and are beyond the scope of this thesis.

### 3.3.5 Limits and restrictions of the model

The assumptions and restrictions of the presented state-of-the-art design model for dowel connections exhibits following limits and restrictions:

- The model is limited to homogeneous connections of fasteners of similar stiffness.
- The bearing capacity of the connection is restricted by the bearing capacity of the decisive single-dowel.
- Plastic deformations of the single-dowel and of the connection respectively are not possible.
- The interaction between the member forces cannot be considered in the structural analysis but only in the verification.

### 3.3.6 Flow chart - State-of-the-art design of dowel connections



## Modeling approach for the calculation of connection slip curves and dowel forces

The model developed in this thesis and discussed in this chapter enables a consistent calculation of the global multi-dowel connection slip curves, as well as the determination of member forces for an arbitrary set of connection deformations. Consequently, in a second step, this model is used to back-calculate dowel forces for a given set of member forces.

Compared to the simplified approach discussed in Section 3.3, which is based on simplified assumptions on the behavior of single-dowels and connections as given in EC 5, the model presented in this chapter is applicable to all kinds of connectors and gives more realistic connection properties. The following weak points of the simplified model have been eliminated, which makes it now possible to:

- allow plastic deformations of the single fasteners, which leads to force redistribution within the connection. Consequently, the increased bearing capacity can be quantified,
- consider inhomogeneous connections. Different types of fasteners with different load-carrying behavior can be combined (including contact conditions) since their stiffness properties are adequately considered,
- use arbitrary (realistic) single-fastener slip curves, which makes it possible to consider the direction dependence of the bearing capacity as well as of the stiffness of the connection,
- choose the reference point at an arbitrary position. Consideration of plastic deformations of the connection requires the independence of the reference point from

the center of gravity (COG), since the COG may change in the plastic regime,

- account for the interaction between the single loadings, by means of deformations ( $u/w/\phi$ ) or member forces ( $N/V/M$ ),
- to consistently describe the load-deformation characteristics of connections, i.e. the deformations at each load level are given,
- consider the deviation between the displacement direction and the force direction.

The model discussed in this chapter is based on the following assumptions:

- compared to the stiffness of the interaction fastener-wood, the wood matrix as well as possible connecting elements (e.g. gusset plates), are assumed to be rigid, and
- the position of the single fasteners is assumed to be fixed among each other.

As a result of these assumptions the model is restricted to:

- materials that are stiff compared to the compliance of the connection. Generally, this is valid for all commonly used wood and wood products, and
- two-dimensional problems. An extension to three-dimensional problems is possible.

In the following, the model for the calculation of slip curves of arbitrary connections is described (Section 4.1) and summarized by means of a flow chart. A description of the single steps of the MATLAB Code can be found in Appendix A. The same structure is used for the application of the model to back-calculate dowel forces for an arbitrary set of member forces (in Section 4.2).

## 4.1 Model for the calculation of connection slip curves

This model discusses the calculation of the behavior of multi-dowel connections for an arbitrary set of global deformations of the connection. More precisely, the local deformation distribution is determined based on the geometry and the global input deformations. Consequently, this local deformations and the single-dowel slip curves of each fastener are used to calculate the reaction force of each dowel. Equilibrium conditions yield the member forces and stiffness matrices of the connection.

### 4.1.1 Description of the model

With exception of the restrictions given previously, the presented model is generally applicable to all kinds of dowel-type fasteners. This means that each joint configuration consisting of timber or engineered timber products with or without gusset plates and arbitrary connection elements is permitted. Even if the descriptions are focused on dowels, also other connectors like e.g. split rings are possible. In the following, the model is described in detail and an overview of the most important calculation steps is given by means of a flow chart.

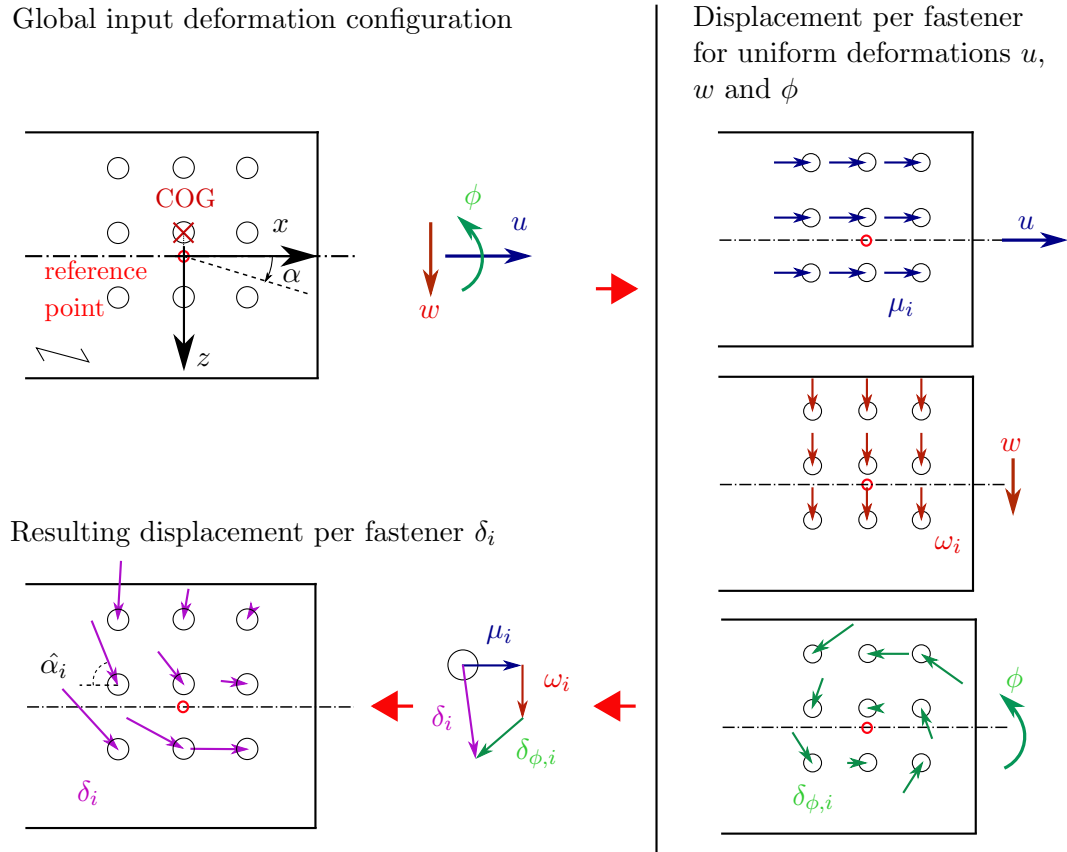


Figure 4.1: Global input deformation ( $u$ ,  $w$ ,  $\phi$ ) and local resulting displacements per dowel ( $\mu_i$ ,  $\omega_i$ ,  $\delta_{\phi,i}$  &  $\delta_i$ ).

## Deformation configuration

The starting point of this model is a prescribed deformation at an arbitrary point of the connection. Advantageous is the definition of the deformations at the beam axis perpendicular to the center of gravity, since it is closest to the real load transformation point. The set of connection deformation configurations is a vector with three elements, including the displacement in axial direction ( $u$ ), the displacement in transverse direction ( $w$ ) and the rotation of the cross section in this plane ( $\phi$ ).

## Resulting displacement and force-to-grain angle of each fastener

Considering the assumptions of a rigid timber matrix and fixed position of the fasteners related to each other, the resulting displacement caused by the given deformation configuration is calculated. This is based on the assumptions that each dowel gets the same axial and transverse deformation as a result of a global axial or transverse deformation. The size and direction of the displacement caused by the rotation of the cross section depends on the position of the specific dowel related to the reference point. The most exposed dowel with the maximum distance from the reference point has the maximum

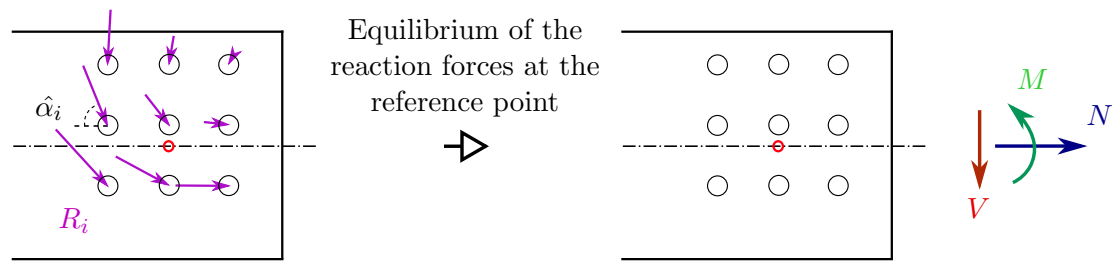


Figure 4.2: Reaction forces per fastener (left) and their resulting member forces (right).

displacement. The direction of the displacement is assumed to be perpendicular to the conjunction fastener - reference point ( $r_i$ ). The size of the displacement is calculated by multiplication of  $r_i$  with the global rotation of the connection.

Finally, the resulting displacement of each dowel ( $\delta_i$ ) is determined by vector addition of the local dowel displacements caused by axial ( $u$ ) and transverse deformation ( $w$ ) as well as by rotation of the connection ( $\phi$ ). Subsequently, the size of the local displacement ( $\delta_i$ ) and the local displacement-to-grain angle ( $\hat{\alpha}_i$ ) is calculated for each dowel. The maximum displacement of the single fastener is restricted by two times of the fastener diameter. Figure 4.1 presents the procedure for the calculation of the resulting displacements per fastener.

### Reaction force per fastener

The resulting displacement of the specific fastener is used as input to the single-dowel slip curve. This allows the determination of the reaction force of the fastener. In order to get a realistic reaction force, a single-dowel slip curve considering the specific force-to-grain angle of the resulting displacement of the fastener should be used. Opportunities for the formulation of slip curves are discussed in Section 2.4. If no single dowel slip curve exists for this specific force-to-grain angle, a linear interpolation between the two closest slip curves is used (see Figure A.1). In general, the direction of the reaction force is assumed to be equal to the displacement direction of the dowel. Alternatively, a deviation between displacement and force direction according to Figure 2.5 can be used.

### Member forces / Stiffness matrix

Definition of the equilibrium of forces at the reference point gives the member forces (Figure 4.2), or in the case of uniform loading conditions the elements of the stiffness matrix at the reference point.

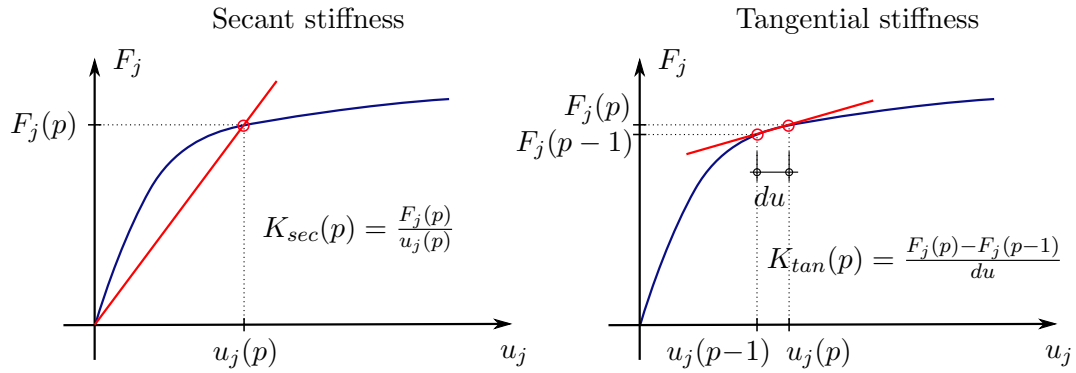
For the determination of the three member forces, containing the normal force  $N$ , the shear force  $V$  and the bending moment  $M$ , the resulting displacement is calculated with the full set of deformations, which means  $\delta_i$  is calculated by the combination  $\mu_i + \omega_i + \delta_{\phi,i}$ .

In order to get the nine elements of the stiffness matrix  $\mathbb{K}$  (see Figure 4.3), the three elements of the deformation vector have to be considered separately. For example, the first column of the stiffness matrix is estimated by a global deformation in axial

$$\begin{bmatrix} u \\ 0 \\ 0 \end{bmatrix} \rightarrow \begin{bmatrix} N_u \\ V_u \\ M_u \end{bmatrix} = \begin{bmatrix} K_{11} \\ K_{21} \\ K_{31} \end{bmatrix} \quad \begin{bmatrix} 0 \\ w \\ 0 \end{bmatrix} \rightarrow \begin{bmatrix} N_w \\ V_w \\ M_w \end{bmatrix} = \begin{bmatrix} K_{12} \\ K_{22} \\ K_{32} \end{bmatrix} \quad \begin{bmatrix} 0 \\ 0 \\ \phi \end{bmatrix} \rightarrow \begin{bmatrix} N_\phi \\ V_\phi \\ M_\phi \end{bmatrix} = \begin{bmatrix} K_{13} \\ K_{23} \\ K_{33} \end{bmatrix}$$
  

$$\begin{bmatrix} N \\ V \\ M \end{bmatrix} = \begin{bmatrix} \begin{bmatrix} K_{11} \\ K_{21} \\ K_{31} \end{bmatrix} & \begin{bmatrix} K_{12} \\ K_{22} \\ K_{32} \end{bmatrix} & \begin{bmatrix} K_{13} \\ K_{23} \\ K_{33} \end{bmatrix} \end{bmatrix} \cdot \begin{bmatrix} u \\ w \\ \phi \end{bmatrix}$$

Figure 4.3: Determination of the stiffness matrix and the slip curves respectively.


 Figure 4.4: Determination of the stiffness properties  $K_{sec}$  and  $K_{tan}$ .

direction (first element of the deformation vector), while the other two elements are equal to zero. For the second column of the stiffness matrix the only non-zero element of the deformation vector is the global transverse displacement (second element of the deformation vector), and for the third column the third element of the deformation vector, respectively (see Figure 4.3). The connection stiffness can be defined by means of the secant stiffness and the tangential stiffness (see Figure 4.4). The notation used at Figure 4.4 is related to the one used in the MATLAB Code (see Appendix A).

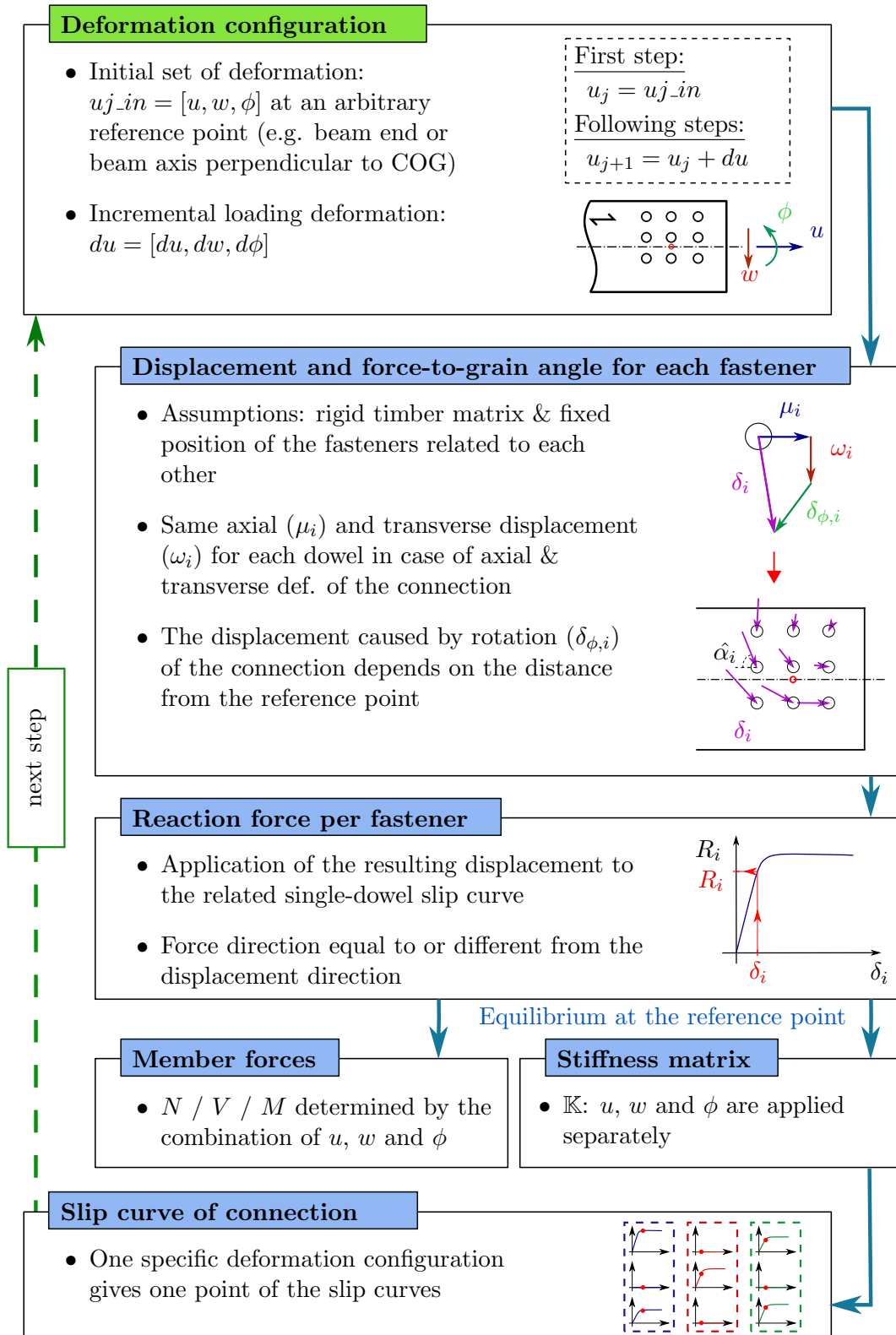
### Determination of the slip curves of the connection

The discussion of the model so far was only related to one specific deformation configuration. With this set of deformations, a resulting displacement per fastener is calculated. Application of the displacement per fastener to the related single-dowel slip curve gives the reaction force per fastener and, finally, equilibrium of the reaction forces leads to the member forces or the stiffness matrix at the reference point. Since only one set of

deformations is considered, the result is also only one set of member forces, which can be interpreted as one point in the related slip curve of the connection. In order to get the slip curve of the connection, by means of a polygonal line, an incremental set of deformations ( $du$ ) is added step-by-step to an arbitrary initial deformation configuration ( $uj_{in}$ ).

A detailed description of the implementation of the model in MATLAB is given in Appendix A.

### 4.1.2 Flow chart - calculation of connection slip curves



## 4.2 Back-calculation of dowel forces

The model presented in Section 4.1 calculates reaction forces (forces per fastener, member forces and stiffness matrices of the connection) based on an arbitrary global set of deformations. In this section, the model is applied in the opposite way. The calculation starts at a given set of member forces ( $N/V/M$ ) and the geometry of the connection. In the following, an iterative process is used to back-calculate the single dowel forces from the given set of member forces. As a result, the single-dowel forces and their force-to-grain directions are determined for each fastener.

### 4.2.1 Description of the model

The presented model is generally applicable to all kinds of dowel-type fasteners, even if the descriptions focus on steel dowels. The model is an extension of the model presented in Section 4.1, which means the calculation steps of the already presented model are not described in detail. In the following, a description of the calculation procedure is given as well as a summary of the calculation steps by means of a flow chart.

#### Member forces

The starting point for calculations is a set of member forces ( $N/V/M$ ), which are generated i.e. by means of a structural analysis software. In order to get the local displacement and force distribution of each dowel, assumptions have to be made since it is not possible to directly calculate the local displacement and forces distributions. Additionally to the geometric properties and the single-dowel slip curves, only the three member forces serve as input data for the model. The global deformation of the connection, the member forces are based on, are unknown. Additionally, it should be highlighted, that the reference point of the input member forces has to be the same as the reference point used in this model.

#### Global deformation of the connection

As a first assumption, the global deformation of the connection ( $u$ ,  $w$  and  $\phi$ ) is determined by application of the input member forces ( $N/V/M$ ) to the global slip curves of the connection. Uniform deformation conditions are assumed, which means a normal force ( $N$ ) causes only an axial deformation ( $u$ ), a shear force ( $V$ ) leads only to a transverse deformation ( $w$ ) and a moment ( $M$ ) only to a rotation of the connection ( $\phi$ ). Consequently, only the three diagonal elements of the stiffness matrix (see Figure 4.3) are unequal to zero. This is true only for very specific conditions, namely for uniform loading of the connection. However, in general, the deformation deviates from the uniform deformation due to the interaction of member forces. The model presented in Section 4.1 is used, for the determination of the global slip curves of the connection.

This first approximation of the global deformation of the connection ( $u$ ,  $w$  and  $\phi$ ) is now the starting point for the calculation of the displacement and force distribution within

the connection. Since the calculation steps are equal to the procedure of the model in Section 4.1, only a short description of each step is given.

### Displacement and force-to-grain angle of each dowel

The global deformations of the connection ( $u$ ,  $w$  and  $\phi$ ) causes local axial deformations ( $\mu_i$ ), local transverse deformations ( $\omega_i$ ) and local deformations perpendicular to the conjunction reference point - fastener ( $\delta_{\phi,i}$ ). Addition of these deformations of each dowel, gives the size ( $d_i$ ) and direction with respect to the grain direction ( $\hat{\alpha}$ ) of the local deformation of each fastener.

### Reaction force per fastener

Application of the local deformations of each dowel to the single-dowel slip curves gives the reaction force for each fastener. The direction of the reaction force can be assumed to be equal to the displacement direction, or a deviation between displacement and force direction according to Figure 2.5 can be considered.

### Member forces

Definition of the equilibrium of forces at the reference point gives the member forces ( $N_{iter}$ ,  $V_{iter}$  and  $M_{iter}$ ) based on the estimated single-dowel forces.

### Comparison of the member forces

The estimated member forces  $N_{iter}$ ,  $V_{iter}$  and  $M_{iter}$  are compared to the input member forces  $N$ ,  $V$  and  $M$ . The input member forces will be equal to estimated member forces only for the specific case of the reference point at the center of gravity (COG) and low member forces. The term low member forces is used, since even the sum of the different deformation components of each fastener ( $\mu_i$ ,  $\omega_i$  and  $\delta_{\phi,i}$ ) has to be in the elastic range. This deformation has to be small in the sense that the reaction force of the single-dowel is independent from the force-to-grain angle.

In general, both sets of member forces do not match each other. In this case, an iterative process for the identification of dowel forces is required.

### Iteration

The global deformations of the connection are modified as long as the input member forces ( $N$ ,  $V$  and  $M$ ) do not correspond to the calculated member forces ( $N_{iter}$ ,  $V_{iter}$  and  $M_{iter}$ ). After adjustment of the deformations of the connection, the following calculation steps are executed:

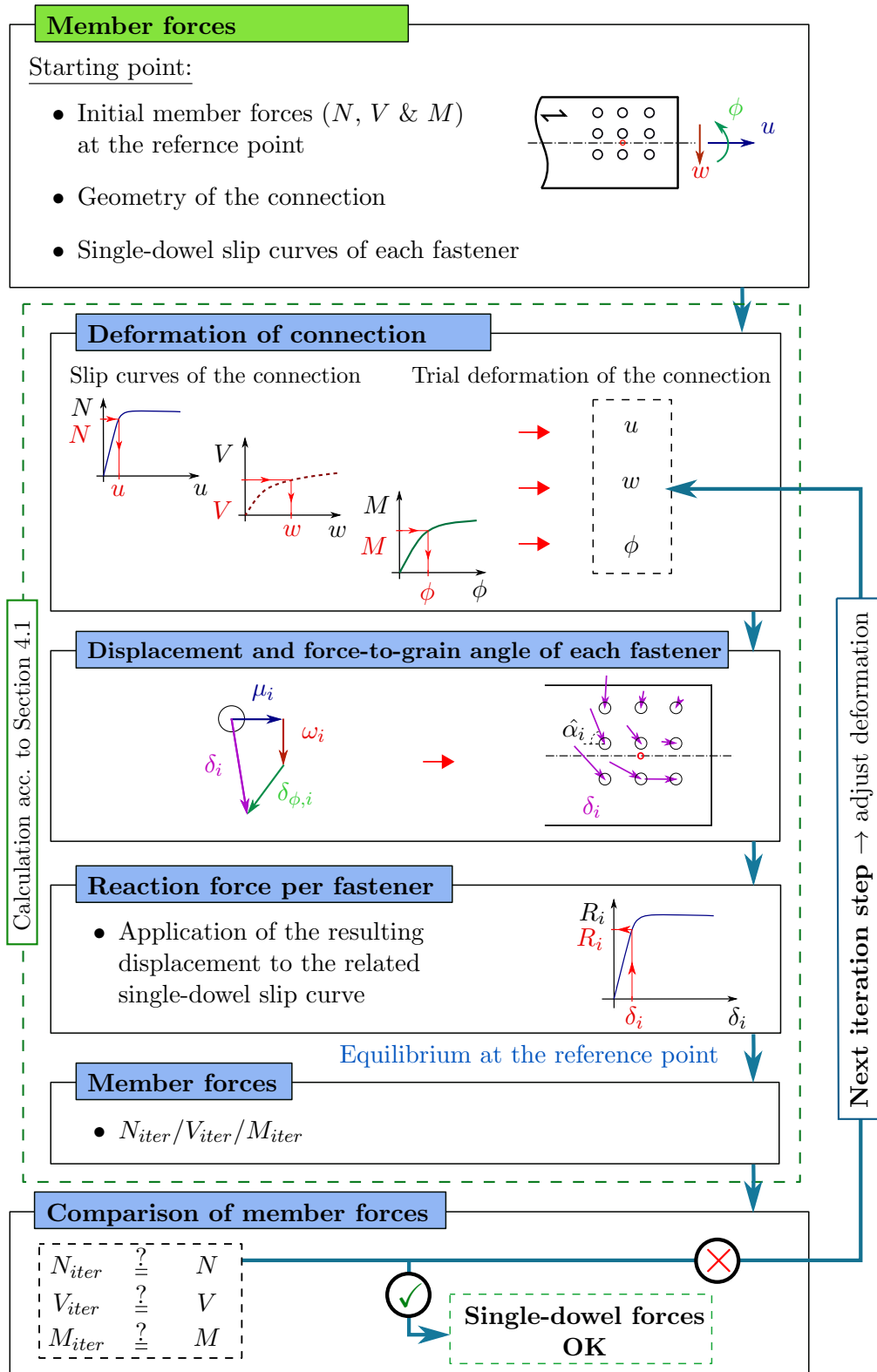
- determination of the displacement and the force-to-grain angle of each fastener,
- calculation of the reaction forces per fastener,

- calculation of the member forces ( $N_{iter}$ ,  $V_{iter}$  and  $M_{iter}$ ),
- comparison of the calculated member forces ( $N_{iter}$ ,  $V_{iter}$  and  $M_{iter}$ ) with the input member forces ( $N$ ,  $V$  and  $M$ ).

This procedure is continuously repeated until the calculated forces match the input member forces. Consequently, the corresponding dowel forces and their direction with respect to the grain direction are identified.

A detailed description of the implementation of the model in MATLAB is given in Appendix B.

### 4.2.2 Flow chart - back-calculation of dowel forces



## Design examples

The application of the model presented in Chapter 4 to single connections and the influence of the connection slip on the behavior of timber structures is shown in the following.

First, the behavior of the connection itself, as predicted by means of the modeling approach presented in Chapter 4, is discussed. In order to study the influence of the definition of single-dowel slip curves on the behavior of dowel connections and, further, on timber structures, different dowel connections and a timber structure are analyzed. Particularly, the structural behavior of a frame structure, based on the connection slip determined in Section 5.1, is investigated. A comparison between the approach considering the compliance of the connections, and the traditional structural analysis (no connection slip) is done.

Following assumptions are made for all design examples studied in this thesis:

- force direction is equal to the displacement direction of the single fastener,
- the bearing capacity and connection slip of the single fastener are based on mean values of timber properties,
- partial factors are not considered in the structural analysis, and
- maximum local deformation per fastener is restricted by two times of the fastener diameter ( $max\delta_i = 2.0 \cdot d$ ).

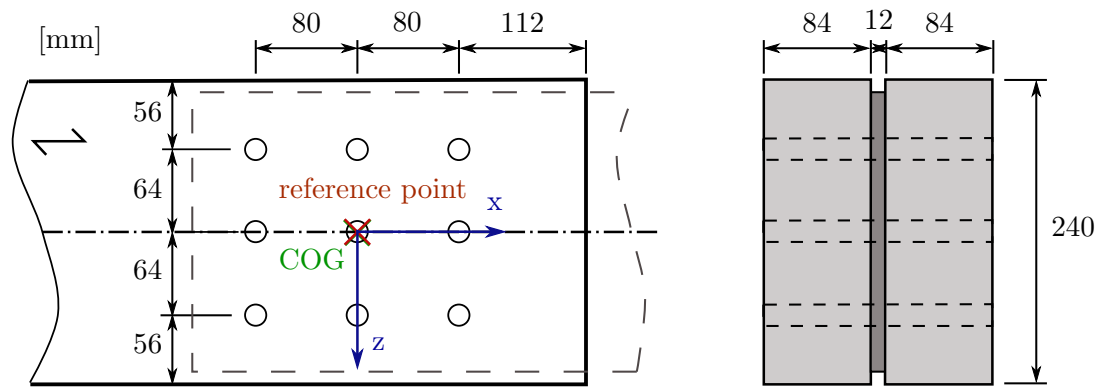


Figure 5.1: Elevation (left) and cross section (right) of a centric dowel connection.

## 5.1 Slip curves and limit surfaces of multi-dowel connections

The model is applied to study the interaction between the member forces  $N/V/M$ , or the deformations  $u/w/\phi$  respectively. For this purpose, limit surfaces related to specific deformation conditions of dowel connections are generated. In addition, the nonlinear load-deformation behavior of single connections is shown by means of connection slip curves. First, a simple multi-dowel connection is investigated. Starting from the centric configuration of this dowel connection within a timber element, modifications are done to show the influence of excentricities on the interaction between the member forces as well as on the slip curves. Moreover, the influence of contact elements in a connection is studied. In addition, the connection slip curves of a frame corner detail and a column base are determined. Unless otherwise specified, several connection slip curves are based on single-dowel slip curves determined by means of the sub-model.

### 5.1.1 Dowel connection design examples

In total, five different connections are investigated, encompassing three different configurations of a design example of a dowel connection and two connections of a typical frame structure.

#### Connection (1) - Centric connection

The basic configuration of this connection is shown in Figure 5.1. Nine dowels are situated symmetric to the reference point in both axis directions. The reference point itself is located at the beam axis. As a result of this configuration, the position of the reference point is equal to the position of the center of gravity of the connection for each load step, which means the single deformations lead only to their related member forces. Only the three diagonal elements of the stiffness matrix are non-zero elements.

Table 5.1: Design example of dowel connection – input parameters

	Simple connection (centric, excentric and contact)
Connection type	double shear steel-to-timber
<b>Fasteners</b>	
type	dowels
number	9
diameter $d$	16 mm
steel quality	S235
<b>Steel plate</b>	
thickness $t$	12 mm
location	center
<b>Timber</b>	
side member thickn. $t_1$	84 mm
strength class	GL28c
<b>Reinforcement</b>	no

### Geometry

Figure 5.1 shows the geometric properties of the centric connection. This multi-dowel steel-to-timber connection in double shear consists of nine dowels ( $d = 16\text{ mm}$ ). The distances between the dowels, as well as the edge distances are in accordance with the minimum distances according to EC 5. A summary of the geometric properties and the material qualities of the centric connection and its modifications is given in Table 5.1.

### Limit surfaces

The failure criterion of single-dowels for calculation of limit surfaces of connections is defined by means of maximum single-dowel deformations ( $\delta_i$ ) of  $0.9\text{ mm}$ ,  $1.0 \cdot d$ ,  $1.5 \cdot d$  and  $2.0 \cdot d$ . This means that the limit of the connection is reached as soon as the dowel with the highest deformation reaches a specific predefined deformation. The  $0.9\text{ mm}$  limit surface can be interpreted as the elastic limit surface, while the surface for  $2.0 \cdot d$  is considered to be the ultimate limit of the connection. Limit surfaces are generated for interactions of the global deformations ( $u/w/\phi$ ) as well as for the corresponding member forces ( $N/V/M$ ). Each point of the limit surfaces is related to a specific set of three member forces  $N/V/M$ , or deformations  $u/w/\phi$ , respectively.

In the following, two three-dimensional surface plots (see Figure 5.2), including four limit surfaces as mentioned above, are discussed. Additionally, two-dimensional profiles of the limit surfaces are presented. For each profile, one deformation is set equal to zero, which means only the interaction between two deformations or loads is considered.

The upper limit surface in Figure 5.2 is related to the interaction of the global deformations ( $u/w/\phi$ ). The limit surface is double-symmetric, which means the interaction of the global deformations is independent of the global deformation direction. The overall shape of the limit surface is more or less like a double cone. Therefore, the interaction between a deformation in beam axis and perpendicular to it and a global rotation is

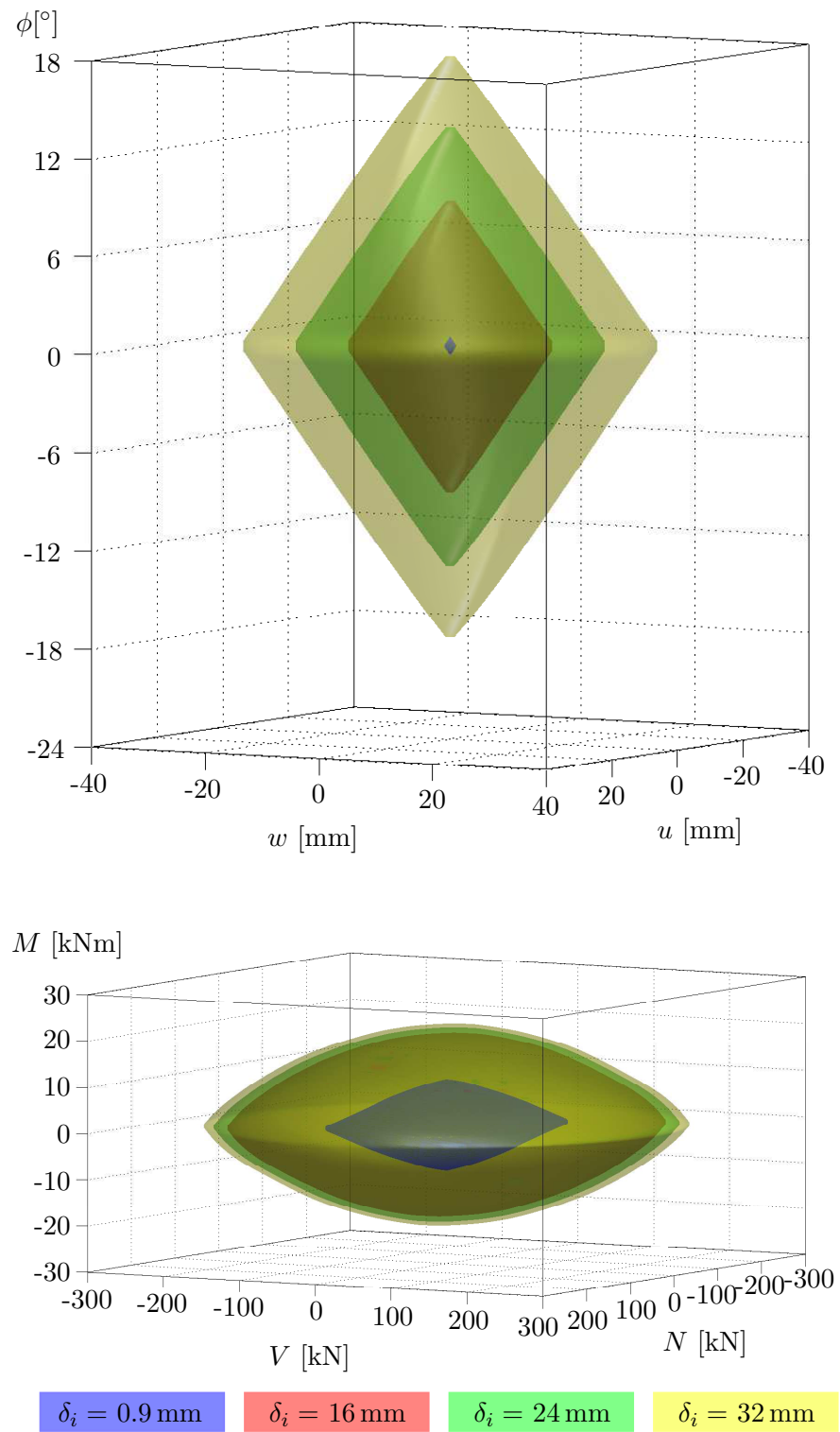


Figure 5.2: Limit surfaces of the deformation interaction (top) and member force interaction (bottom) for the maximum single-dowel deformation  $\delta_i$  - centric dowel connection.

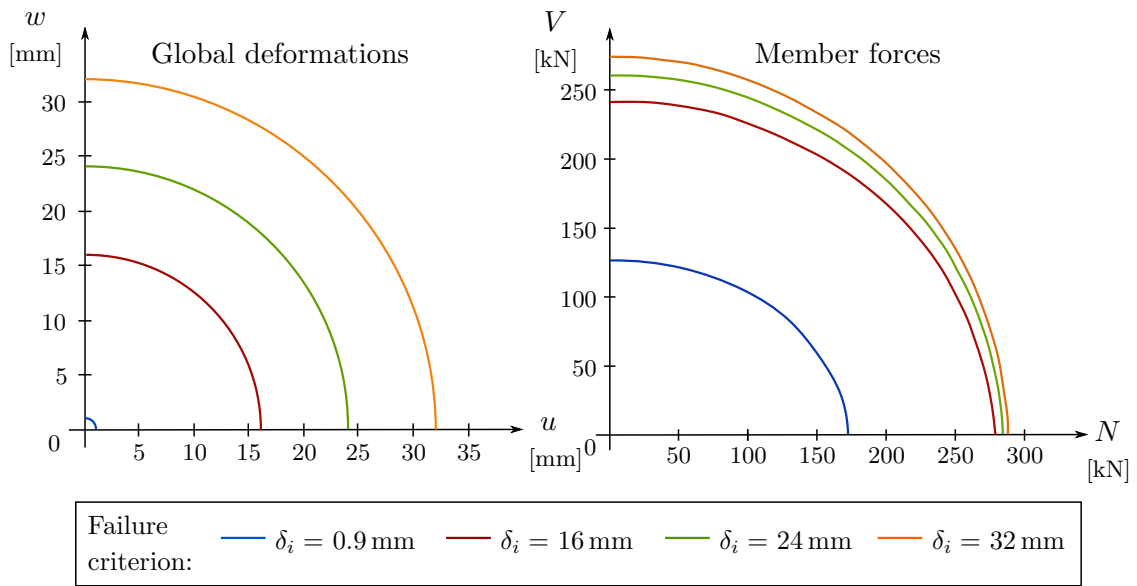


Figure 5.3: Interaction of  $u - w$  (left figure) and of  $N - V$  (right figure) for the maximum single-dowel deformation  $\delta_i$  - centric connection.

more or less linear, while the interaction between deformation  $u$  and  $w$  follows a circular path. The different cones in Figure 5.2 are related to different failure criteria of maximum single-dowel deformations of  $2.0 \cdot d$  (yellow),  $1.5 \cdot d$  (green),  $1.0 \cdot d$  (red). The blue double rotational cone in the middle is determined for  $\delta_i = 0.9$  mm. The double symmetric shape is due to the position of the reference point being equal to the center of gravity of the connection. Consequently, local deformation of the dowels are symmetric.

The second limit surface in Figure 5.2 shows the surfaces of the member force interaction. The shape of the limit surface is again double-symmetric. Compared to the deformation surface plot, the limit surface for  $\delta_i = 0.9$  mm is larger in relation to the other limit surfaces. This is due to the nonlinear single-dowel behavior. After the elastic limit (approximately at  $\delta_i = 0.9$  mm), only minor additional bearing forces can be activated, even for large dowel deformations.

Figure 5.3 to 5.5 show the interaction of specific deformation and member force interactions. Due to the symmetric behavior, only one quadrant of the limit surface is shown. In Figure 5.3, the interaction of the global axial ( $u$ ) and transverse ( $w$ ) deformation, and the interaction of the corresponding member forces is illustrated. This centric connection configuration causes only member forces related to the corresponding global deformations, which means normal ( $N$ ) and transverse ( $V$ ) forces for the interaction of  $u$  and  $w$ . The left figure shows the deformation interaction ( $u - w$ ). All curves of the limit surfaces are circles with a radius of the size of the failure criterion. In comparison, the interaction of the member forces is different. The shape is approximately elliptic, since the same deformation in transverse and in axial direction yields higher reaction forces in axial direction than in transverse direction. Nevertheless, for a uniform shear force, the bearing capacity corresponding to the plastic failure criteria ( $\delta_i = 2.0 \cdot d$ ) almost at the

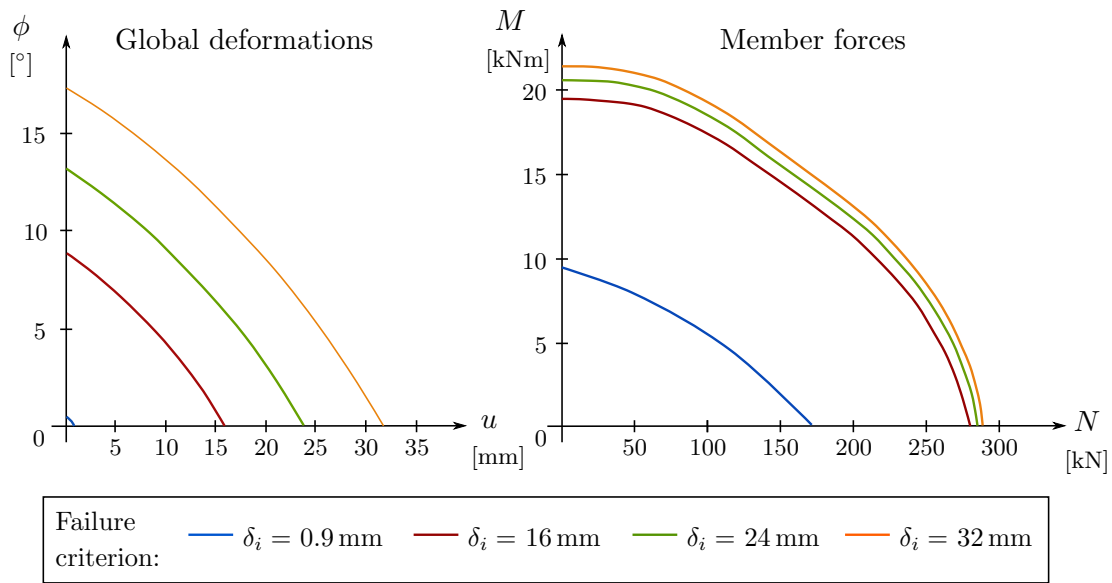


Figure 5.4: Interaction of  $u - \phi$  (left figure) and of  $N - M$  (right figure) for the maximum single-dowel deformation  $\delta_i$  - centric connection.

level of the normal force, since the effect of hardening for wood loaded perpendicular to the grain leads to increasing reaction forces of the single-dowels.

The interaction of axial deformation ( $u$ ) and rotation of the cross section ( $\phi$ ) is presented in Figure 5.4. The deformation interaction (left figure) is almost linear, only a minor positive curvature can be seen. The interaction of the member forces  $N - M$  can be separated into three parts. Small moments or small normal forces slightly reduce the bearing capacity of the other member force. Particularly, small normal forces have only a minor influence on the moment bearing capacity, which is indicated by the almost horizontal lines in Figure 5.4. For higher normal forces and moments, there is more or less linear interaction.

The interaction of transverse deformation ( $w$ ) and rotation of the cross section ( $\phi$ ), illustrated in Figure 5.5, is similar to the one of the interaction  $u - \phi$ . The overall shape of the curves is the same. The only difference is given in the size of the shear force ( $V$ ), which is lower than the normal force ( $N$ ) in the interaction  $u - \phi$ . The reason lies in the lower reaction force perpendicular to the grain compared to the reaction force in grain direction at the same local deformation of the single-dowel.

### Connection slip curves

Connection slip curves calculated by means of the model presented at Chapter 4 are discussed. Again, it should be highlighted, that the connection slip curves are determined by means of uniform global deformations, which means the interaction between the global deformations, or the member forces respectively, as previously shown with limit surfaces is not considered here. The same position of the reference point and center of gravity of the connection leads to a stiffness matrix with non-zero elements at the diagonal only.

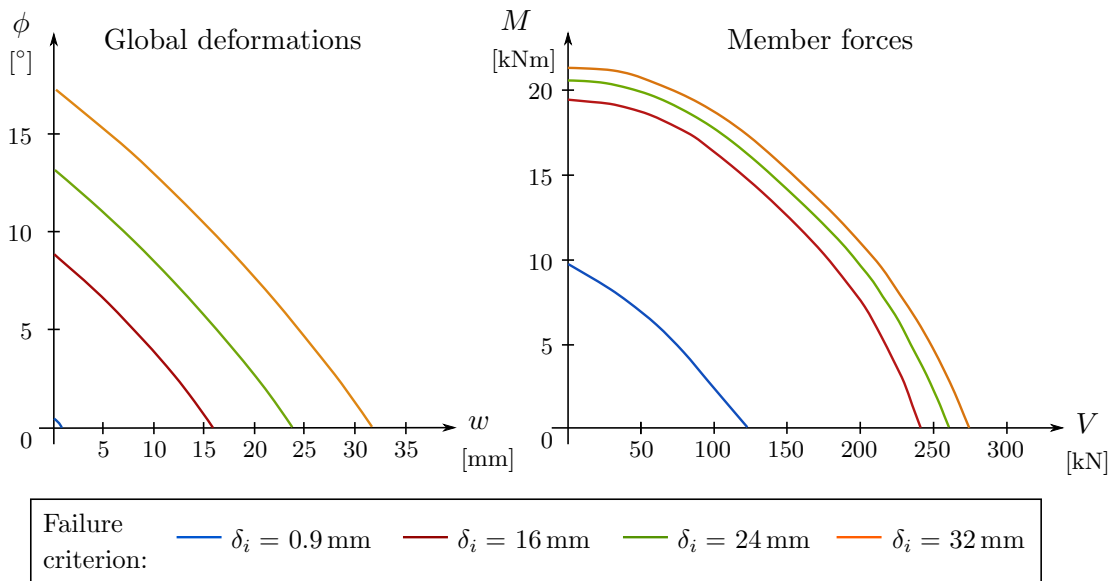


Figure 5.5: Interaction of  $w - \phi$  (left figure) and of  $V - M$  (right figure) for the maximum single-dowel deformation  $\delta_i$  - centric connection.

Connection slip curves of the centric configuration of the dowels are illustrated as continuous blue lines in Figure 5.6. Since the connection slip curves are based on the nonlinear single-dowel slip curves, determined by means of the sub-model (method 3), the connection slip curves are also nonlinear. The top-left curve in Figure 5.6 is related to the normal forces ( $N$ ) caused by global axial deformations ( $u$ ). In this special case, the reaction force of the connection (normal force) is the sum of the reaction forces of the single dowels and, as a result, the shape of the connection slip curve is the same as the corresponding one of the single dowel. In this special case, only a global axial deformation is applied, which leads to axial single dowel deformations only (no interaction). The slip curve can be separated approximately into an elastic part of high stiffness and a plastic part with minor increasing normal forces. However, between this two parts a transition zone can be found.

The upper right plot in Figure 5.6 is related to the shear forces ( $V$ ) caused by transverse deformations ( $w$ ). In general, the comments given for the slip curve ( $u - N$ ) are also valid. Compared to the normal force slip curve, the slip curve for the shear forces is characterized by a plastic zone with a remarkable increase of the shear force. This increasing forces are based on hardening and the rope effect of wood perpendicular to the grain direction as considered in the single-dowel slip curve. The ultimate bearing capacity in case of the normal force and the shear force are at approximately the same level. The shape of the moment - rotation slip curve ( $M - \phi$ ) is something in-between the curves for the normal force and the shear force, since the moment is based on single-dowel reaction forces with different force-to-grain directions (see Figure 5.6). As a result, the moment is partly based on single-dowels with hardening effects. Additionally, each fastener has a different local displacement depending on the distance between the fastener and the center of rotation. Different displacements mean different reaction forces

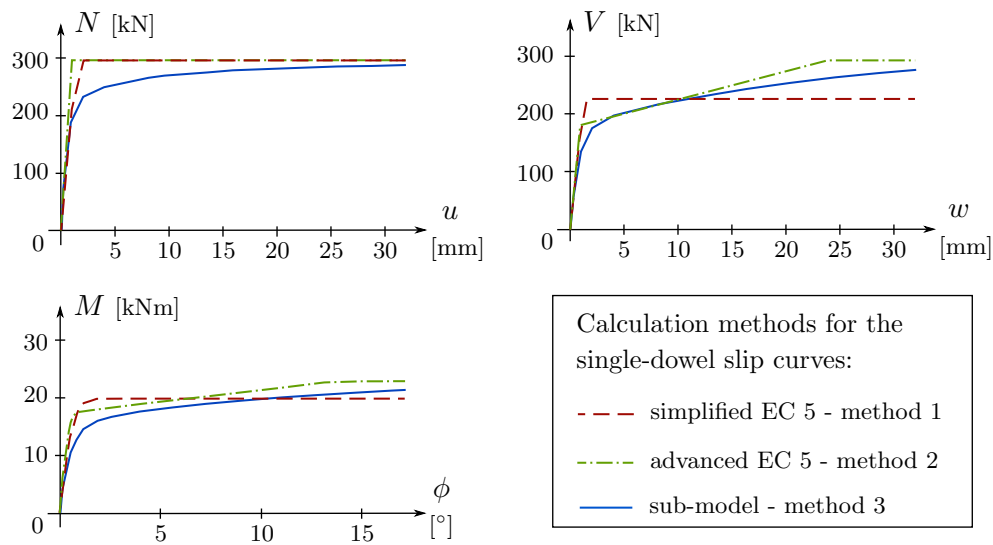


Figure 5.6: Comparison of the global connection slip curves, calculated by means of the three different calculation methods for single-dowel slip curves - centric connection.

for each fastener. Increasing rotation of the cross section leads to force redistribution, since the maximum stressed fastener is probably at a plastic stage, while other dowels still behave elastic and, take therefore take higher additional forces.

Finally, the connection slip curves based on the three different single-dowel calculation methods are compared to each other (see Figure 5.6). As regards the normal force slip curves, the bearing capacity of all three methods is very similar. However, at low plastic deformations the normal forces determined by the methods based on EC 5 are considerably higher than based on the sub-model method. In the second figure (shear force  $V$ ) and third figure (moment  $M$ ), a good correlation between the advanced EC 5 method and the sub-model method is given. The simplified method however, overestimates the reaction forces for low plastic deformations and underestimates the reaction forces for high plastic deformations as compared to the two other methods.

## Connection (2) - Excentric connection

Compared to the centric configuration, the dowel group is moved 40 mm in vertical direction to model an excentric connection. As a result of the excentricity, additional member forces appear in the stiffness of the connection as well as in the slip curves, which are, additionally, changed.

### Geometry

Geometric properties are shown in Figure 5.7 and summarized in Table 5.1. The center of gravity (COG) of the connection is not marked, since the COG changes its position due to force redistribution for increasing loading. All the other properties are equal to the basic centric configuration (see Connection (1)).

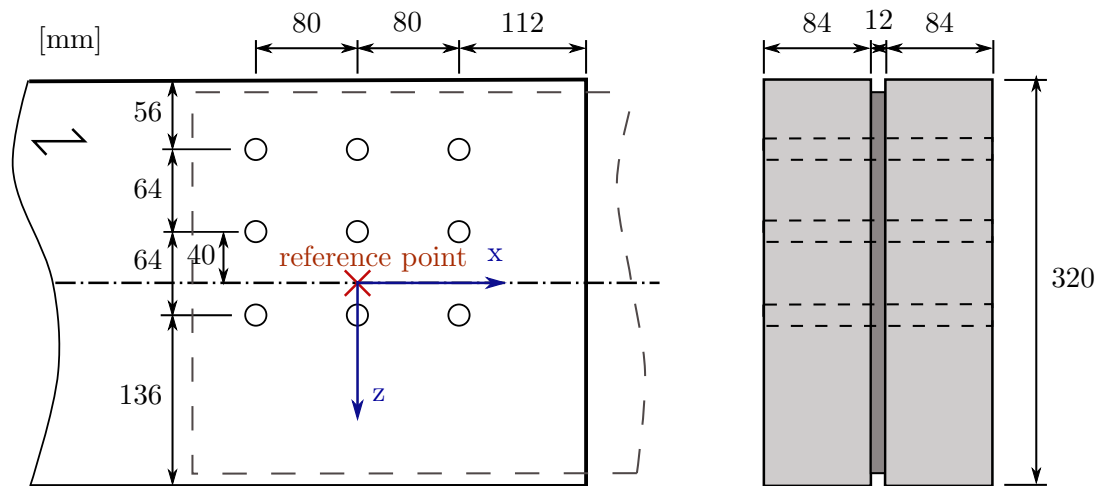


Figure 5.7: Elevation (left) and cross section (right) of a excentric dowel connection.

### Limit surfaces

The same failure criteria as used for the centric connection are applied, namely maximum single-dowel deformations ( $\delta_i$ ) of  $0.9 \text{ mm}$ ,  $1.0 \cdot d$ ,  $1.5 \cdot d$  and  $2.0 \cdot d$ . Again, three-dimensional figures by means of deformation limit surfaces and member force limit surfaces are generated. Additionally, profiles of this figures showing the interaction of specific deformations are discussed.

The upper limit surface in Figure 5.8 is related to the interaction of the global deformations ( $u/w/\phi$ ). Compared to the centric connection, the shape of the limit surface is non-symmetric, which is an indicator for an excentric connection since uniform global deformations cause additional deformations in other directions. As a result of the asymmetric shape, the interactions of the global deformations dependent on the direction of the single global deformations. E.g. the interaction of a positive axial deformation ( $u$ ) and a positive rotation ( $\phi$ ), is not the same as the interaction of a positive axial deformation ( $u$ ) and a negative rotation ( $\phi$ ). Similar to the centric connection, the yellow surface is related to the failure criterion  $\delta_i = 2.0 \cdot d$ , the green surface to  $\delta_i = 1.5 \cdot d$ , the red surface to  $\delta_i = 1.0 \cdot d$  and the point in the middle to  $\delta_i = 0.9 \text{ mm}$ .

The second plot in Figure 5.8 shows the member force interaction. Since the deformation limit surface is asymmetric, also the member force limit surface is asymmetric. Basically, the limit surface seems to be the centric member force limit surface rotated around the  $N - V$  plane. Therefore, the same  $N - V$  bearing capacity as for the centric connection is given for the excentric connection with an additional moment that compensates the excentricity (cf. Figure 5.2).

In the following, the deformation interaction as well as the member force interaction are discussed. Since both, the deformation and the member force interaction are asymmetric, the entire profile is shown.

In Figure 5.9, the interaction of the global axial ( $u$ ) and transverse ( $w$ ) deformation, and the interaction of their resulting member forces are shown. Besides normal forces

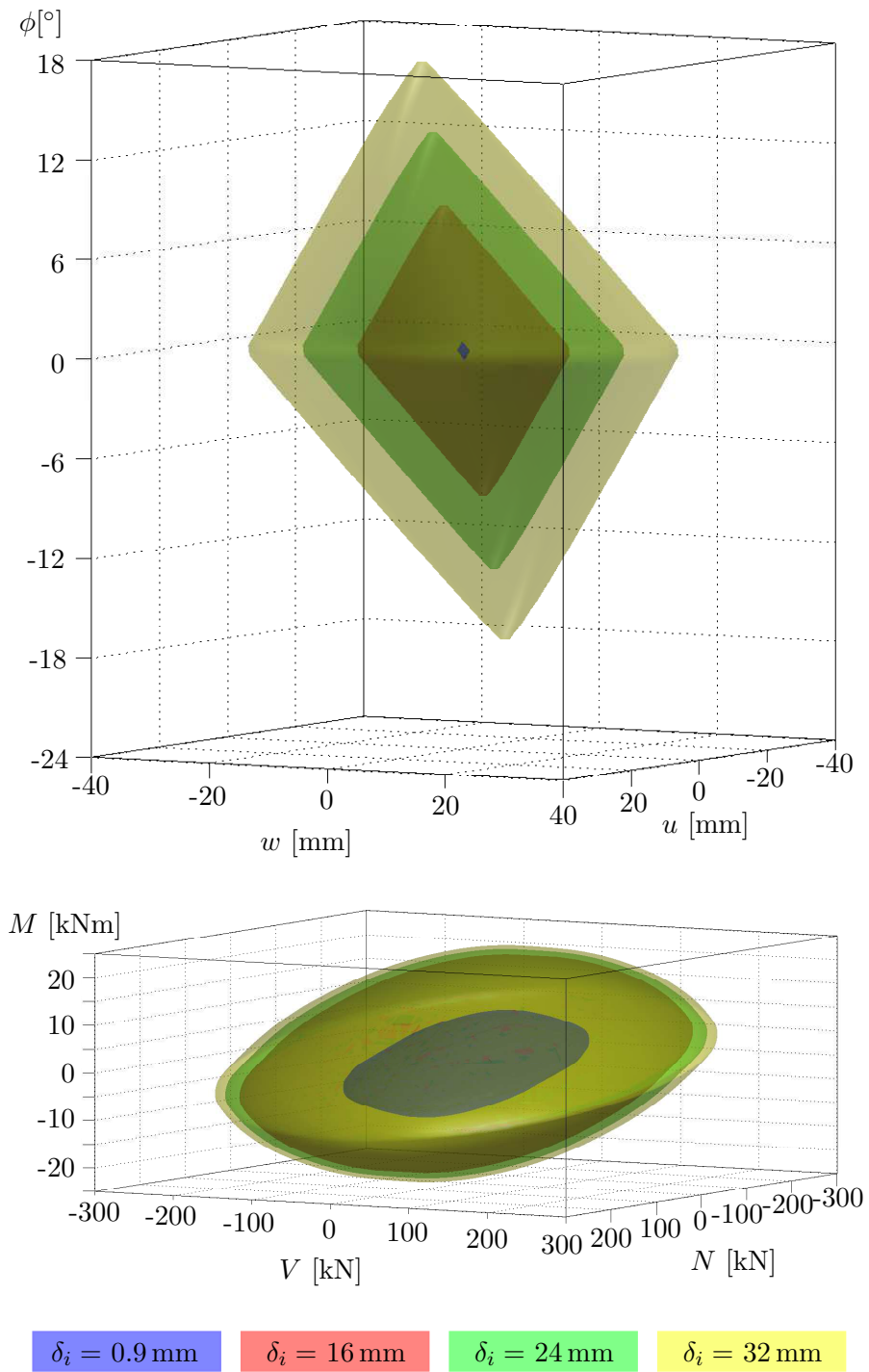


Figure 5.8: Limit surfaces of the deformation interaction (top) and member force interaction (bottom) for the maximum single-dowel deformation  $\delta_i$  - eccentric dowel connection.

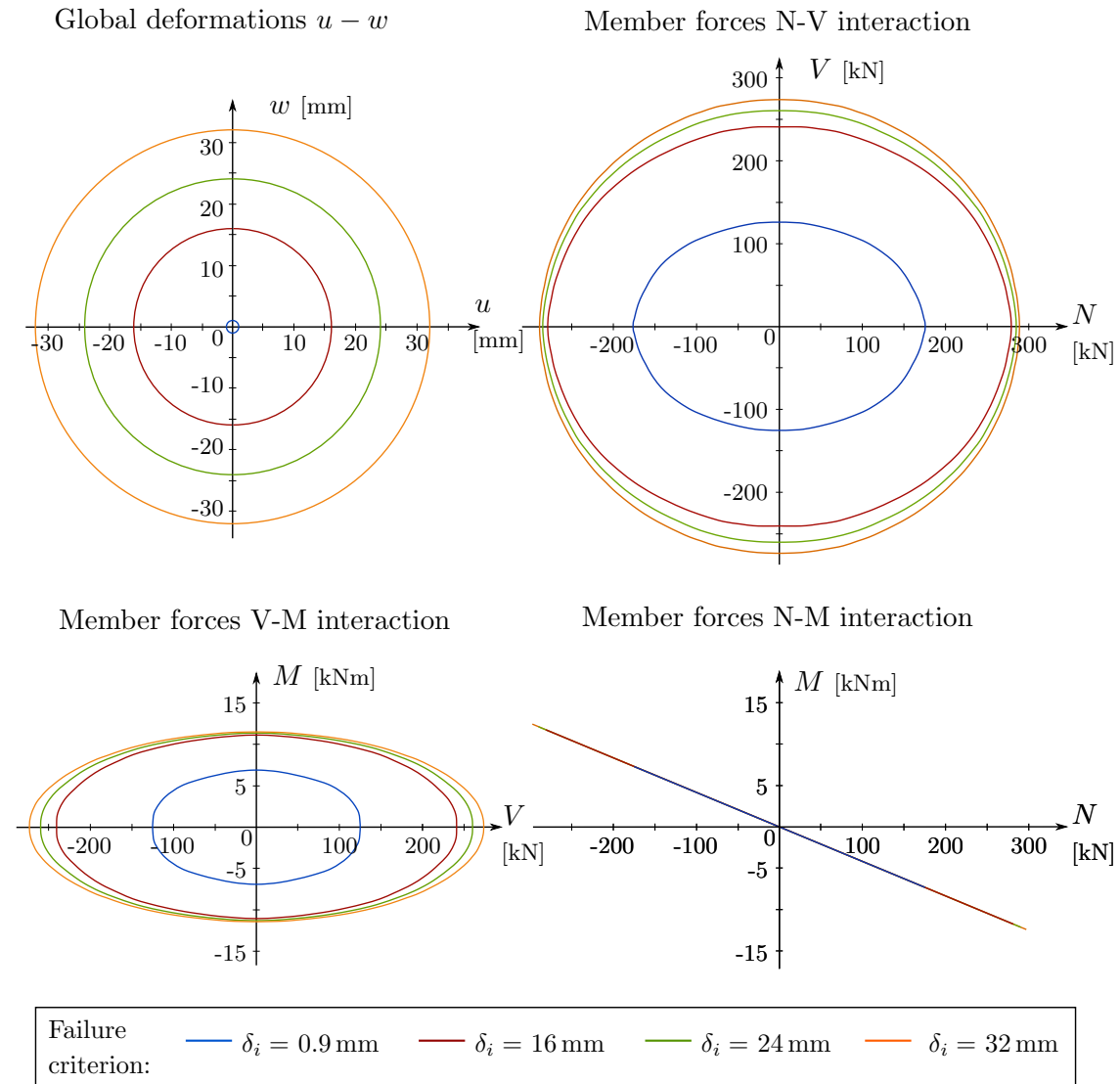


Figure 5.9: Interaction of  $u - w$  (top left figure) and of member forces caused by these deformations: interactions of  $N - V$  (top right figure),  $V - M$  (bottom left figure) and  $N - M$  (bottom right figure) for the maximum single-dowel deformation  $\delta_i$  - excentric connection.

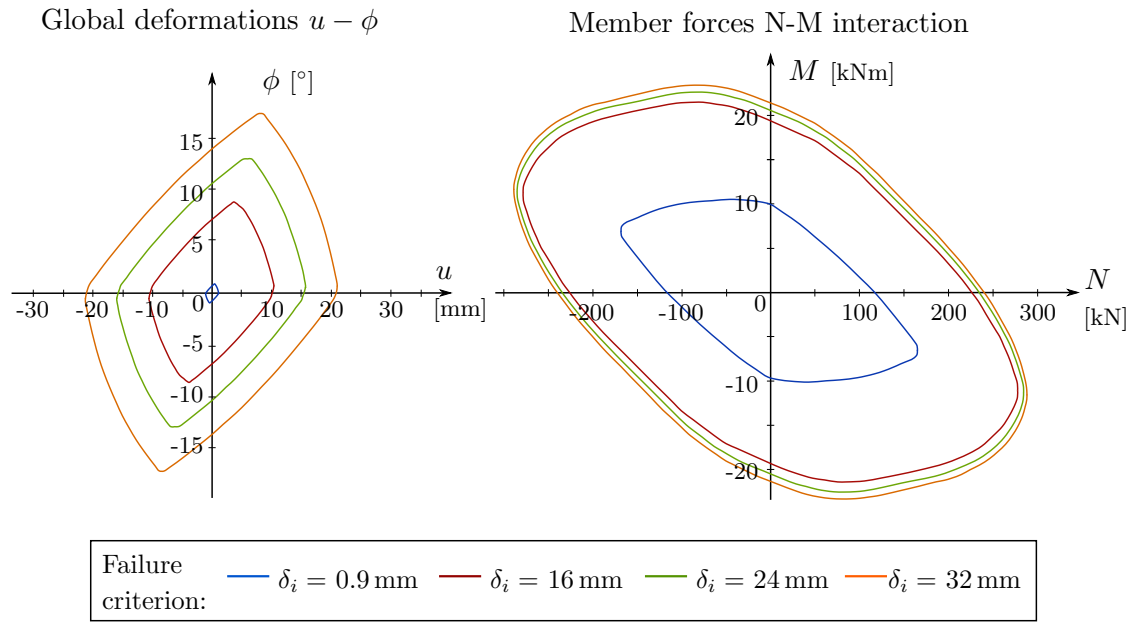


Figure 5.10: Interaction of  $u - \phi$  (left figure) and of member forces caused by these deformations: interactions of  $N - M$  (right figure) for the maximum single-dowel deformation  $\delta_i$  - excentric connection.

( $N$ ) and shear forces ( $V$ ), this excentric connection configuration causes also moments ( $M$ ). The interaction of  $u - w$  is again a circle with a radius of the failure criterion, i.e. the limit deformation. The shape of the normal force  $N$  and shear force  $V$  interaction is similar to the one of the centric connection. Again, elliptical curve for the  $N - V$  interaction corresponds to the interaction  $u - w$ . However, compared to the centric connection, the excentricity of the connection yields in additional moment (bottom left and bottom right plot in Figure 5.9). The linear interaction of  $N - M$  is illustrated in Figure 5.9.

The next plot (see Figure 5.10) is related to the interaction of  $u - \phi$  and of the member forces caused by this interaction. Both figures, the one of the deformation limit surface, as well as the member force limit surface can be seen as rotated and slightly deformed limit surfaces of the centric connection (cf. Figure 5.4). The right plot in Figure 5.10 shows the normal force ( $N$ ) - moment ( $M$ ) interaction. The excentricity of the connection leads to the effect that for certain normal forces, the moment bearing capacity even increases. This means that for these combinations, the moment bearing capacity is even higher than for an uniformly acting moment. The same effect holds for normal force. There are no shear forces caused by the combination of axial deformations and rotation of the cross section since the connection is only excentric to the longitudinal axis.

Figure 5.11 shows the interaction of transverse deformations ( $w$ ) and rotation of the cross section ( $\phi$ ). The shape of the curves of the interaction  $w - \phi$ , as well as of the interaction  $V - M$  is similar to the one of the centric connection (cf. Figure 5.5). However, the excentricity of the connection causes also normal forces, which is shown in

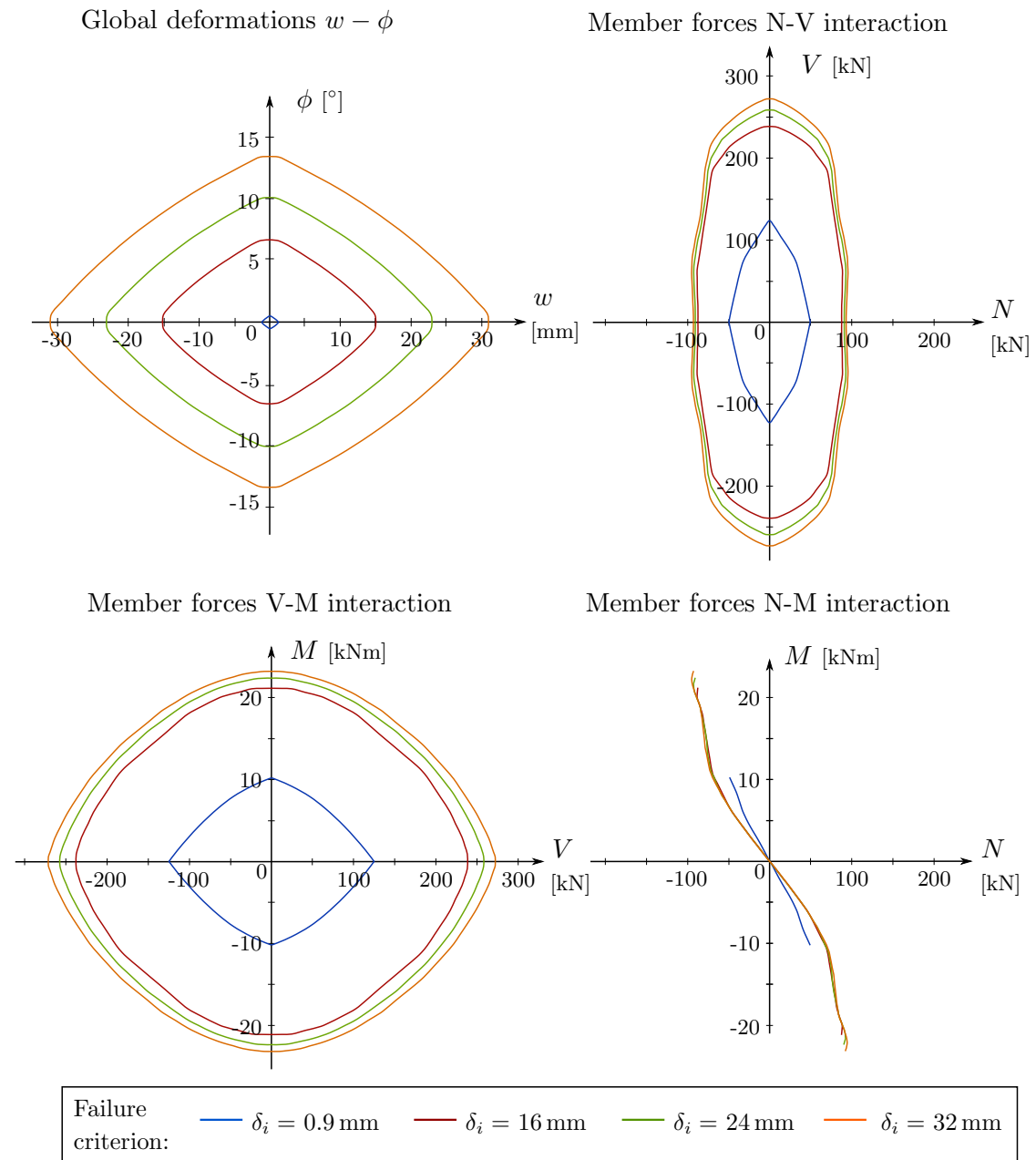


Figure 5.11: Interaction of  $w - \phi$  (top left figure) and of member forces caused by these deformations: interactions of  $N - V$  (top right figure),  $V - M$  (bottom left figure) and  $N - M$  (bottom right figure) for the maximum single-dowel deformation  $\delta_i$  - excentric connection.

the top right plot in Figure 5.11 ( $N - V$  interaction) and bottom right figure ( $N - M$  interaction). Both curves are highly nonlinear. This non-linearity is mainly a reason of force redistributions within the connection and the non-linearity of the single-dowel slip curves used as input for the model of the connection.

### Connection slip curves

Connection slip curves of the excentric connection are presented in Figure 5.12. Only positive global deformations are shown, since several curves are symmetric in compression and tension. Slip curves are calculated using the method discussed in Chapter 4, based on the single-dowel slip curves determined by a sub-model (method 3). The red dashed lines in Figure 5.12 are related to the excentric connection, which are compared to the slip curves of the centric connection (blue continuous lines). In case of the excentric connection, five non-zero global slip curves exist. In addition to the slip curves for the relationship between  $N - u$ ,  $V - w$  and  $M - \phi$ , a global axial deformation causes also moments ( $M - u$ ) and a normal force causes a rotation of the cross section ( $N - \phi$ ). The slip curves for  $N - u$  and  $V - w$  are identical to the slip curves of the centric connection. Moments caused by a rotation of the cross section ( $M - \phi$ ) are even higher than the one of the centric connection since the distance between the reference point and the most exposed dowel is higher. Normal forces as a result of the rotation of the cross section are about one third of the normal forces caused by an axial deformation, but with opposite direction. The maximum moment caused by an axial deformation of the connection is approximately half of the moment caused by rotation, but again with opposite direction. The other slip curves in Figure 5.12 are again zero for the excentric as well as for the centric connection (cf. Figure 5.6).

### Connection (3) - Centric connection with contact elements

The last design example of a dowel connection is related to the introduction of an additional contact condition. The influence of a contact area on the connection behavior shall be shown.

#### Geometry

Geometric properties of the connection are identical to the one of the centric connection. However, additionally to the steel dowels, a contact area is considered at the end of the beam (see Figure 5.13). For implementation in the MATLAB code (see Chapter 4), the contact area is approximated by 8 contact points along the beam edge (see Figure 5.14). The contact behavior allows forces in positive longitudinal beam direction to be transferred, i.e. compressive loads only. Forces caused by friction between the beam end and the contact area are neglected. Consequently, the behavior of the connection depends on the dowels as well as on the contact characteristics. Moreover, the behavior becomes load direction dependent for loads in beam axis. For positive deformations, the dowels act in combination with the stiff contact area, while only the dowels are able to transfer loads in case of negative deformations  $u$ .

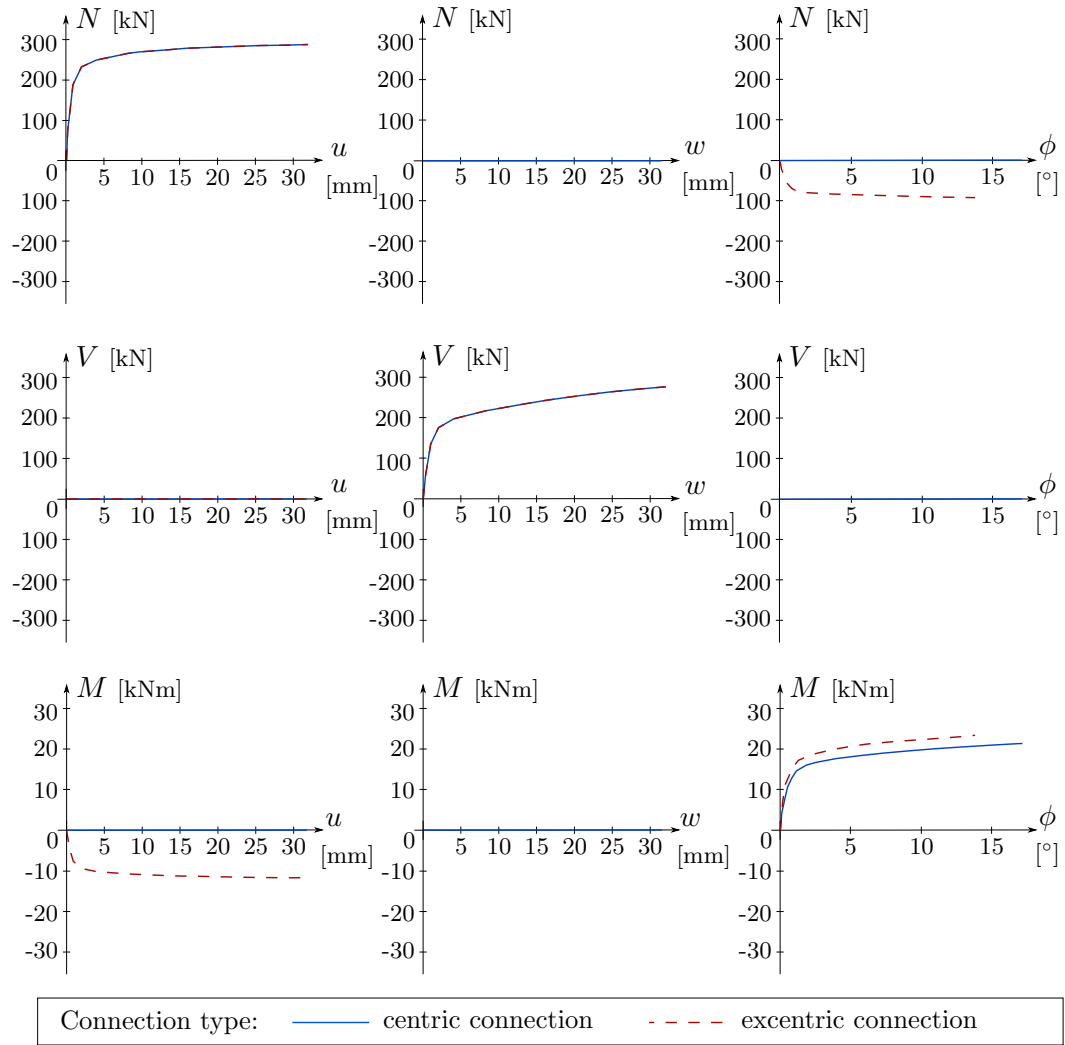


Figure 5.12: Comparison of global connection slip curves for Connection 1 - Centric connection (continuous - blue line) and Connection 2 - Excentric connection (dashed - red line) simple (based on method 3 for the single-dowel slip curves).

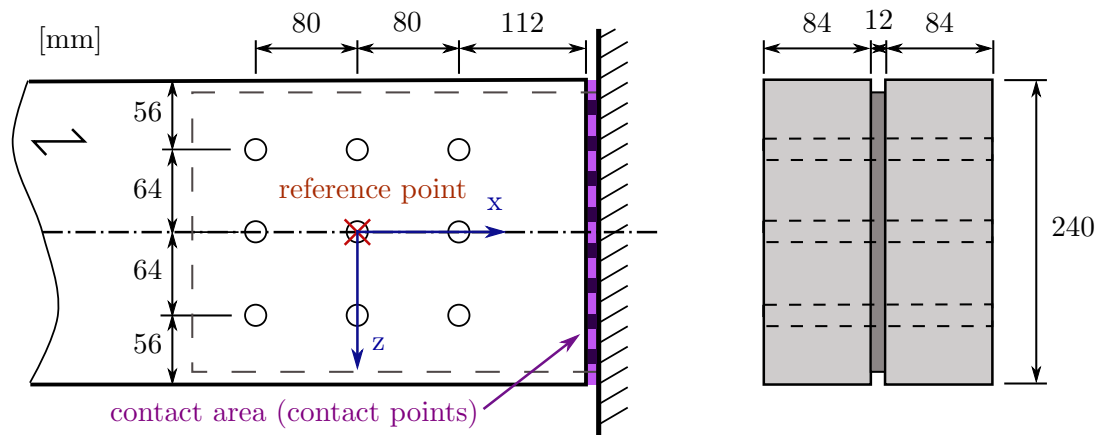


Figure 5.13: Elevation (left) and cross section (right) of the centric connection, including a contact condition.

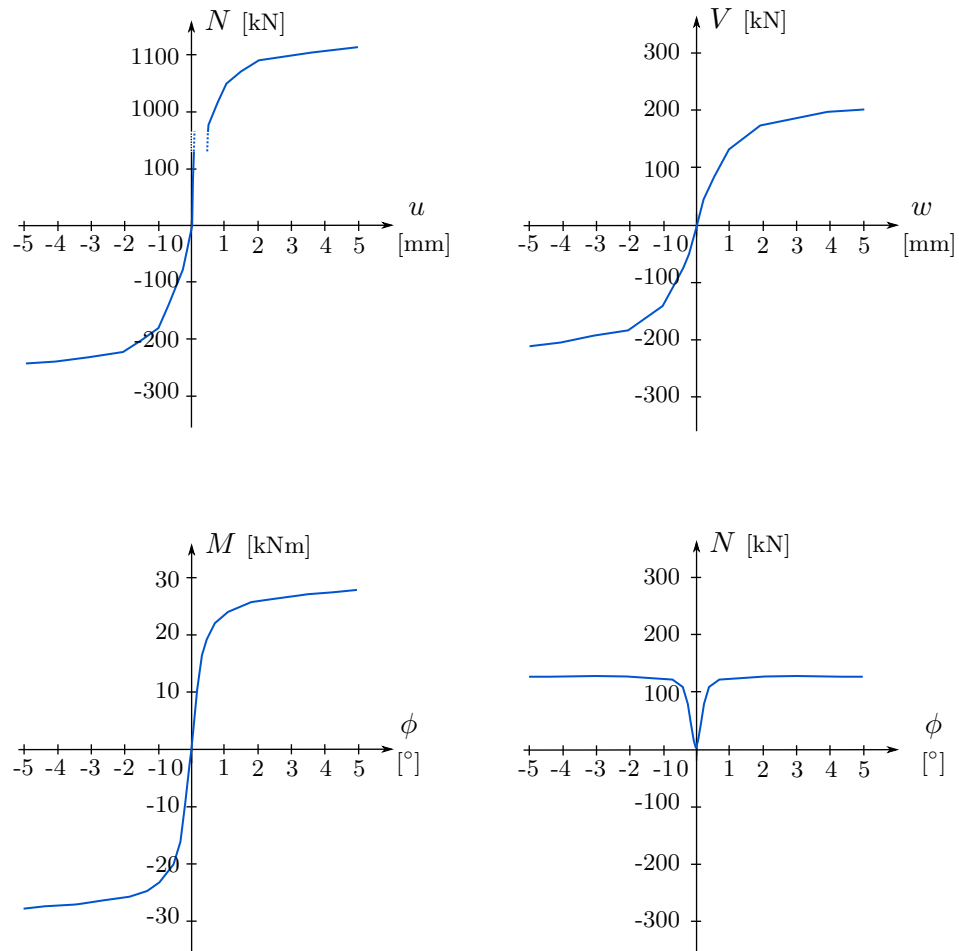


Figure 5.14: Connection slip curves for the centric connection including a contact condition in x-direction.

### Connection slip curves

Global slip curves for the centric connection with a contact area are shown in Figure 5.14. The slip curves for the relationship between  $V - w$  and  $M - \phi$  are antisymmetric. The shear force - transverse deformation relation (top right figure) is independent from the contact area, which means that the slip curve is the same as for the connection without contact condition (see Figure 5.14). The moment bearing capacity (bottom left figure) increases by about 50% compared to the connection without contact since the moment is partly carried by the contact area. Additionally, the rotation of the cross section causes normal forces (bottom right figure) in positive direction, since a rotation leads to reaction forces in axial direction in the contact area. The top left plot in Figure 5.14 shows the normal forces caused by axial deformation of the connection. For positive axial deformations, the contact condition is activated, which leads to a considerable increase of the normal forces. Until the limit of the contact area is reached (approximately at 0.5 mm), the load-deformation behavior is dominated by the behavior of the contact area. Thereon, also the dowels are activated, which leads to a further increase of the normal forces. For deformations on the negative longitudinal direction the contact area has no effect, which means that the entire load is carried by the dowel group. As a result, the bearing capacity in positive direction is approximately five times higher than in negative longitudinal direction (see Figure 5.14).

### 5.1.2 Typical connections of a timber frame structure

The following two connections are related to the frame system presented in the following Section 5.2. A description of the frame corner and the column base, followed by the description of the connection slip curves, is given. Both connections, the column bases and the frame corners, are of the same connection type. Multiple dowel steel-to-timber connections in double-shear are used. The steel plate is located in the middle of the cross section.

#### Connection (A) - Frame corner

##### Geometry

Figure 5.15 shows the elevation and cross section of the connection between the timber column and the beam. Transmission of the forces from one timber element to the other is done indirectly via a 12 mm thick steel plate located in the middle of the timber members. The column and the beam are connected by 28 dowels to the steel plate on each end. Dowels of a steel quality S235 and a diameter of  $d = 16$  mm are used. The dowels are set at grid points with a mesh width of  $80 \times 80$  mm. In order to prevent brittle failure modes, such as lateral splitting, in total, 12 screws of the dimension of  $8 \times 330$  mm are installed as reinforcement of the connection. On each side of the steel plate, six screws in vertical direction of the beam are situated. Several geometric properties and material qualities are summarized in Table 5.2.

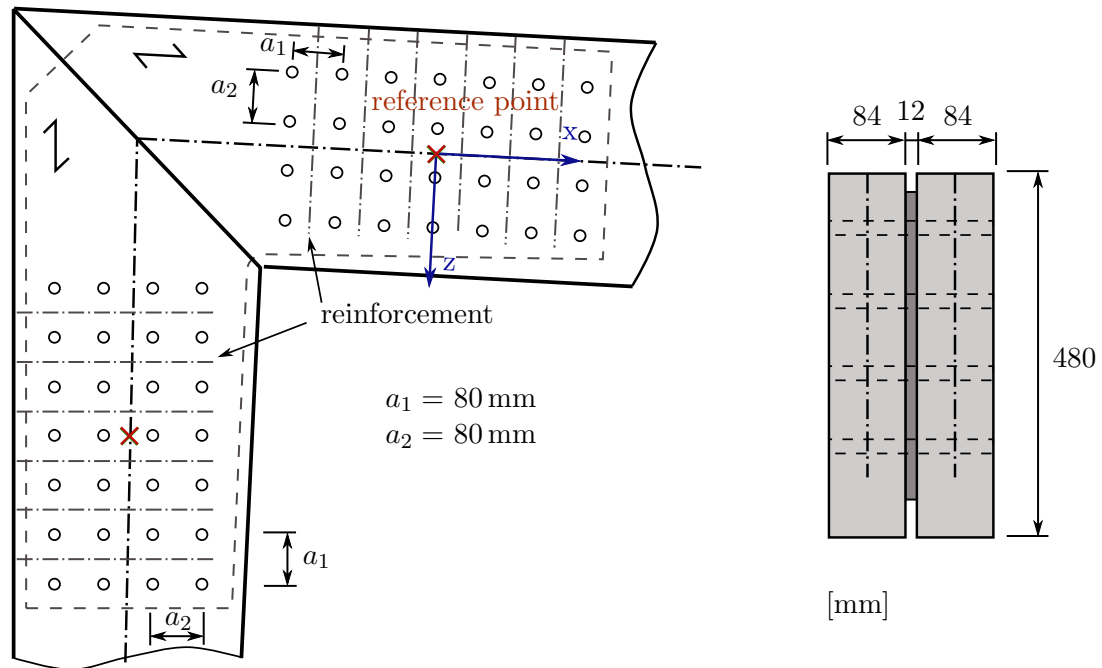


Figure 5.15: Frame corner (Connection (A) in Figure 5.20).

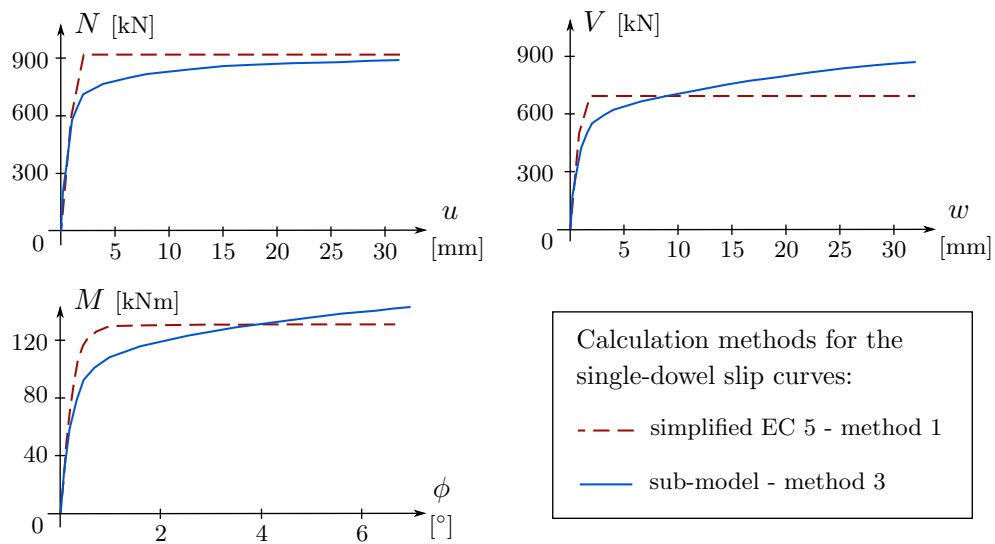


Figure 5.16: Connection slip curves of Connection (A) - Frame corner. Based on single-dowel slip curves determined by method 1 (simplified EC 5) and method 3 (sub-model).

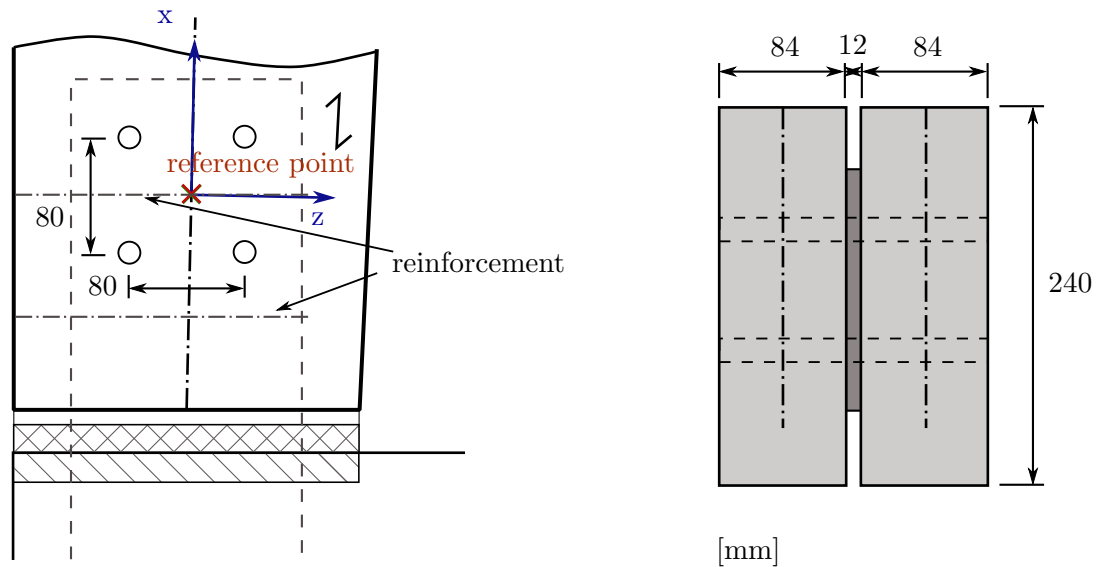


Figure 5.17: Column base (Connection (B) in Figure 5.20).

### Connection slip curves

The geometric configuration and the material properties are identical to the simple connection design examples presented in Section 5.1.1, which means the shape of the frame corner slip curves can be compared with the connection slip curves of the simple design example. In Figure 5.16, the three non-zero slip curves of the frame corner are shown. The blue continuous slip curves are based on the single-dowel slip curves determined by means of the sub-model (method 3) and the red dashed lines are related to the calculation based on the simplified EC 5 determination (method 1). As discussed in the previous section, the sub-model slip curves are nonlinear. Compared to the simplified method based on EC 5 (red dashed line), the normal force are underestimated for low plastic deformations. The bearing capacities of  $N$  is about the same for both methods. Shear forces ( $V$ ) as calculated by method 1 are mainly lower than determined by method 3, since hardening is neglected. The same difference is found for the moment slip curve ( $M - \phi$ ). Since the connection is double-symmetric to the reference point, the slip curves in Figure 5.16 are the only non-zero slip curves.

### Connection (B) - Column base

#### Geometry

In general, the same connection type as for the frame corner is used. Four dowels of a diameter of 16 mm transfer the loads through a 12 mm thick steel plate to the basis. Dowels are installed at distance of 80 mm between the dowels. Since the cross section of the column changes linearly from the basis to the frame corner, a negligible small excentricity between center of gravity of the dowel-group and the column axis exists (see Figure 5.20). In total, 4 screws of the dimension of  $8 \times 200$  mm are installed as reinforcement of the connection. On each side of the steel plate, two screws in transverse

Table 5.2: Frame - Connection parameters.

	Frame corner	Column base
Connection type	double shear steel-to-timber	double shear steel-to-timber
<b>Fasteners</b>		
type	dowels	dowels
number	28	4
diameter $d$	16 mm	16 mm
steel quality	S235	S235
<b>Steel plate</b>		
thickness $t$	12 mm	12 mm
location	center	center
<b>Timber</b>		
side member thickn. $t_1$	84 mm	84 mm
strength class	GL28c	GL28c
<b>Reinforcement</b>	yes	yes

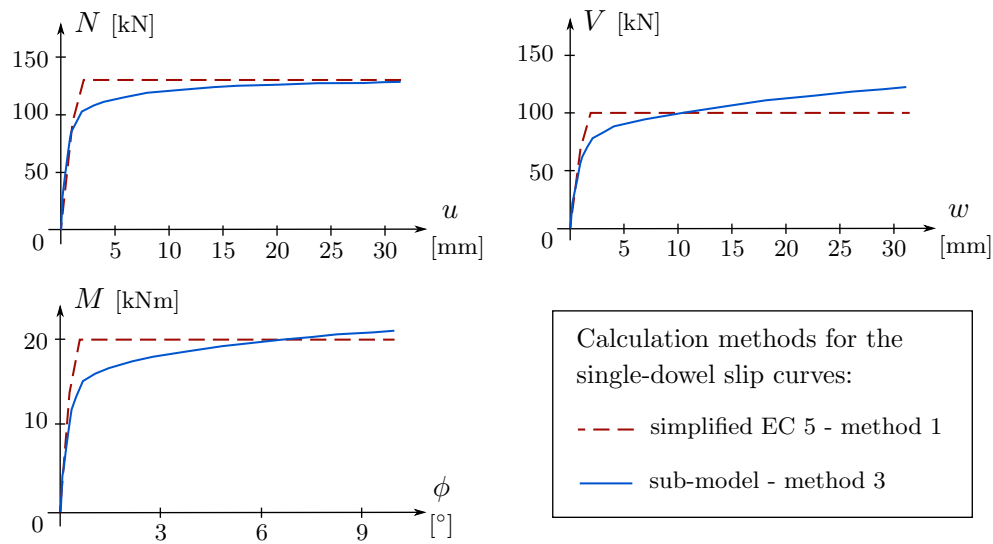


Figure 5.18: Connection slip curves of Connection (B) - Column base. Based on single-dowel slip curves determined by method 1 (simplified EC 5) and method 3 (sub-model).

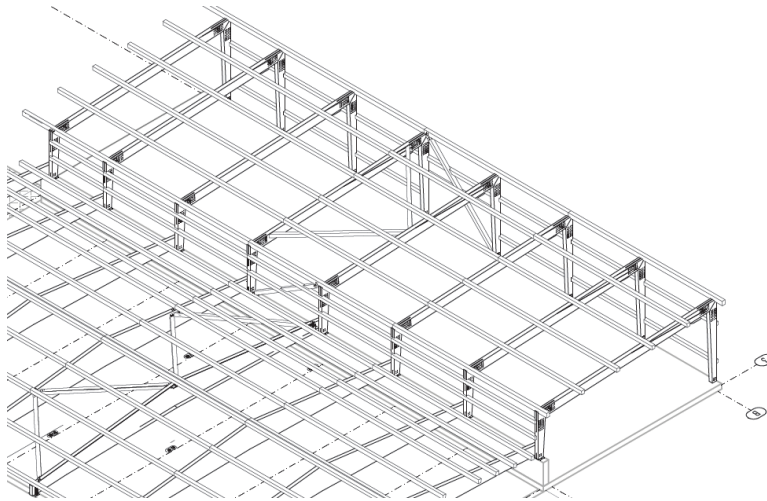


Figure 5.19: Investigated timber frame structure.

direction of the beam are situated. A summary of geometric and material properties is given in Table 5.2.

### Connection slip curves

The three connection slip curves are shown in Figure 5.18. The corresponding curves are determined based on single-dowel slip curves calculated by the sub-model (method 3) and the simplified EC 5 method (method 1). A description of the connection slip curves is not given, since the shape of the curves is identical to the shapes of the frame corner connection slip curves. However, the normal force ( $N$ ) and shear force ( $V$ ) bearing capacity of the column base is only considerably lower than the frame corner bearing capacity. Furthermore, the moment bearing capacity ( $M$ ) of the frame corner is approximately seven times higher than the one of the column base.

## 5.2 Influence of connection slip on structural behavior

In this section, the influence of the connection compliance on the structural behavior of a typical timber structure is discussed. The analysis is related to the force redistribution within the structure and the change of deformations. Particularly, necessity of considering the connection slip shall be shown. Therefore, the structural behavior of a two-dimensional frame structure is discussed. Since this frame structure is statically indetermined, a change of the system stiffness leads to force redistributions in the structure. The connection slip curves determined in Section 5.1.2 are considered and compared to the traditional approach of rigid/hinged connections.

### System

The investigated frame structure is part of a building complex used for offices (see Figure 5.19). The building consists of eight frames with a distance of approximately

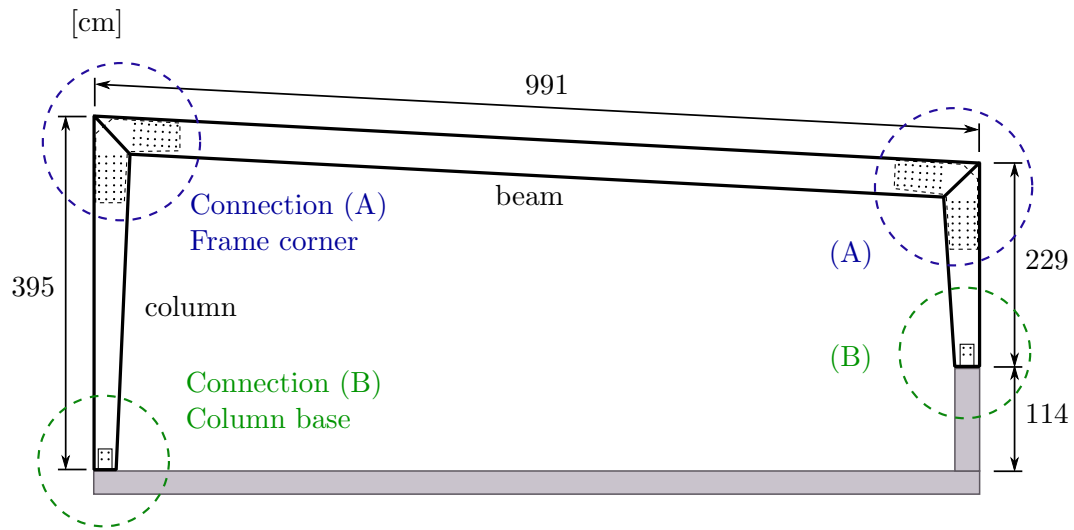


Figure 5.20: Timber frame structure.

Table 5.3: Geometric data and material properties of the frame members.

	left column	girder	right column
length (approx.)	375 cm	950 cm	209 cm
cross section	18/24-40 cm	18/40 cm	18/29-40 cm
timber	GL28c	GL28c	GL28c
steel members	S235	S235	S235

4.0 m. In vertical and cross direction, loads are transferred through stringers to the frames. A wind bracing, located in the middle of the hall, carries the loads in longitudinal direction.

In order to simplify the system for the study of the influence of compliant connections, a single frame has been modeled as a 2D load-bearing structure. The frame is about 4.0 m high and exhibits a span of approximately 10 m.

## Geometry – Materials

Table 5.3 gives an overview of the geometric parameters and the materials of the frame.

## Structural analysis model

For the model of a traditional static approach, the structural elements are connected by a hinge to the basis. The basis made of reinforced concrete is considered to be rigid. For the first model, the frame corner is approximated as rigid connection. From the statics point of view, a frame with two hinges is one times statically indetermined, which means the member forces of this system depend on the stiffness distribution within the system.

Figure 5.21 shows the corresponding structural analysis model of the frame. Red points

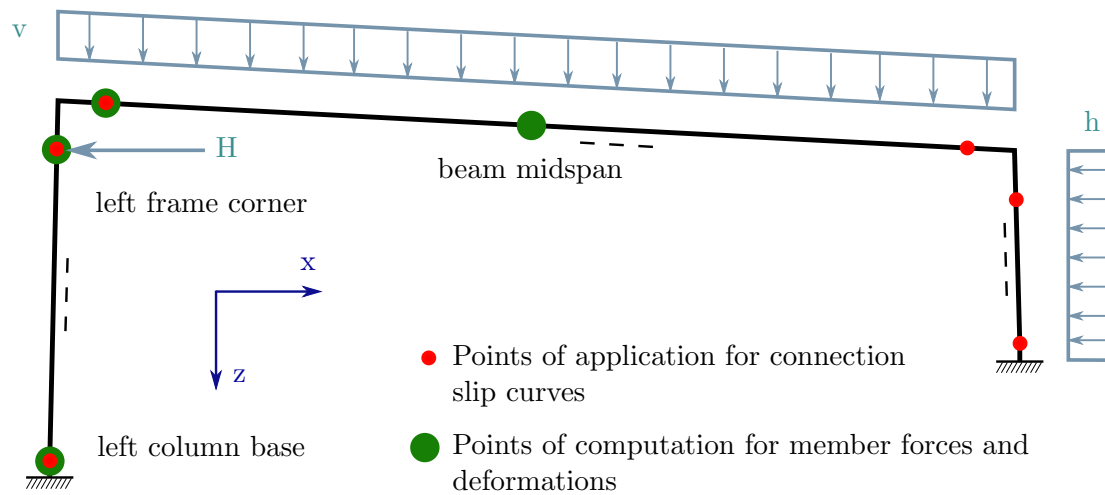


Figure 5.21: Structural analysis model of timber frame structure.

Table 5.4: Loading of the frame.

	SLS	ULS
uniform vertical load ( $v$ )	10,47 kN/m	24,20 kN/m
uniform horizontal load ( $h$ )	8,40 kN/m	11,88 kN/m
single horizontal load ( $H$ )	11,20 kN	15,84 kN

are related to the points of application of the connection slip curves. Green points mark the position of the calculated member forces and deformations used for the comparison of the approaches. In total, three different configurations of the frame are compared. The traditional structural analysis approach is chosen as reference configuration. The second configuration is the frame system with application of the connection slip curves based on the simplified EC 5 approach for the single-dowel (method 1 in Figure 5.16 and Figure 5.18). For the third configuration, connection slip curves calculated based on the single-dowel slip curves according to the sub-model are used (method 3 in Figure 5.16 and Figure 5.18).

## Loading

Two load levels, related to the serviceability limit state (SLS) and the ultimate limit state (ULS) respectively, are applied to the frame structure. Several uniformly distributed vertical loads (dead weight, snow,...) and horizontal loads (wind,...) are summed up to one uniformly distributed vertical load ( $v$ ) and one uniformly distributed horizontal load ( $h$ ). Additionally, one single horizontal load ( $H$ ) acts on the structure. The size of these loads is given in Table 5.4. Several loads are design loads.

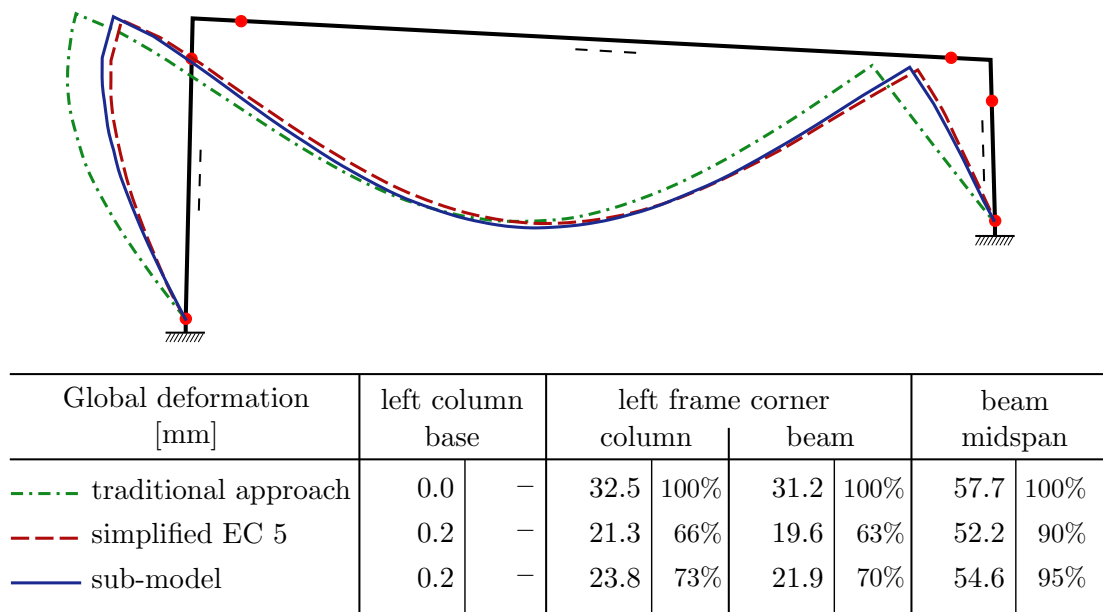


Figure 5.22: Comparison of the deformation in the SLS.

## Comparison of the results

The structural analysis is performed in the engineering design software RSTAB (Ing. Dlubal GmbH, Germany).

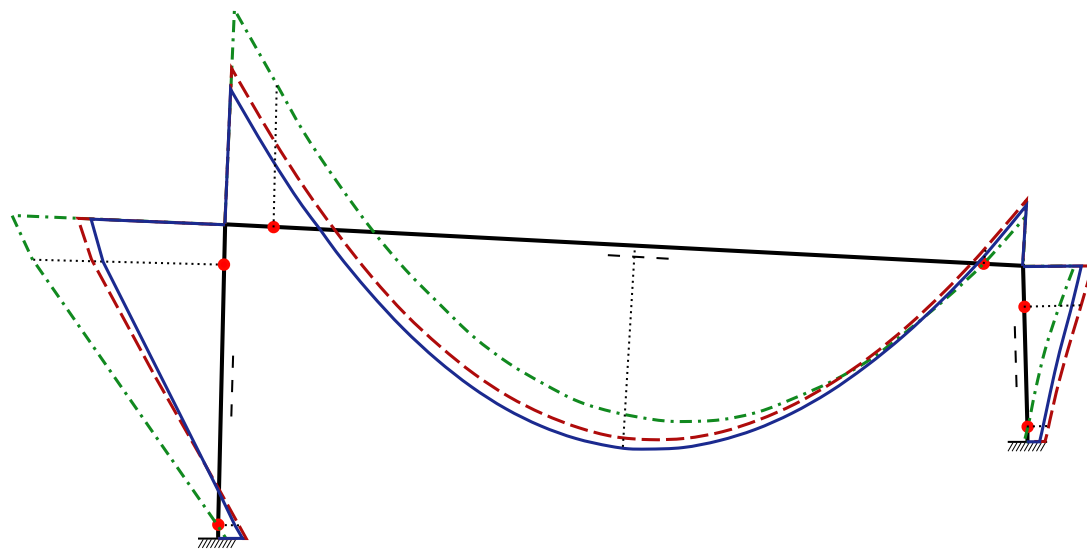
### Serviceability limit state (SLS)

The serviceability limit state is related to elastic deformations of the connections. The elastic limit is first reached for the normal force at the left column base for the model based on the sub-model for the single dowel. Moments at the column base as well as at the frame corner are slightly below the elastic limit.

Figure 5.22 shows the global deformation of the timber frame structure. The three deformation figures correspond to the calculation methods for the connection slip. The values given in Figure 5.22 are the absolute deformations of the corresponding points of the structure. The green, dash-dotted line describes the deformation behavior of the traditional design approach.

Consideration of the compliance of connections leads to a stiffer behavior in horizontal direction ( $u$ ) (see Figure 5.22). This is due to the rotational stiffness of the column base not considered in the traditional approach. The deformations are reduced up to 40 %. In vertical direction ( $w$ ), the deformations are slightly increased. For the sub-model configuration, the deformations at midspan are only 4 % higher compared to the rigid/hinged approach.

A considerable force redistribution becomes obvious. Member forces at the frame corner are reduced up to 30 %. Changes at midspan are smaller but still significant. A remarkable moment at the column base near the elastic limit builds up, which is not considered in the hinged/rigid model.



Moment [kNm]	left column base		left frame corner				beam midspan	
			column		beam			
--- traditional approach	0.0	—	-183.0	100%	-138.4	100%	160.7	100%
- - - simplified EC 5	19.6	—	-128.9	70%	-82.6	60%	181.7	113%
— sub-model	16.9	—	-116.2	63%	-68.4	49%	192.8	120%

Figure 5.23: Comparison of the moment distribution in the ULS.

### Ultimate limit state (ULS)

The ultimate limit state is related to the bearing capacity of the structure and connection respectively. The comparison should focus on the member forces. However, also the influence on the deformations of the structure is considerable and therefore, discussed. Similar to the SLS, the bearing capacity is first reached for the normal force at the column base.

Compared to the SLS, the horizontal deformations ( $u$ ) of the frame in the models considering the connection slip, are of the same order as the one in the traditional approach. This can be explained by the softer behavior of the connections in the plastic domain. Also the vertical displacements of the connection slip models are clearly higher than the rigid/hinged approach.

The moment distribution in the frame structure is shown in Figure 5.23. Due to force redistribution, the member forces at the frame corner are reduced and member forces at the midspan of the beam are increased. The moment at midspan of the beam is increased by 20 % compared to the traditional approach. The member forces of the frame corner are reduced up to 50 %. Special attention should be given to the column base. In addition to the normal forces, also a considerable moment in the size of the bearing capacity of the connection develops. An interaction of this two member forces may cause a failure of the connection. The simplified approach based on EC 5 exhibits

a slightly stiffer behavior than the approach based on the connection slip calculated by means of a sub-model. Therefore, the moment at the frame corner is higher and the moment at midspan is lower for the simplified approach based on EC 5.

### **Current restrictions**

The structural analysis is performed in the engineering software RSTAB (Ing. Dlubal GmbH, Germany), which allows to consider the connection slip. However, currently, the interaction of internal forces and corresponding relative deformations are not considered. Therefore, the load bearing capacity of the connection is overestimated and relative deformations are underestimated in the corresponding model. Nevertheless, the significance of dowel slips on the behavior of the timber structures has been shown.

Consideration of the appropriate interaction of local internal forces at connections would even lead to lower internal forces and consequently, to higher relative deformations at connections. Particularly in case of reinforced connections and the exploitation of plastic deformation characteristic in the design of timber structures, a realistic model for the behavior of the connection is indispensable.

# Chapter 6

---

## Summary and conclusions

In this thesis, the load-deformation behavior of dowel connections and the influence of the connection slip on the structural behavior of timber structures was studied. The work was particularly focused on the development of a generally applicable numerical model for the calculation of multi-dowel connection slip curves.

As a basis for the modeling of dowel connections, properties of single-dowel connections have been presented. Different reactions of wood in case of different loading directions, as well as several models to calculate single-dowel slip curves were discussed. The state-of-the-art model to determine the connection slip curves has been shown. Since this model is limited to some special design situations, a generally applicable model has been developed. This model enables a straight forward determination of member forces and connection slip curves for an arbitrary set of deformations. Furthermore, a modification of the model to determine the deformation and force distribution within the connection for specific member forces was discussed.

The model was applied to different connections to illustrate their behavior for simple design examples. Moreover, connection slip curves have been implemented in the structural analysis of a static indetermined system, to show the necessity of considering the compliance of connections in the design of timber structures.

The model developed in this thesis gives access to the relationship between global connection deformation and corresponding member forces, as well as between member forces and local force distribution within the connection. The consistent formulation of the connection deformation and loading ensures the model to be applicable to all kinds of single-connectors, and is therefore not limited to dowel-type fasteners. Even load direction dependent behavior, as shown for contact properties, can be considered. Force redistribution and increasing deformations as a result of compliant connections has been shown in the behavior of a timber frame structure. Furthermore, this design example makes it evident that a realistic single-dowel slip curve is essential to model the connec-

tion realistically. Particularly for the consistent definition of loads and corresponding deformations. Currently, this is only possible by using a sub-model.

The behavior of centric connections has been found to be symmetric by means of member force interaction. An approximately quadratic interaction has been shown for the interaction of normal force and shear force. The interaction for normal force and moment, and shear forces and moments respectively are almost linear. Excentricity of the reference point related to the beam axis causes asymmetric member force interactions.

The model presented in this thesis considers ductile embedment failure. Further work should be focused on implementation of brittle failure modes, such as lateral splitting or block shear failure. Moreover, detailed investigations on the deviation between force direction and displacement should be performed. An implementation of the model in structural analysis software should be aimed for, to make the model suitable for commercial purposes.

# Bibliography

- [1] DIN 1052:2008. Entwurf, Berechnung und Bemessung von Holzbauwerken – Allgemeine Bemessungsregeln und Bemessungsregeln für den Hochbau (Design of timber structures – General rules and rules for buildings). *Deutsches Institut für Normung*, 2008.
- [2] ÖNORM EN 1995-1-1:2009. Eurocode 5: Bemessung und Konstruktion von Holzbauten – Teil 1-1: Allgemeines – Allgemeine Regeln und Regeln für den Holzbau (Eurocode 5: Design of timber structures – Part 1-1: General – Common rules and rules for buildings). *Austrian Standards Institute*, 2009.
- [3] ÖNORM EN 383:2007. Holzbauwerke – Prüfverfahren – Bestimmung der Lochleibungsfestigkeit und Bettungswerte für stiftförmige Verbindungsmittel (Timber structures – Test methods – Determination of embedment strength and foundation values for dowel type fasteners). *Austrian Standards Institute*, 2007.
- [4] A. Awaludin, W. Smittakorn, T. Hirai and T. Hayashikawa. Bearing properties of shorea obtusa beneath a laterally loaded bolt. *Journal of wood science*, 53(3):204–210, 2007.
- [5] H. J. Blaß, A. Bienhaus and V. Kramer. Effective bending capacity of dowel-type fasteners. *Proceedings PRO 22, International RILEM Symposium on Joints in Timber Structures*, 71–80, 2001.
- [6] L. Bleron, J.F. Bocquet, G. Duchanois and P. Triboulot. Contribution to the optimization of timber joints performances-analysis of dowel type fasteners embedment strength. *Proceedings PRO 22, International RILEM Symposium on Joints in Timber Structures*, 23–32, 2001.
- [7] F. Brühl, U. Kuhlmann and A. Jorissen. Consideration of plasticity within the design of timber structures due to connection ductility. *Engineering Structures*, 33(11):3007–3017, 2011.
- [8] M. Dorn. Investigations on the serviceability limit state of dowel-type timber connections. *Doctoral Thesis – TU Wien*, 2012.
- [9] S. Franke and P. Quenneville. Embedding strength of New zealand timber and recommendation for the NZ standard. *Proceedings of CIBW18, CIB-W18/42-7-4*, 2009.

- [10] G. Hochreiner, T. K. Bader, K. de Borst and J. Eberhardsteiner. Stiftförmige Verbindungsmittel im EC5 und baustatische Modellbildung mittels kommerzieller Statiksoftware (in german). *Bauingenieur*, 88:1–15, 2013.
- [11] U. Hübner, T. Bogensberger and G. Schickhofer. Embedding strength of european hardwoods. *Proceedings of CIBW18*, CIB-W18/41-7-5, 2008.
- [12] K. W. Johansen. Theory of timber connections. *International Association of Bridge and Structural Engineering*, 9:249–262, 1949.
- [13] A. Jorissen and M. Fragiacomio. General notes on ductility in timber structures. *Engineering structures*, 33(11):2987–2997, 2011.
- [14] H. J. Larsen and V. Enjily. Practical design of timber structures to Eurocode 5. *Thomas Telford*, 2009.
- [15] M. Masuda and K. Tabata. Theoretical and experimental analyses of fracture of wood in pinned joint using DIC and FSAFC (Finite Small Area Fracture Criterion). *Proceedings PRO 22, International RILEM Symposium on Joints in Timber Structures*, 3–12, 2001.
- [16] M. N. Nonbo. Numerical simulation of timber connections with slotted-in steel plates. *Master Thesis DTU*, 2010.
- [17] S. Ormarsson and M. Blond. An improved method for calculating force distributions in moment-stiff timber connections. *World Conference on Timber Engineering*, 25(8):361–366, 2012.
- [18] M. B. U. Pedersen, C. O. Cloriosa, L. Damkilde, P. Hoffmeyer, and L. Eskildsen. Dowel type connections with slotted-in steel plates. *Proceedings of CIBW18*, CIB-W18/32-7-8, 1999.
- [19] C. Santana and N. Mascia. Modeling of semi-rigid nailed joints for application in structural analysis. *Proceedings PRO 22, International RILEM Symposium on Joints in Timber Structures*, 111–120, 2001.
- [20] J. Schänzlin, U. Kuhlmann, F. Brühl and B. Deam. Design of timber structures considering the plastic behavior of steel fasteners. *University of Canterbury, Department of Civil Engineering Christchurch, New Zealand*.
- [21] K. Yasumura and M. Sawata. Determination of yield strength and ultimate strength of dowel-type timber joints. *Proceedings of CIBW18*, CIB-W18/33-7-1, 2000.

# Appendix **A**

---

## Description of MATLAB Code for the calculation of connection slip curves

In general the MATLAB Code consists of one main script called *Connection\_03*, and several subscripts (functions) hosted at this script. The main script itself is divided in an input and an output part. The input part includes settings regarding the deformation of neighboring cross sections (i.e. beam ends), geometric properties, material properties of steel and wood, and the type of the single-dowel slip curve. Compared to the input part, the output part is only used for calculation and visualization. The deformation per fastener in combination with the related single-dowel slip curve of each fastener is used to determine the reaction force per fastener. This is followed by the determination of the stiffness matrix and resulting member forces (internal forces). Finally, plots of the input single-dowel slip curves, the force distribution within the connection as well as the slip curves of the multi-dowel connection are generated.

First, several scripts and functions of the MATLAB Code are listed in chronological order. The *Connection\_03.m* is the basic script, which hosts several functions and subscripts of this code. The following itemization uses the same subdivision as implemented in the script *Connection\_03.m*.

### **Connection\_03.m**

#### Input

- InputData\_03.m
- Slipcurve01\_03-01.m

- bearcapsingledowtypesteel01mean.m
- bearcapsingledowtypetimber01mean.m
- ...
- Slipcurve01\_02.m

### Calculation - Output

- InitialMatrices01.m
- ReactionValues03.m
  - ResultingForce03.m
    - \* SectionalLinearCurve03.m
  - SectionalLinearCurve01.m
- StiffnessMatrices01.m

### Plots

- FigureSlipCurves03.m
- FigureSketch03.m
- FigureMemberForces01.m

In the following, a detailed description of the scripts and functions of the MATLAB Code is given. In general, the description of each script/function is divided in input, calculation and output. The structure of the code is illustrated at the end of Appendix A.

## **Connection\_03.m**

*Connection\_03.m* is the basic script which has to be executed in order to estimate the connection behavior. The script is divided in an input and an output part. The main task of the script is to execute other functions, only some settings are done directly in *Connection\_03.m*.

### **Input**

The input part of *Connection\_03.m* contains all necessary input values for the calculations, which means settings are only done directly in the input part of *Connection\_03.m* or in the functions called in this script. For the calculation and for the output, no further settings have to be made.

The following prescriptions are done directly in *Connection\_03.m*:

**Deformations of neighboring cross sections:** A set of deformations of neighboring cross sections, by means of relative deformations between the dowel group of the beam

and the connecting structural element, is the starting point of the calculation. All deformations are applied to the connection at the specified reference point. This set of deformations may consist of the following two parts:

- **Initial relative deformations of neighboring cross sections  $uj\_in$** , is a vector with three elements, including the displacements in x-direction (axial displacement)  $u$  in mm, the displacements in z-direction (transverse displacement)  $w$  in mm and the rotation of the cross sections around the y-axis  $\phi$  in radian.
- **Additional incremental deformations of neighboring cross sections  $du$** , is a vector with the length of three. Their entries are related to the ones of  $uj\_in$ . The number of incremental deformations that are added to the initial deformation configuration is defined at  $pu$  (number of investigation points).

A visualization of the input deformations, as well as the definition of the coordinate system (including the definition of the positive angle direction) can be found in Figure 4.1.

The three prescriptions  $uj\_in$ ,  $du$  and  $pu$  enable the user to determine the connection behavior for one specific set of deformations, e.g. calculated by a structural analysis of a timber structure, or for several deformation sets. In the first case, the elements of  $du$  are chosen to be zero,  $pu = 1$  and  $uj\_in$  equal to a specific set of deformations. The second case is used to determine slip curves of the connection. For this purpose, an arbitrary starting point is chosen  $uj\_in$ . Thereon, the additional incremental deformations  $du$  are added as often as specified by  $pu$ .

Further settings are done in the subscript *InputData\_03.m* and *Slipcurve01\_03\_01.m* for the calculation of single-dowel slip curves.

## Calculation

After initialization of the necessary matrices the main *calculation core* is started. It consists of a loop, where step-by-step input deformations are extracted from the matrix of input deformations, and applied to the calculation of the member forces and stiffness matrices. Finally, the data are stored at the initial matrices and the next input deformations are called. This procedure is repeatedly executed for the specified number of investigation points  $pu$ .

In general, the calculation procedure is done twice. Once to calculate the member forces and once to calculate the stiffness matrices. In order to determine the member forces, the resulting displacement as interaction of the axial and transverse displacement as well as the displacement caused by rotation of the cross sections is used. Compared to the determination of the member forces, the calculation of the stiffness matrices is based on a separate consideration of the three deformations described above. Each deformation is considered to be isolated and leads to one column of the stiffness matrix (see Figure 4.3). In order to get the entire stiffness matrix, the calculation has to be done three times.

Since the calculation procedure for the member forces is identical to the calculation of the stiffness matrices, the description is given only ones. This calculations are done by the function *ReactionValues03.m*, which consists of several sub-functions.

## Output

- resulting displacement per fastener  $\mathbf{dji}$ ,
- reaction forces per fastener  $\mathbf{Ri}$ ,
- force-to-grain angle per fastener  $\hat{\alpha}$ ,
- member forces  $N, V$  &  $M$ ,
- secant and tangential stiffness matrix  $\mathbb{K}_{sec}$  and  $\mathbb{K}_{tan}$ , and
- illustration of the determined values (plots).

## I1) InputData\_03.m

All input data in this subscript are set by the user. In this function, the geometrical and mechanical properties as well as the calculation methods of the reaction forces and single-dowel slip curves are defined.

## Input

- **Geometry**
  - coordinates and corresponding slip curves of the fasteners in an arbitrary input coordinate system  $\mathbf{X}_-$ , and
  - additionally, a translation vector  $\mathbf{eX}_-$  in mm and a rotation  $ny$  in  $^\circ$  can be specified, in order to move the coordinates from the input to the reference coordinate system. The reference coordinate system is usually located on the beam axis perpendicular to the center of gravity.
- **System data**
  - safety concept: Specification of modification factor  $k_{mod}$  of timber elements,
  - material: Mechanical properties and geometry of the connection elements (side member(s), gusset plate(s), fasteners, ...), as well as the grain direction with respect to the beam axis of the timber elements,
  - calculation method - related to the force/displacement direction  $cm$ : Opportunity to consider the deviation between force and displacement direction of the single-dowel loaded at an angle to the grain,
  - calculation method - related to the type of the single-dowel slip curve  $m_{sc01}$ : Possibility to choose between method 1 to 8 (extension to further methods is possible). Three different calculation principles are presented in Table 2.2.

## Calculation

- transformation of the coordinates from the input coordinate system to the reference system.

## Output

Identical to Input.

## I2) Slipcurve01\_03\_01.m / I3) Slipcurve02.m

While in *Slipcurve02.m* the singel-dowel slip curve (contact condition) is generated automatically, in *Slipcurve01\_03\_01.m* the procedure for the calculation of the single-dowel slip curve depends on the chosen calculation method. The general shape of the different slip curves determined in *Slipcurve01\_03\_01.m* is presented at Table 2.2. Detailed explanations are given in Section 2.4.

## Input

- calculation method - related to the type of the single-dowel slip curve *m\_sc01*, and
- geometrical data and system data defined in *InputData\_03.m*

## Calculation

Dependent on the chosen calculation method *m\_sc01*, different procedures are executed. Three different types are listed consecutively. A detailed description of these methods is given in Section 2.4.

- simplified method based on EC 5 (*m\_sc01* = 1),
- advanced method based on EC 5 (*m\_sc01* = 2),
- slip curve determined by a sub-model (*m\_sc01* = 3 – 8).

## Output

The output of these function are single-dowel slip curves, by means of a displacement vector (**d01\_sc**) and force vector (**Fv01\_sc**) for as many force-to-grain angles as specified in *Slipcurve01\_03\_01.m*.

The following functions are related to the calculation - output part of the main script *Connection\_03.m*.

### O1) InitialMatrices01.m O1)

The function *InitialMatrices01.m* provides empty matrices or vectors. On the one hand, the generated input deformations for each step ( $\mathbf{uj\_in}$ ;  $\mathbf{uj\_in} + \mathbf{du}$ ; ...) are stored and, on the other hand, the calculated values, regarding the displacement of the fasteners ( $\mathbf{djiv}$ ), the reaction forces ( $\mathbf{Ri}$ ), force-to-grain angle ( $\hat{\alpha}i$ ) and the member forces ( $N/V/M$ ) are summarized.

#### Input

- input relative deformations of neighboring cross sections ( $\mathbf{uji\_in}$ ),
- additional incremental deformations of neighboring cross sections ( $\mathbf{du}$ ),
- number of investigation points ( $pu$ ), and
- number of fasteners ( $n$ ).

#### Calculation

- initialization of empty matrices (vectors) with their necessary size, and calculation plus storage of the input deformations for each calculation step.

#### Output

- matrix including the input deformations for each calculation step ( $\mathbf{uj}$ ).

Empty matrices (vectors) for:

- displacements of the fasteners ( $\mathbf{djiv}$ ),
- reaction forces ( $\mathbf{Ri}$ ),
- force-to-grain angles ( $\hat{\alpha}i$ ), and
- member forces ( $N/V/M$ ).

## O2) ReactionValues03.m

This function determines the reaction values of the connection due to the prescribed input deformation. First, the displacements of each dowel due to the input deformations are calculated. As a result of the assumptions regarding rigidity of the timber matrix and fixed position of the fasteners below each other, every fastener experiences the same axial ( $u_{ji}$ ) and transverse displacement ( $w_{ji}$ ). The displacement caused by the rotation of the cross section ( $d_{ji\_phi}$ ) depends on the distance of the dowel from the reference point. Vector addition of these three displacements gives the resulting displacement vector (see Figure 4.1). The length of the single displacement vector (=size of the displacement  $d_{ji}$ ) and the direction of the vector  $\hat{\alpha}$  (related to the grain direction) is determined.

Application of the resulting displacements per fastener to the related slip curve (defined by the slip curve type and force-to-grain angle) gives the reaction force vector. The calculations are done in the function *ResultingForce03.m* for the slip curve category  $sc = 1$ , and in *SectionalLinearCurve01* for  $sc = 2$ .

Equilibrium of the forces at the reference point gives the member forces  $N/V/M$  (see Figure 4.2). Finally, the displacement of the fasteners, the force-to-grain direction, the reaction forces and the member forces are stored in the corresponding matrices.

### Input

- input deformation vector  $\mathbf{u_j}$ ,
- geometry of the connection  $\mathbf{x}$ ,  $\mathbf{z}$  &  $n$ ,
- single-dowel slip curve type per fastener  $sc$ ,
- grain angle  $\alpha$ ,
- single-dowel slip curves, and
- calculation method regarding the force/displacement direction  $cm$ .

### Calculation - Output

- resulting displacement per fastener  $d_{ji}$ ,
- displacement-to-grain angle per fastener  $\hat{\alpha}1$ ,
- reaction forces per fastener  $R_i$ ,
- force-to-grain angle  $\hat{\alpha}$  (if the deviation of force - displacement direction is not consider, then  $\hat{\alpha}1 = \hat{\alpha}$ ), and
- member forces  $N, V$  &  $M$ .

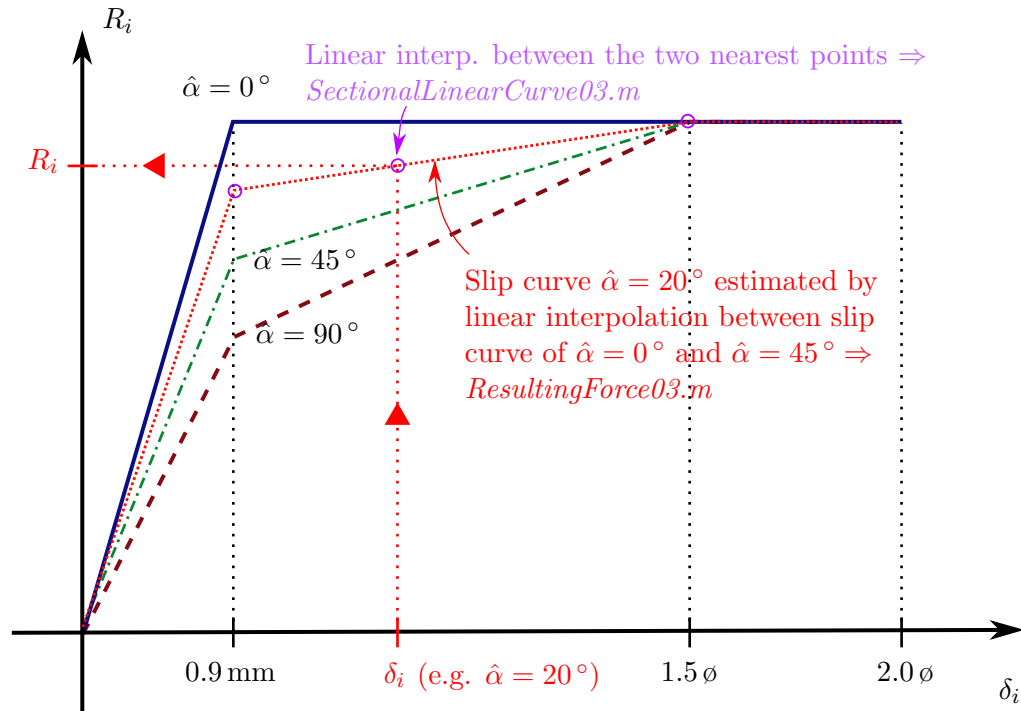


Figure A.1: Determination of the reaction force per fastener.

### O3) ResultingForce03.m / O4) O5) SectionalLinearCurve01(03).m

These two functions determine the reaction forces per fastener by means of single-dowel slip curves, starting at the resulting displacement per fastener. While *SectionalLinearCurve01(03).m* determines the reaction force  $R_i$  within the polygonal slip curve, the function *ResultingForce03.m* additionally interpolates between the single-dowel slip curves, in the case the force-to-grain angle of the resulting displacement does not match a force-to-grain angle, for which the single-dowel slip curves are determined (see Figure A.1). Since the contact condition ( $sc = 2$ ) depends on the grain direction, only the function *SectionalLinearCurve01(03).m* is used in this case.

#### Input

- single-dowel slip curve,
- resulting displacement of the fastener  $d_{ji}$ , and
- force-to-grain angle  $\hat{\alpha}$  (only for *ResultingForce03.m*).

#### Calculation - Output

- reaction force per fastener  $R_i$ .

### O6) StiffnessMatrices01.m

This function calculates the secant and tangential stiffness for a specific point of the connection slip curve. The secant stiffness is calculated by division of the current member force by the current deformation. For each deformation configuration nine secant and nine tangential stiffnesses are determined. The tangential stiffness is calculated by division of the difference between the current member forces ( $Nj(p)$ ,  $Vj(p)$  &  $Mj(p)$ ) and the previous member forces ( $Nj(p-1)$ ,  $Vj(p-1)$  &  $Mj(p-1)$ ) by the incremental deformation  $du$ . It should be highlighted that stiffnesses are calculated by isolated consideration of each deformation component. Figure 4.4 illustrates the stiffness determination.

#### Input

- vector of member forces ( $\mathbf{Nj}$ ,  $\mathbf{Vj}$  &  $\mathbf{Mj}$ ),
- current global deformation  $\mathbf{uj\_cu}$ , and
- incremental global deformation  $\mathbf{du}$ .

#### Calculation - Output

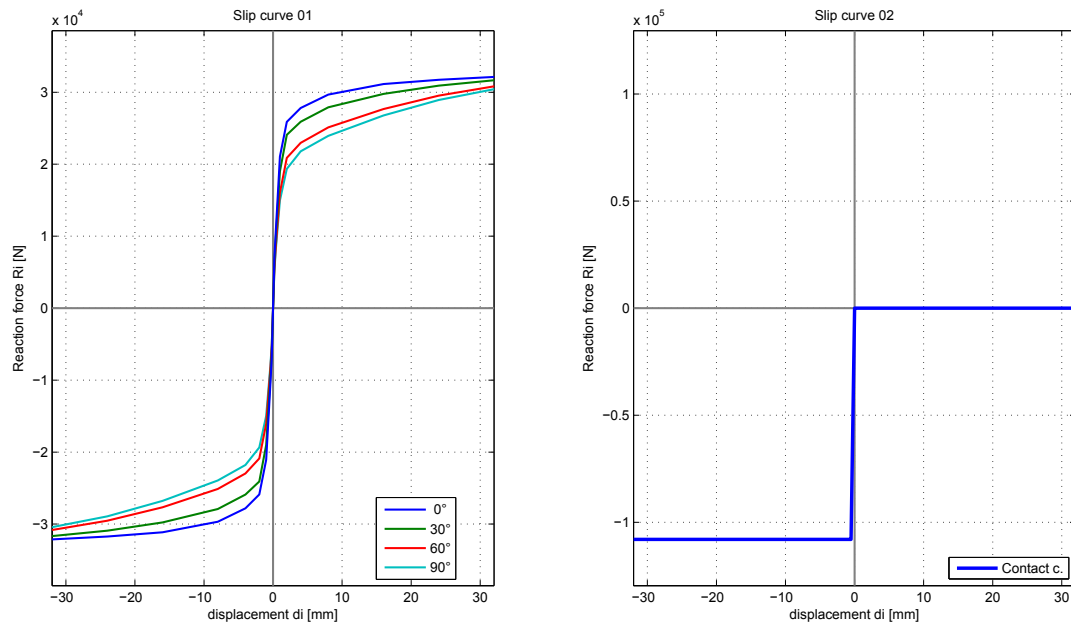
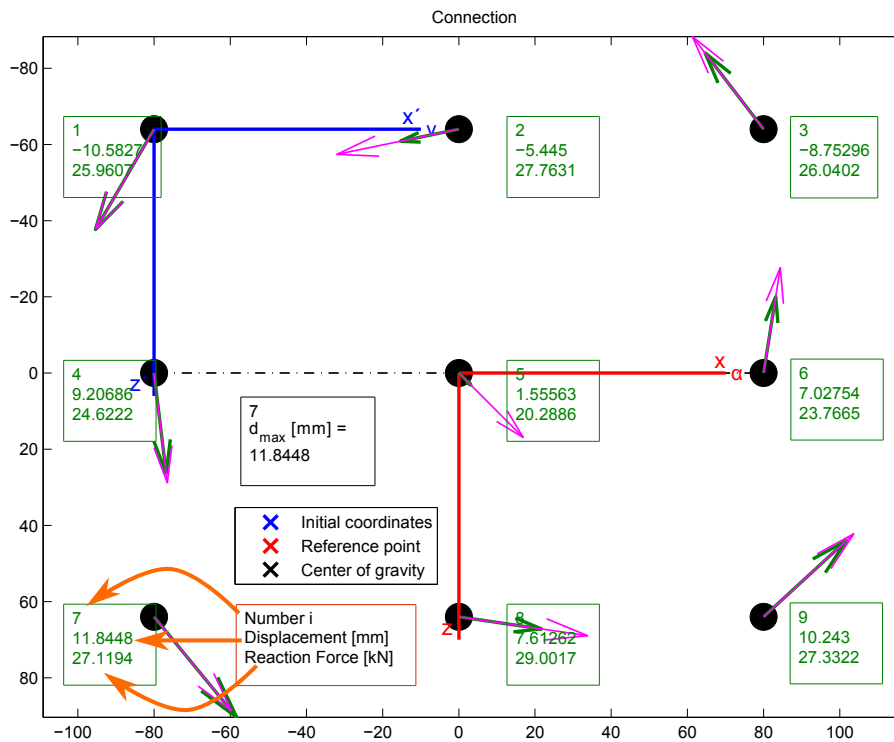
- secant stiffness matrix  $\mathbb{K}_{sec}$ , and
- tangential stiffness matrix  $\mathbb{K}_{tan}$ .

### O7) FigureSlipCurves03.m

This plot shows the single-dowel slip curves generated in *Slipcurve01\_03\_01.m* (left plot) and the contact condition defined in *Slipcurve02.m* (right plot). The horizontal axis is related to the displacement  $\delta_i$  and the vertical axis to the reaction force  $R_i$ . The different curves (left plot) are related to the different force-to-grain angles of the slip curves (see Figure A.2).

### O8) FigureSketch03.m

On the one hand, the second plot serves to visualize the geometric properties of the connection and, on the other hand, the displacement and force distribution within the connection is shown. The plot includes the position of the fasteners, the input and reference coordinate system, the center of gravity of the connection (COG), the grain direction and the beam axis. Furthermore, the length and direction of the displacement vector of each fastener (green arrows) is shown graphically and, additionally the size of the displacement is computed. The same is done for the reaction force vector (magenta arrows). Also, the maximum fastener displacement and its position are highlighted (see Figure A.3).

Figure A.2: Single-dowel slip curves for centric design example - *FigureSlipCurves03.m*.Figure A.3: Configuration of the connection, and displacement and force distribution - *FigureSketch03.m*.

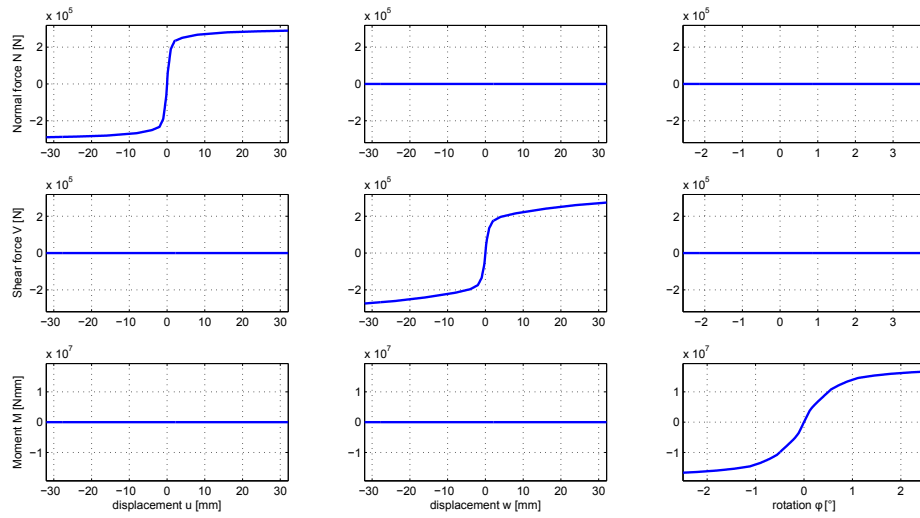
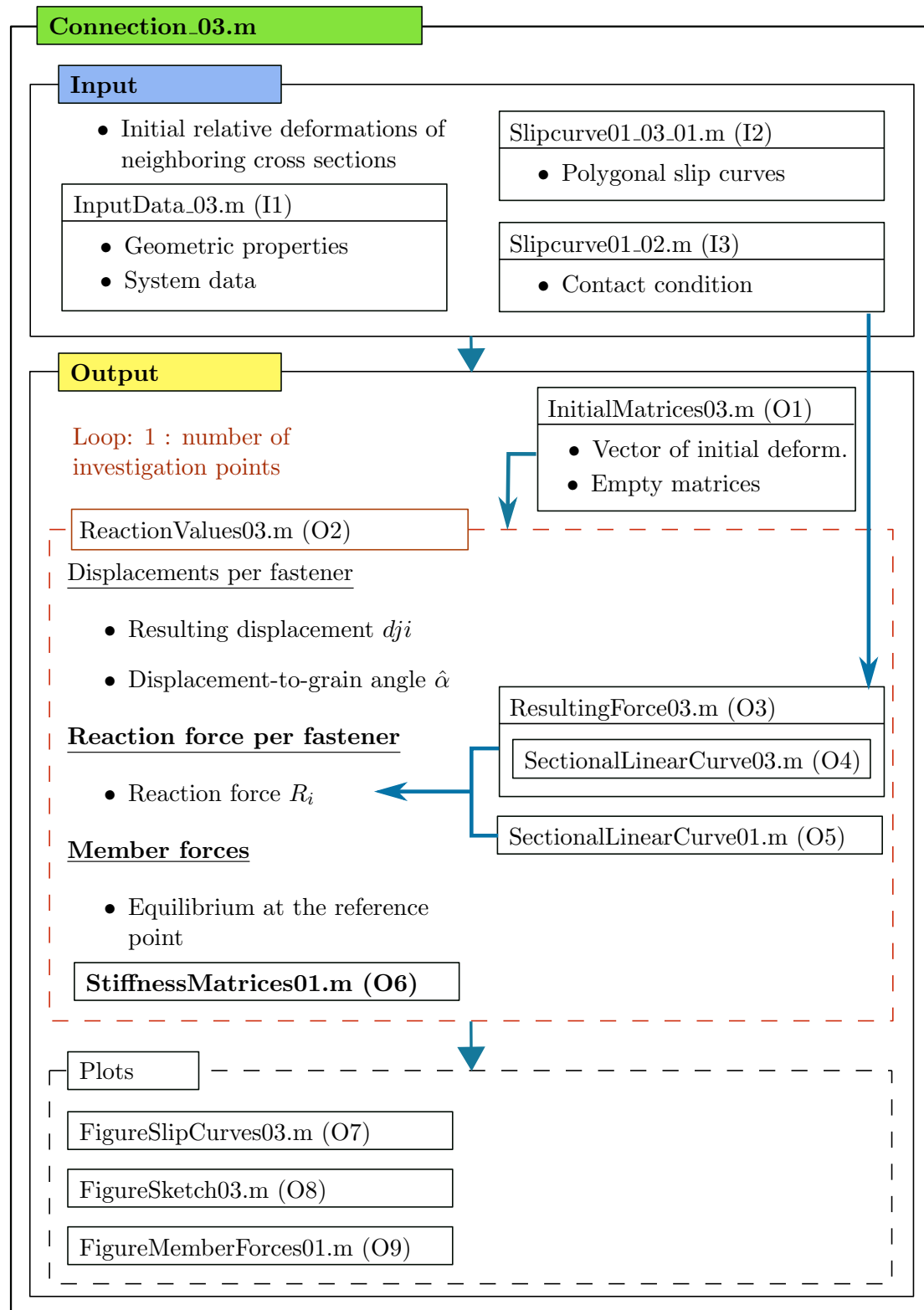


Figure A.4: Connection slip curves for centric design example - *FigureMemberForces01.m*.

## O9) FigureMemberForces01.m

The plot *FigureMemberForces01.m* illustrates member forces, by means of nine different slip curves. The position of the slip curves within the plot is related to the position within the stiffness matrices (see Figure A.4).

## Flow chart - MATLAB Code - calculation of connection slip curves



# Appendix B

---

## Description of MATLAB Code for back-calculation of dowel forces

In general the MATLAB Code consists of one main script called *MemberForces\_03\_01.m*, and several subscripts (functions) hosted at this script. Additionally, the MATLAB script *Connection\_03.m*, described in Appendix A, has to be executed before the main script is called. *Connection\_03.m* generates the global slip curves of the connection, which are used as input of *MemberForces\_03\_01.m*.

The main script itself is divided in an input, calculation, and an output part. The input part includes settings regarding the input member forces, geometric and material properties of the connection, the type of the single-dowel slip curves, and the iteration procedure. As a starting point for the calculation, a first estimation of the global deformations of the connection, based on the input member forces is done using the slip curves of the connection. These global deformations are used to determine the local deformations for each fastener. Application of the local deformations to the single-dowel slip curves gives the reaction forces per fastener. In the following, the member forces are calculated by means of equilibrium conditions of the forces at the reference point. These member forces are compared to the input member forces. If the two sets of member forces match each other, the deformation and force distribution within the connection has been found. Otherwise, the global deformations of the connection are adjusted, until the input member forces match the calculated member forces (→ iterative process).

Finally, plots of the displacement and force distribution within the connection as well as the slip curves of the multi-dowel connection are generated.

First, several scripts and functions of the MATLAB Code are listed in chronological order. The *MemberForces\_03\_01.m* is the basic script, which hosts several functions and subscripts of this code. The subscripts and functions of the input script *Connection\_03.m* are not listed here (see Appendix A). The following itemization uses the same subdivision

as implemented in the script *MemberForces\_03\_01.m*.

### **Connection\_03.m**

see Appendix A

### **MemberForces\_03\_01.m**

#### Input

- InitialDeformation\_01.m
- InputData\_03.m
- Slipcurve01\_03\_01.m
  - bearcapsingledowtypesteel01mean.m
  - bearcapsingledowtypetimber01mean.m
  - ...
- Slipcurve01\_02.m

#### Calculation - Output

- InitialMatrices01.m
- ReactionValues03.m
  - ResultingForce03.m
    - \* SectionalLinearCurve03.m
  - SectionalLinearCurve01.m
- StiffnessMatrices01.m
- NewtonRaphson\_01.m

#### Plots

- FigureSketch\_MF\_01.m
- FigureMemberForces01\_02.m

In the following, a detailed description of the individual scripts and functions used in the MATLAB Code is given. Some of the scripts/functions are already described in Appendix A. Nevertheless, the description of this scripts are repeated here in order to have an enclosed description of the MATLAB Code for back-calculation of the dowel forces. In general, the description of each script/function is divided in an input, calculation and output part. The structure of the code is illustrated at the end of Appendix B.

## I1) Connection\_03.m

*Connection\_03.m* is the MATLAB script for the calculation of member forces and slip curves of the connection, respectively. Here, the script is used to determine the slip curves of the connection, which serve as input to *MemberForces\_03\_01.m*. A detailed description of the calculation steps of the script *Connection\_03.m* can be found in Appendix A.

## MemberForces\_03\_01.m

*MemberForces\_03\_01.m* is the basic script, which has to be executed in order to back-calculate dowel forces. As mentioned before, the script is divided in an input and an output part. The main task of the script is to execute other functions, only some settings are done directly in *MemberForces\_03\_01.m*.

### Input

The input part of *MemberForces\_03\_01.m* contains all necessary input values for the calculations. Settings are done directly in the input part of *MemberForces\_03\_01.m* or in the functions called at this part.

The following specifications are necessary in *MemberForces\_03\_01.m*:

- **Input member forces MF:** As starting point of the calculation, the three member forces  $N$ ,  $V$  and  $M$  are prescribed.
- **Iteration settings:** An incremental deformation  $du$ , which is needed to determine the gradient of the slip curves of the connection, has to be defined. The gradient of the global slip curve is necessary for the iterative process, to adjust the global deformation. The Newton-Raphson method is applied for the iteration process. Additionally, the maximum number of iteration cycles *max\_iter* has to be defined, in order to exit the execution of the MATLAB code, for the case of a non-convergent setting of input member forces.

Further settings are done in the subscript *InputData\_03.m* and in the function to apply single-dowel slip curves (*Slipcurve01\_03\_01.m*). No settings have to be done at the functions *InitialDeform\_01* and *Slipcurve02*.

### Calculation

Basically, the input for the calculation is the first approximation of the global deformation of the connection at the reference point ( $uj_{in}$ ), the coordinates of the fasteners in the reference system and the single-dowel slip curves. This part of the MATLAB Code is more or less the calculation core, where the resulting displacements of each fastener are calculated and applied to the corresponding single-dowel slip curves. The application to the single-dowel slip curves yields a reaction force per fastener. Equilibrium of these forces at the reference point leads to the member forces. The calculated member forces are compared with the input member forces, and if necessary the input deformations of

the connection are modified. This modified deformations are used to calculate revised member forces, which are again compared with the input member forces. This procedure is executed until a satisfactorily low residue  $Rn$  (less than  $10^{-6}$ ) between the two sets of member forces, or the maximum number of iteration cycles is reached.

### Output

- resulting displacement per fastener  $\mathbf{d}_{ji}$ ,
- reaction forces per fastener  $\mathbf{R}_i$ , and
- force-to-grain angle per fastener  $\hat{\alpha}$ .

## I2) InitialDeform\_01.m

The object of this function is to estimate the initial global deformations  $\mathbf{u}_{j\_in}$  based on the input member forces  $\mathbf{MF}$ , as a starting point for the iterative determination of the deformation and force distribution within the connection. For this purpose, the slip curves of the connection, determined by the script *Connection\_03.m* are used.

### Input

- input member forces  $\mathbf{MF}$ , and
- slip curves of the connection.

### Calculation

- linear interpolation within the polygonal slip curve.

### Output

- first approximation of the global deformation of the connection  $\mathbf{u}_{j\_in}$ .

## I3) InputData\_03.m

All input data in this subscript are set by the user. Basically, the geometrical and mechanical properties as well as the calculation methods for the reaction forces and single-dowel slip curves have to be defined here.

## Input

- **Geometry**

- coordinates and corresponding slip curves of the fasteners in an arbitrary input coordinate system  $\mathbf{X}_-$ , and
- additionally, a translation vector  $\mathbf{eX}_-$  in mm and a rotation  $ny$  in  $^\circ$  can be specified, in order to move the coordinates from the input to the reference coordinate system. The reference coordinate system is usually located on the beam axis perpendicular to the center of gravity.

- **System data**

- safety concept: Specification of modification factor  $k_{mod}$  of timber elements,
- material: Mechanical properties and geometry of the connection elements (side member(s), gusset plate(s), fasteners, ...), as well as the grain direction with respect to the beam axis of the timber elements,
- calculation method - related to the force/displacement direction  $cm$ : Opportunity to consider the deviation between force and displacement direction of the single dowel loaded at an angle to the grain, and
- calculation method - related to the type of the single-dowel slip curve  $msc01$ : Possibility to choose between method 1 to 8 (extension to further methods is possible). Three different calculation principles are presented in Table 2.2.

## Calculation

- transformation of the coordinates from the input coordinate system to the reference system.

## Output

Identical to Input.

### I4) Slipcurve01\_03\_01.m / I5) Slipcurve02.m

While in *Slipcurve02.m* the single-dowel slip curve (contact condition) is generated automatically, in *Slipcurve01\_03\_01.m* the procedure for the calculation of the single-dowel slip curve depends on the chosen calculation method. The general shape of the different slip curves determined in *Slipcurve01\_03\_01.m* is presented at Table 2.2. Detailed explanations are given in Section 2.4.

## Input

- calculation method - related to the type of the single-dowel slip curve  $msc01$ , and

- geometrical data and system data defined in *InputData\_03.m*.

### Calculation

Dependent on the chosen calculation method *m\_sc01*, different procedures are executed. Three different types are listed consecutively. A detailed description of these methods is given in Section 2.4.

- simplified method based on EC 5 (*m\_sc01* = 1),
- advanced method based on EC 5 (*m\_sc01* = 2),
- slip curve determined by a sub-model (*m\_sc01* = 3 – 8).

### Output

The output of these function are single-dowel slip curves, by means of a displacement vector (**d01\_sc**) and force vector (**Fv01\_sc**) for as many force-to-grain angles as specified in *Slipcurve01\_03\_01.m*.

The following functions are related to the calculation - output part of the main script *MemberForces\_03\_01.m*.

### O1) InitialMatrices01.m

The function *InitialMatrices01.m* provides empty matrices or vectors. On the one hand, the generated input deformations for both steps (**uj\_in** & **uj\_in** + **du**) are stored. On the other hand, the calculated values, namely the displacement of the fasteners (**djiv**), the reaction forces (**Ri**), force-to-grain angle ( $\hat{\alpha}i$ ) and the member forces ( $N/V/M$ ) are summarized.

### Input

- input relative deformations of neighboring cross sections (**uj\_in**),
- additional incremental deformations of neighboring cross sections (**du**),
- number of investigation points ( $pu = 2$ ), and
- number of fasteners ( $n$ ).

### Calculation

- initialization of empty matrices (vectors) with their necessary size, and calculation plus storage of the input deformations for both steps.

## Output

- matrix including the input deformations for both calculation steps ( $\mathbf{u_j}$ ).

Empty matrices (vectors) for:

- displacements of the fasteners ( $\mathbf{d_{jiv}}$ ),
- reaction forces ( $\mathbf{R_i}$ ),
- force-to-grain angles ( $\hat{\alpha_i}$ ), and
- member forces ( $N_{iter}/V_{iter}/M_{iter}$ ).

## O2) ReactionValues03.m

This function determines the reaction values of the connection due to the prescribed input deformation.

First, the displacements of each dowel due to the input deformations are calculated. As a result of the assumptions regarding rigidity of the timber matrix and fixed position of the fasteners below each other, every fastener experiences the same axial ( $u_{ji}$ ) and transverse displacement ( $w_{ji}$ ). The displacement caused by the rotation of the cross section ( $d_{ji-\phi}$ ) depends on the distance of the dowel from the reference point. Vector addition of this three displacements gives the resulting displacement vector (see Figure 4.1). The length of the vector (=size of the displacement  $d_{ji}$ ) and the direction of the vector  $\hat{\alpha}$  (related to the grain direction) is determined.

Application of the resulting displacements per fastener to the related slip curve (defined by the slip curve type and force-to-grain angle) gives the reaction force vector. The calculations are done in the function *ResultingForce03.m* for the slip curve category  $sc = 1$ , and in *SectionalLinearCurve01* for  $sc = 2$ .

Equilibrium of the forces at the reference point gives the member forces  $N_{iter}/V_{iter}/M_{iter}$  (see Figure 4.2). Finally, the displacement of the fasteners, the force-to-grain direction, the reaction forces and the member forces are stored in the corresponding matrices.

## Input

- input deformation vector  $\mathbf{u_j}$ ,
- geometry of the connection  $\mathbf{x}$ ,  $\mathbf{z}$  &  $n$ ,
- single-dowel slip curve type per fastener  $sc$ ,
- grain angle  $\alpha$ ,
- single-dowel slip curves, and
- calculation method regarding the force/displacement direction  $cm$ .

### Calculation - Output

- resulting displacement per fastener  $dji$ ,
- displacement-to-grain angle per fastener  $\hat{\alpha}1$ ,
- reaction forces per fastener  $Ri$ ,
- force-to-grain angle  $\hat{\alpha}$  (if the deviation of force - displacement direction is not consider, then  $\hat{\alpha}1 = \hat{\alpha}$ ), and
- member forces  $N_{iter}$ ,  $V_{iter}$  &  $M_{iter}$ .

### O3) ResultingForce03.m / O4) O5) SectionalLinearCurve01(03).m

These two functions determine the reaction forces per fastener by means of single-dowel slip curves, starting at the resulting displacement per fastener. While *SectionalLinearCurve01(03).m* determines the reaction force  $Ri$  within the polygonal slip curve, the function *ResultingForce03.m* additionally interpolates between the single-dowel slip curves, in the case the force-to-grain angle of the resulting displacement does not match a force-to-grain angle, for which the single-dowel slip curves are determined (see Figure A.1). Since the contact condition ( $sc = 2$ ) depends on the grain direction, only the function *SectionalLinearCurve01(03).m* is used in this case.

### Input

- single-dowel slip curve,
- resulting displacement of the fastener  $dji$ , and
- force-to-grain angle  $\hat{\alpha}$  (only for *ResultingForce03.m*).

### Calculation - Output

- reaction force per fastener  $Ri$ .

### O6) StiffnessMatrices01.m

This function determines the secant and tangential stiffness for a specific global deformation. In the case of back-calculation of the dowel forces, only the tangential stiffness matrix is needed. The stiffness of the connection, which is equal to the gradient of the slip curve is used as input to the Newton-Raphson method. The tangential stiffness is calculated by division of the difference between the current member forces ( $N_{iter}(p)$ ,  $V_{iter}(p)$  &  $M_{iter}(p)$ ) and the previous member forces ( $N_{iter}(p-1)$ ,  $V_{iter}(p-1)$  &  $M_{iter}(p-1)$ ) by the incremental deformation  $du$ . It should be highlighted that the stiffness is calculated by isolated consideration of each deformation. Figure 4.4 illustrates the stiffness determination.

**Input**

- vector of member forces ( $\mathbf{N}_{iter}$ ,  $\mathbf{V}_{iter}$  &  $\mathbf{M}_{iter}$ ),
- current global deformation  $\mathbf{u}_{j-cu}$ , and
- incremental global deformation  $\mathbf{du}$ .

**Calculation - Output**

- tangential stiffness matrix  $\mathbb{K}tan$ .

**O7) NewtonRaphson\_01.m**

Finally, the calculated member forces  $N_{iter}$ ,  $V_{iter}$  &  $M_{iter}$  are compared with the input member forces  $N$ ,  $V$  &  $M$ . The residue of the member forces ( $Rn$ ) is calculated as the difference between both sets of member forces, divided by the set of input member forces. If the residue is lower than the exit criterion, than the displacement and force distribution has been found. Otherwise the global deformation of the connection is adjusted by means of the Newton-Raphson method. The incremental change of the global deformations ( $\mathbf{deltaUj}$ ) is calculated by division of the difference between the input member forces and calculated member forces ( $\mathbf{deltaMF}$ ) with the corresponding gradient of the global slip curve ( $\mathbf{Ktan}$ ). This incremental change of the global deformation is added to the previous deformation set of the connection ( $\mathbf{u}_{j+1} = \mathbf{u}_j + \mathbf{deltaUj}$ ). The new global deformation ( $\mathbf{u}_{j+1}$ ) is then used as input for the next iteration cycle.

**Input**

- input member forces ( $N$ ,  $V$  &  $M$ ),
- calculated member forces ( $N_{iter}$ ,  $V_{iter}$  &  $M_{iter}$ ),
- stiffness matrix ( $\mathbb{K}tan$ ), and
- current global deformation ( $\mathbf{u}_j$ ).

**Calculation**

- residue of the member forces ( $Rn$ ),
- incremental change of the global deformation ( $\mathbf{deltaUj}$ ), and
- global deformation for the next iteration step ( $\mathbf{u}_{j+1}$ ).

**Output**

- residue of the member forces ( $Rn$ ), and
- global deformation configuration for the next iteration step ( $u_{j+1}$ ).

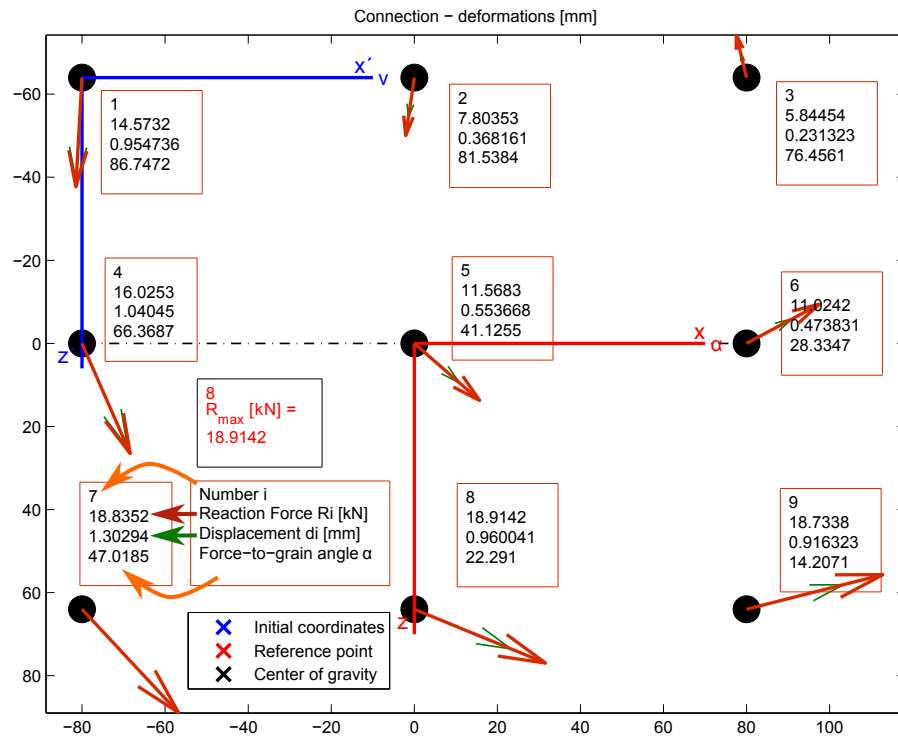


Figure B.1: Configuration of the connection, and displacement and force distribution - *FigureSketch\_MF\_01.m*.

## O8) FigureSketch\_MF\_01.m

On the one hand, this plot serves to visualize the geometric properties of the connection and, on the other hand, the displacement and force distribution within the connection is shown. The plot includes the position of the fasteners, the input and reference coordinate system, the center of gravity of the connection (COG), the grain direction and the beam axis. Furthermore, the length and direction of the displacement vector (green arrow) of each fastener is shown graphically and, additionally, the size of the displacement is computed. The same is done for the reaction force vector (red arrow). The force-to-grain angle is computed for each fastener. Also, the maximum fastener reaction force and its position is highlighted (see Figure B.1).

## O9) FigureMemberForces01\_02.m

The plot *FigureMemberForces01\_02.m* illustrates the three slip curves of the connection, based on uniformly loading. The position of the input member forces within the global slip curves is marked (see Figure B.2).

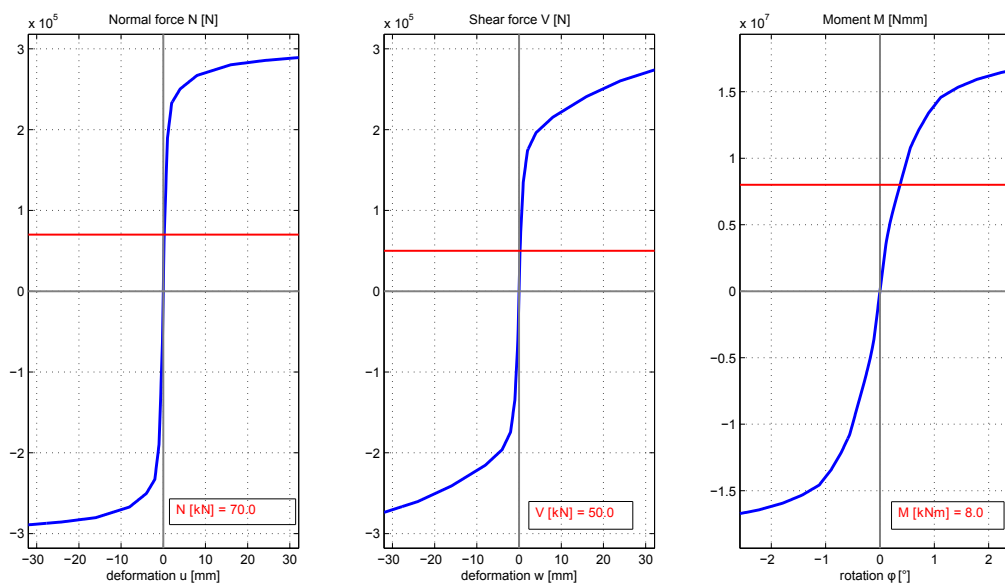


Figure B.2: Connection slip curves for centric design example - *FigureMember-Forces01\_02.m*.

## Flow chart - MATLAB Code - back-calculation of dowel forces

